Nouveaux gels organiques et carbonés dérivés de composés phénoliques naturels et synthétiques

Andrzej Szczurek

THÈSE

Présentée devant l'Université Henri Poincaré, Nancy 1

pour l'obtention du grade de

DOCTEUR DE L'UNIVERSITÉ HENRI POINCARÉ, NANCY 1

Ecole doctorale EMMA

Spécialité: Chimie du Solide

par

Andrzej SZCZUREK

NOUVEAUX GELS ORGANIQUES ET CARBONÉS DÉRIVÉS DE COMPOSÉS PHÉNOLIQUES NATURELS ET SYNTHÉTIQUES

Sous la responsabilité d'Alain CELZARD et Antonio PIZZI

Co-encadrée par Vanessa FIERRO

Soutenue publiquement le 7 Novembre 2011 devant la Commission d'examen

Rapporteurs :

M. Bernard DE JESO, Professeur, Université de Bordeaux I

M. Bertrand CHARRIER, Professeur, Université de Pau

Examinateurs:

M. Lionel FLANDIN, Professeur, Université de Savoie – *Président du jury*

M. Antonio PIZZI, Professeur, Université de Nancy I

Mme Vanessa FIERRO, Chargée de Recherches CNRS

M. Alain CELZARD, Professeur, Université de Nancy I

Thèse préparée à l'Institut Jean Lamour – UMR CNRS 7198 en étroite collaboration avec le LERMAB – EA 4370, sur le Campus Fibres d'Epinal.

Acknowledgements

To my Professors:

Prof Alain Celzard for an extensive knowledge, availability and the sea of patience,

Prof Antonio Pizzi for good advices and plenty of formulations,

Mme Vanessa Fierro for her availability and sense of humour,

My commission for availability

To my Friends:

Wei, for hundreds of samples changed in Micromeritics 2020 without any word of complaining

Gisele, for companion in the lab and help with analysis of my gels,

Cesar, Karin, Katty and Paula, for an infinite support,

Veronica and Gianluca, for the many great moments,

Paola and Jerome, for petanque, bikes and great sense of humour

Flavia, for smile and good mood every season of our life in ENSTIB,

Mr Jean – Jacques Balland and all people from Atelier for infinite support

Miriam, Rami, Lei Hong, you are still in my memory. It was a pleasure to meet you.

Special thanks for my family for love and support.

Very special thanks to my wife, Anna, for her trust, love and happiness which gives me every day.

Table des matières

Introduction

Les gels de carbone sont des matériaux qui ont été découverts il y a un peu plus de vingt ans. Ils sont le résultat de la pyrolyse de gels organiques non fusibles dont ils conservent la structure de départ. Cette dernière est habituellement décrite comme entre un entrelacs de longues chaînes, elles-mêmes constituées de particules sphériques poreuses (modèle du collier de perles). Entre ces chaînes, une porosité plus large existe, saturée par le solvant dans lequel les gels organiques précurseurs ont été préparés. Le remplacement de ce solvant par de l'air permet donc d'obtenir un solide à porosité hiérarchisée : macro et mésopores entre les nodules sphériques, et microporosité dans les nodules. Un matériau carboné présentant ces caractéristiques poreuses, en plus des propriétés typiques du carbone telles que résistances chimique et thermique et conductivité électrique, a donc une variété d'applications possibles. Parmi celles-ci, les plus intéressantes sont le stockage électrochimique sous forme d'électrode poreuse dans des condensateurs à capacité de double-couche, l'adsorption de molécules gazeuses ou dissoutes en phase liquide, et la catalyse en tant que catalyseur ou simplement de support.

Ces différentes applications ont en effet été proposées assez rapidement après que les premières descriptions de gels de carbone aient été rapportées. Néanmoins, ces gels étaient toujours du même type. Ils étaient pour la grande majorité synthétisés à partir d'une résine résorcinol – formaldéhyde (RF) dans l'eau en conditions faiblement alcalines, puis séchés à l'air ou en conditions supercritiques avec du dioxyde de carbone. Dans les deux cas, les matériaux étaient appelés « aérogels de carbone ». Il régnait d'ailleurs une certaine confusion dans la terminologie, tout carbone amorphe de très basse densité étant qualifié d'aérogel. Les débouchés applicatifs, pour être envisagés à l'échelle industrielle, ont ensuite amené les chercheurs à s'intéresser à d'autres précurseurs possibles. En effet, en raison du coût prohibitif du résorcinol, d'autres résines ont été proposées, toutes moins chères mais toutes d'origine synthétique, à de rares exceptions près. D'authentiques aérogels de carbone à très bas coût ont d'ailleurs été obtenus à partir de cellulose. Cependant, le rendement en carbone de la cellulose étant très bas, la plupart des auteurs ont continué à s'intéresser aux résines phénoliques.

Dans le même temps, des modes de séchage alternatifs ont été suggérés pour éviter l'étape mettant en œuvre le CO_2 supercritique, tout en permettant d'obtenir des porosités bien développées : séchage micro-ondes, séchage convectif, séchage supercritique dans des solvants organiques (acétone, éther de pétrole, …), et lyophilisation. Bien sûr, cette démarche de réduction des coûts n'a réellement d'intérêt que pour un marché de masse assez peu exigeant. Lorsqu'au contraire une pureté absolue est requise et que le précurseur ne représente qu'une fraction minime du coût final, cet effort pour trouver des substituts à la résine RF est inutile. C'est par exemple le cas des supports de catalyseur pour piles à combustible basse température à échange de protons (PEMFC), très sensibles aux impuretés, et sur lesquels du platine est dispersé. C'est aussi le cas, mais dans une moindre mesure, des électrodes de supercondensateurs à électrolyte organique, dans lesquels la présence de minéraux réduit la durée de vie du système. Dans tous les autres cas, obtenir des carbones poreux aux propriétés équivalentes à celles des aérogels dérivés de résine RF séchés par CO_2 supercritique est d'un réel intérêt.

Dans cette thèse, la préparation de nouveaux carbones poreux aux caractéristiques comparables, et si possible meilleures du point de vue applicatif, que celles de matériaux plus chers ou plus complexes à produire, a été notre ligne directrice. Cette démarche a été réalisée en plusieurs étapes nécessaires à l'acquisition des connaissances que nous n'avions pas au départ. C'est ainsi que nous avons commencé par reproduire des synthèses de gels RF, que nous avons rapidement modifiées afin d'obtenir des gels de carbone très différents les uns des

autres. En séchant les résines par de l'acétone ou de l'éthanol supercritique, en les faisant sécher à l'air ou en les lyophilisant, ce sont autant de nouveaux matériaux qui ont été obtenus et, pour la majorité d'entre eux, caractérisés complètement. Des charbons actifs totalement inédits en ont été dérivés. Le précurseur a ensuite été changé, pour produire de nouveaux gels de carbone au coût progressivement décroissant : phénol d'abord, et polyphénols naturels ensuite : des tannins de mimosa. De manière à étudier leur comportement en solution diluée et en obtenir des gels, ces tannins ont d'abord été utilisés en mélange avec du résorcinol (celui-ci restant minoritaire), puis seuls. Combinés à des modes de séchage moins onéreux que celui utilisant le CO_2, les gels de carbone d'origine phénolique les moins chers, jusqu'à cinq fois moins que leurs homologues RF, ont été obtenus et caractérisés.

Le but premier de cette thèse a donc été atteint même si d'autres formulations, qui n'ont été abordées que partiellement et qui n'ont pas été décrites ici, méritent encore d'être étudiées. Peu de temps a pu être dédié aux propriétés applicatives, exception faite de l'électrochimie dans le cas des cryogels de carbone dérivés de phénol – formaldéhyde. La mise au point des synthèses, la multiplicité des formulations (résines précurseurs) et de leurs différents paramètres (dilution, pH, rapports molaires de réactifs), et les différents séchages mis en jeu (subcritique, supercritique, lyophilisation) a en effet pleinement occupé la durée de la thèse. La somme de résultats qui ont été produits ont permis la publication de 8 articles au cours de ces trois dernières années. Ils sont donnés in extenso dans les pages suivantes.

Ce mémoire est donc présenté « par articles ». Cette manière de procéder présente des avantages et quelques inconvénients. Elle permet de présenter un travail abouti et concis, allant à l'essentiel, et déjà jugé « par les pairs » puisque les publications ont toutes été acceptées dans des revues de rang A avec comité de lecture. Elle permet donc de réduire considérablement le nombre de pages à rédiger, afin d'éviter les redondances. Par contre, elle ne rend pas bien compte du travail fourni, puisque les articles ne présentent que les résultats les plus marquants, sans faire allusion ni aux développements implicites qu'il a fallu faire, ni aux résultats de moindre importance, mais néanmoins intéressants, qui ont été obtenus.

Ce mémoire est organisé comme suit. Après cette introduction, un résumé d'une vingtaine de pages est donné. Il permet au lecteur d'entrevoir toute la démarche intellectuelle et expérimentale de la thèse. Ce long résumé est parsemé d'encadrés de contenu scientifique, qui peuvent être lus indépendamment du texte principal et indépendamment les uns des autres. Ces encadrés donnent des explications plus détaillées sur quelques points de science abordés rapidement dans le texte principal.

Le sujet de ces différents encadrés est ensuite repris de manière approfondie dans les pages qui suivent le résumé : tout d'abord sous forme de cinq chapitres rédigés en anglais et de la bibliographie correspondante, et enfin des huit publications parues ou sous presse. Les cinq chapitres décrivent ainsi, respectivement, la chimie des gels, leur séchage, leurs carbones dérivés, les applications des gels de carbone, et les principales techniques analytiques utilisées au cours de ce travail de thèse. Les publications qui suivent, en anglais toujours, sont précédées d'un résumé d'une page en français. Le mémoire se termine par une conclusion générale.

Résumé des travaux et démarche entreprise

Ce travail est le résultat d'une collaboration fructueuse entre deux laboratoires Nancéiens possédant chacun une antenne sur le Campus Fibres d'Epinal, hébergée dans les locaux de l'ENSTIB : Ecole Nationale Supérieure des Techniques et Industries du Bois. Il s'agit de l'Institut Jean Lamour (IJL – UMR CNRS 7198) et du Laboratoire d'Etudes et de Recherches sur le Matériau Bois (LERMAB – EA 4370). L'idée directrice ayant conduit à la réalisation de cette thèse est la mise en commun de compétences très différentes pour converger vers un but clairement identifié : la préparation, la caractérisation et les applications de nouveaux matériaux poreux. Dans ce but, l'IJL apportait sa connaissance des solides poreux et désordonnés, essentiellement minéraux, et le LERMAB son expertise dans le domaine de la chimie organique, et en particulier des résines. La possibilité d'obtenir des matériaux poreux originaux est née du constat que le LERMAB préparait des adhésifs pour le bois à partir de nombreuses formulations envisageables. Ces résines, avant de durcir, passent par un stade de gel qui, au final, doit être le moins poreux possible. L'IJL a alors proposé de « détourner » de telles formulations pour, au contraire, en préparer des gels de haute porosité qui pourraient ensuite être convertis en gels de carbone. Ces derniers, finement caractérisés avec des méthodes ad-hoc typiques de la chimie du solide, seraient ensuite testés dans les applications habituellement suggérées pour de tels matériaux : adsorption, stockage d'énergie électrochimique, isolation thermique, etc.

Cette partie de la thèse résume quelle démarche a été la notre au cours de cette thèse et propose quelques digressions (encadrées) pour approfondir certains points du texte.

Les réactions sol-gel

En milieu solvant dilué, des monomères peuvent subir des réactions de polycondensation conduisant à la formation d'un squelette solide. Très schématiquement, le précurseur est d'abord dissous dans un solvant auquel sont ajoutés les réactifs qui vont permettre la condensation : eau, catalyseur, réticulant si besoin, etc. La solution de départ, parfaitement transparente et homogène (Fig. 1a), se transforme quelques temps après en un sol, c'est-à-dire une suspension de très fines particules solides (Fig. 1b). Le sol peut être polymérique, à savoir constitué de chaînes de polymères plus ou moins longues et plus ou moins ramifiées, ou être particulaire, c'est-à-dire constitué d'embryons de solide plus ou moins sphériques. Néanmoins cette distinction est historique et n'est réellement utilisée que dans le cas des gels de silice. Il est en effet difficile de différencier un morceau de réseau polymérique d'un solide particulaire, tout solide de composition homogène pouvant être considéré comme un

fragment de polymère. Les particules du sol sont si petites qu'elles sont en agitation permanente (mouvement Brownien) et ne pas soumises à la gravitation. Elles grossissent au fur et à mesure que les réactions se poursuivent, et leur rencontre conduit à la formation d'amas de taille finie. Le nombre croissant de liens qui se forment entre particules fait diverger la viscosité et aboutit finalement à une percolation du système. A cet instant, appelé point de gel, la première liaison pour qu'un amas « géant », dit « infini », se forme, apparaît. Cette macromolécule a la taille du récipient qui la contient (Fig. 1c). Au-delà du point de gel, il n'est plus possible de mesurer de viscosité, par contre un module élastique peut être déterminé. Cependant, ce dernier va augmenter de plusieurs ordres de grandeur au fur et à mesure que de nouveaux liens viennent consolider le gel, et que les amas finis viennent rejoindre l'amas infini. Cette étape, dite de vieillissement (aging or curing), est nécessaire pour obtenir un gel de propriétés mécaniques correctes, et pour que tout le précurseur initialement présent en solution se retrouve dans la réseau solide.

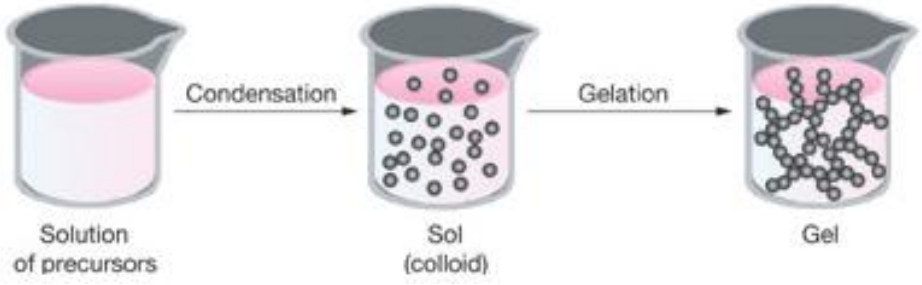

(a) (b) (c)

Fig. 1 : Principe d'une réaction sol-gel. (a) Solution homogène de départ ; (b) Sol ; (c) Gel.

Il fallait néanmoins, avant de faire des gels à partir de formulations d'adhésifs, y ajouter la condition nécessaire que les développements suggérés n'avaient pas déjà été largement étudiés – et donc publiés – par le passé. Une première étude bibliographique montra alors que l'essentiel des études réalisées portaient sur un même système : le couple résorcinol – formaldéhyde (RF) gélifié dans l'eau selon différents conditions. En effet, la résine RF, utilisée dans la préparation d'adhésifs, a l'avantage de produire de très beaux gels élastiques, présentant d'excellentes propriétés mécaniques. En outre, la synthèse est facile, rapide, et très reproductible. Lorsqu'il s'agissait d'en produire des aérogels, la technique restait majoritairement celle proposée en 1989 par Pekala, à savoir le séchage par CO_2 supercritique. Cette pré-étude nous a rapidement suggéré les deux constats suivants : (1) tout nouvel aérogel devrait être suffisamment différent du système RF séché par CO_2 supercritique, très largement étudié de par le monde, et (2) le résorcinol est une résine particulièrement onéreuse, comme

l'indiquent la plupart des publications sur le sujet. Par conséquent, nous avons souhaité préparer des gels de carbone (et donc des précurseurs organiques) qui se différencient des autres par le coût, tout en gardant des caractéristiques et des propriétés finales similaires.

Les gels de résorcinol – formaldéhyde (RF)

La Fig. 2a montre schématiquement la réaction sol-gel du résorcinol avec le formaldéhyde dans le solvant eau. Chaque molécule de résorcinol réagit avec deux molécules de formaldéhyde, conduisant, par condensations successives, à des chaînes de polymère RF. Ces chaînes se ramifient au gré des réticulations, avec pour conséquence la formation de particules très poreuses et sphériques en moyenne (Fig. 2b). L'agglomération de telles particules conduit in fine à un solide avec une structure nodulaire typique dite « en collier de perles », telle que représentée en Fig. 1c. La Fig. 2c montre les tubes hermétiquement fermés dans lesquels les gélations ont été faites, ainsi que des gels RF avec leur coloration brun-rouge habituelle.

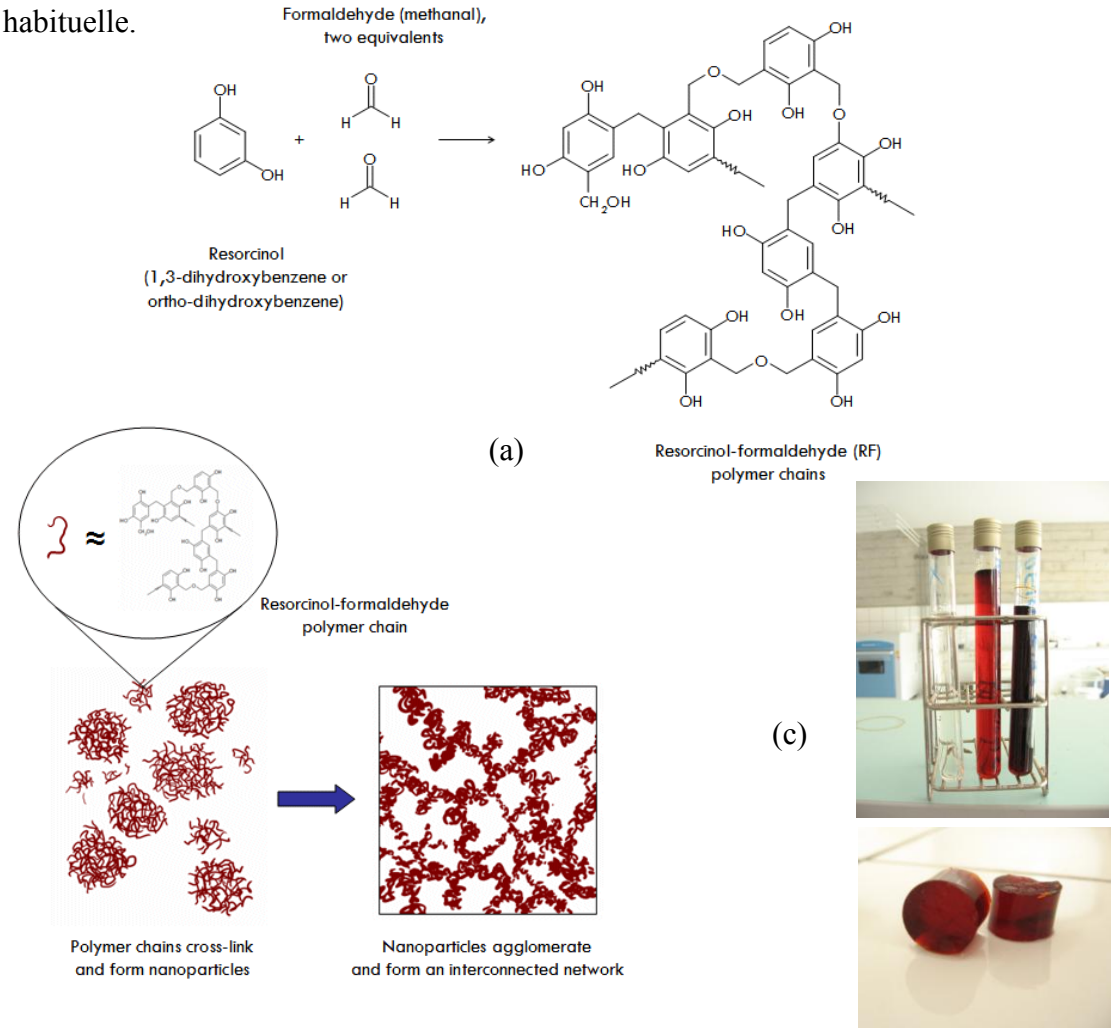

Fig. 2. Formation d'un gel de résorcinol-formaldéhyde dans l'eau. (a) Structure chimique ; (b) Structure poreuse ; (c) Hydrogels RF typiques.

Des matériaux poreux dérivés de gels

Un gel, ou plus exactement un hydrogel ou un alcogel, selon qu'il a été obtenu dans l'eau ou dans un alcool, respectivement, est donc un solide dont le squelette est très ténu et présente une porosité considérable mais saturée du solvant dans lequel il a été préparé. Si, comme dans notre cas, le but est de préparer des matériaux poreux, il convient d'extraire ce solvant de telle manière que la porosité n'en soit pas trop affectée. Autrement dit, il faut sécher le gel, donc remplacer le liquide présent dans les pores par sa vapeur ou par tout autre gaz. Pour ce faire, le diagramme de phase qualitatif du solvant, quel qu'il soit, mérite très considéré (Fig. 3).

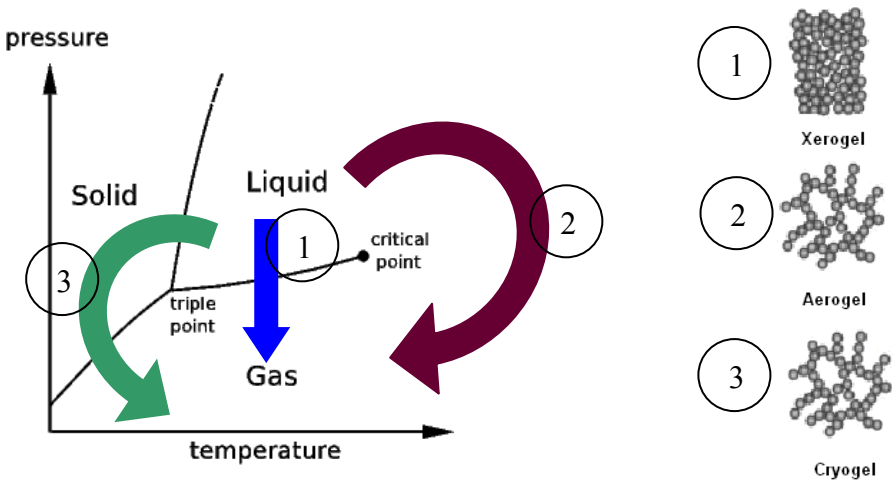

Fig. 3 : Diagramme de phase qualitatif du solvant saturant les pores d'un gel, chemins possibles pour le séchage du gel (1), (2) et (3), et résultats correspondants.

A pression et température ambiante, le point représentatif du solvant se trouve dans le domaine du liquide. Cependant, la pression de vapeur du solvant tend vers zéro dès lors que le gel mouillé est maintenu en atmosphère non confinée. Le solvant en surface d'un gel mouillé et laissé à l'air à température ambiante a donc son point représentatif sur la courbe d'équilibre liquide – vapeur. Autrement dit, le solvant s'évapore par les bords de l'échantillon, et un ménisque liquide existe au niveau de chaque pore (chemin 1 de la Fig. 3). A l'échelle du nanomètre, les forces capillaires mises en jeu sont très intenses, et le mince squelette solide subit donc des tensions considérables, conduisant à un retrait très important et souvent à de la fissuration. En résultat, le gel a perdu beaucoup de sa porosité initiale. Séché ainsi, de manière subcritique, il est qualifié de xérogel (du grec « xero » : sec).

Pour éviter la contraction lors du séchage et conserver l'aspect monolithique du gel, il faut faire disparaître les forces capillaires, et donc éviter que liquide et vapeur coexistent. Le

contournement du point critique (chemin 2 de la Fig. 3) ou le passage par la phase solide (chemin 3) permettent cela, et sont qualifiés de séchage supercritique et de lyophilisation, respectivement. Les matériaux obtenus ont en première approximation la même structure microscopique que celle des gels mouillés initiaux, et sont qualifiés d'aérogels et de cryogels, respectivement. Ces gels secs sont ainsi caractérisés par une extrême légèreté, et donc une porosité très développée. Cependant, au niveau macroscopique, la texture n'est pas exactement la même. En raison de la congélation du solvant qui donne des cristaux de glace plus ou moins gros, la porosité des cryogels est toujours nettement plus grossière que celle des aérogels de même densité et de même nature. La Fig. 4 montre ainsi des gels de carbone issus d'hydrogels RF séchés de manière différente. Au niveau microscopique, la structure reste nodulaire et indifférenciable.

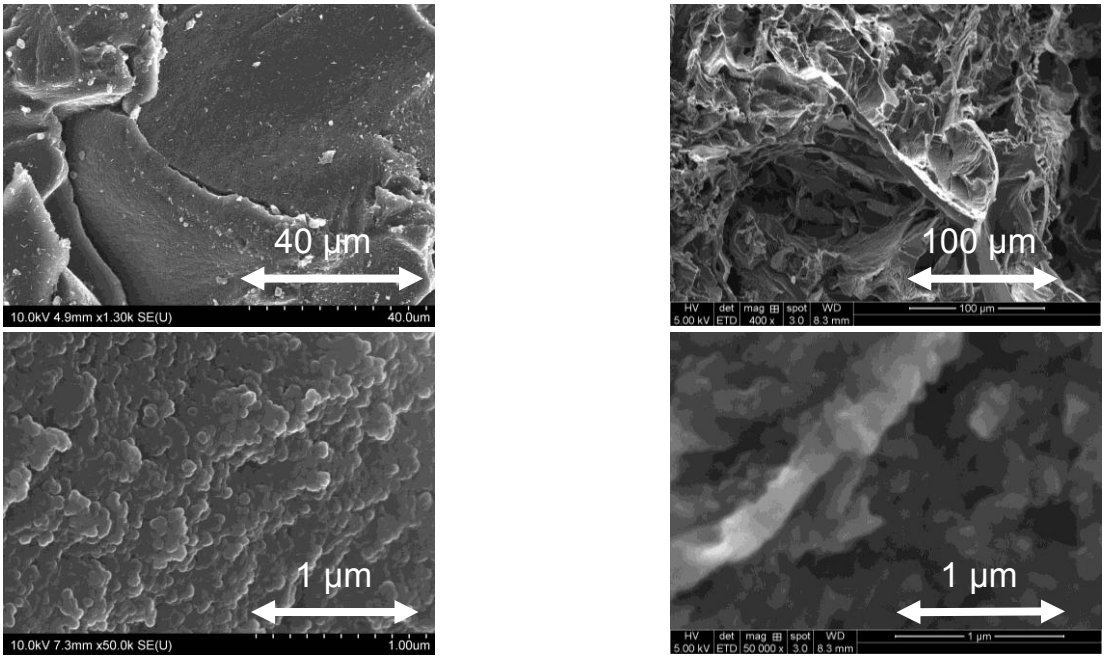

(a) (b)

Fig. 4 : Gels de carbone RF vus à différents grossissements en microscopie électronique à balayage. (a) Aérogel ; (b) Cryogel.

Pour atteindre l'objectif de réduction des coûts liés à la production de ces solides poreux, nous avons travaillé selon deux approches permettant d'obtenir des matériaux suffisamment nouveaux : le précurseur d'une part, et le mode de séchage d'autre part. En effet, les nombreuses formulations offertes par le LERMAB pouvaient être utilisées pour réaliser des aérogels qui n'avaient jamais été obtenus auparavant. Inversement, le résorcinol pouvait être utilisé mais pour produire des gels séchés par des méthodes alternatives, et donc présentant des textures poreuses inédites. Dans les deux cas, que l'on se concentre sur le précurseur ou

sur le mode de séchage des gels, des matériaux nouveaux – et à moindre coût – étaient obtenus.

C'est donc dans cette optique que cette thèse a été réalisée. Lors de son démarrage en automne 2008, aucune synthèse de gel organique n'avait alors jamais été réalisée par l'IJL. La seule expérience consistait à avoir mis au point dans les années 2000 une méthode d'obtention d'aérogels de silice. Cette méthode, basée sur un séchage dans l'éthanol supercritique, avait été développée dans le cadre des Travaux Pratiques dispensés par Alain Celzard en Maîtrise de Chimie, à Nancy. Elle a ensuite fait l'objet, entre autres applications de la méthode sol-gel, d'un article dans Journal of Chemical Education paru en 2002[1]. Préparer des gels organiques ne paraissait a priori pas plus difficile que faire des gels minéraux. En outre, le matériel nécessaire (four, autoclave et vannes haute-pression) était disponible. Nous avons néanmoins préféré faire nos premiers pas en tentant de reproduire des synthèses de résines RF déjà publiées. Notre premier contact avec le résorcinol a ainsi permis de mener à bien une courte étude sur sa réaction avec les adhésifs de type polyuréthane, et a fait l'objet du premier article produit lors de cette thèse (article n°1).

Article n°1 : **L'hydroxyméthyl résorcinol en tant que promoteur d'adhésion dans les colles polyuréthane pour le bois**

Dans ce travail, sans lien avec les matériaux poreux mais mettant en jeu le résorcinol avec lequel nous devions nous familiariser, les mécanismes de réaction de l'hydroxyméthyl résorcinol (HMR) avec une résine polyuréthane ont été considérés. Le but était de mieux comprendre comment l'HMR améliorait les performances des colles PU monocomposantes (comportant des groupes –N=C=O toujours réactifs) auxquelles du HMR est parfois ajouté.

Deux produits, l'un issu de la réaction du HMR avec de la PU monocomposante, l'autre issu de la réaction du résorcinol seul (donc sans formaldéhyde, contrairement au cas précédent) avec cette même PU, ont été synthétisés et étudiés par RMN du ^{13}C. Il apparaît que le résorcinol seul donne, au moment du séchage, des liaisons uréthanes entre les groupements isocyanates résiduels et les hydroxyls du résorcinol (Fig. 5a). Le HMR donne aussi cette réaction en dernier ressort mais, avant le séchage, en donne également une autre entre ces mêmes isocyanates et les groupes méthylols du HMR (Fig. 5b). Cette réaction supplémentaire mise en évidence pour la première fois explique, entre autres raisons déjà reportées dans la

[1] A. Celzard, J.F. Marêché. Demonstrative applications of the sol-gel process through well-tested recipes. Journal of Chemical Education 79 (2002), 854-859

littérature, les meilleures performances des adhésifs comportant du HMR.

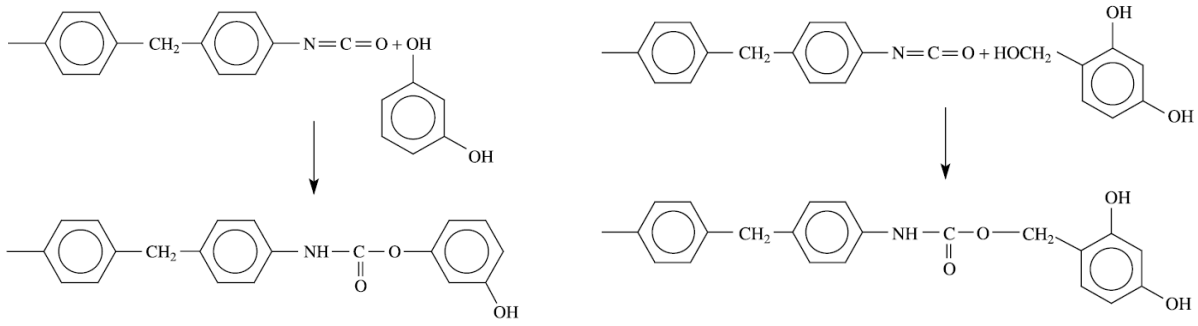

(a) (b)

Fig. 5 : Réaction présente dans le mélange : (a) résorcinol-pMDI monocomposant et HMR-pMDI monocomposant ; (b) HMR- pMDI monocomposant.

La facilité de produire la résine RF à différentes dilutions, différents pH et différents solvants, nous a donné de nombreux échantillons de gels qui ont ensuite été séchés. Outre le séchage supercritique, nous avons rapidement pu avoir accès à un lyophilisateur. Des gels ont été également laissés libres de sécher à l'air. En combinant les différentes formulations et les différents modes de séchage, ce sont plusieurs dizaines de matériaux qui ont été obtenus. Leur synthèse et leur caractérisation a pris plusieurs mois. Cependant, les résultats ont indiqué le plus souvent que, comparées aux données de la littérature, les textures poreuses obtenues étaient tout à fait quelconques. Pis, la découverte d'articles plus confidentiels révéla que de tels essais comparatifs pour évaluer les différents paramètres de synthèse sur la porosité finale avaient déjà été réalisés, avec des conclusions pas toujours bien tranchées. Même si nos propres expériences n'étaient pas identiques à celles qui avaient déjà été rapportées, nous avons renoncé à publier ces résultats, dont le caractère original aurait pu être mis en doute.

Gels de carbone et charbons actifs

Un gel de carbone est le produit de la pyrolyse, par définition un traitement thermique sous atmosphère inerte, d'un gel organique. Etant donné que ce dernier est constitué d'une résine thermodurcissable, donc infusible, la structure de départ est conservée. Autrement dit, le matériau est progressivement converti en carbone, en maintenant la porosité et les nodules dont le gel est constitué. Si le chauffage est suffisamment lent, quelques degrés par minute, les tensions éventuelles liées à la réorganisation du solide en cours de carbonisation et le départ de matières volatiles n'affectent ni la forme ni le caractère monolithique du gel. Le matériau obtenu est donc un solide très léger, noir, non fissuré, mais plus petit que le gel de

départ. La pyrolyse entraîne en effet un retrait important (au moins 50% en volume) et une perte de masse de la même ampleur. En conséquence, la densité apparente du gel de carbone final est assez voisine de celle du gel sec initial.

Un charbon actif est un solide carboné dont la porosité a été ouverte et développée par un processus appelé activation. Un tel matériau, dont la surface spécifique peut atteindre environ 3000 m^2/g, est un excellent adsorbant et utilisé comme tel dans de nombreux procédés industriels. Si le précurseur est déjà un carbone, les pores sont généralement créés par gazéification contrôlée, en faisant passer un gaz oxydant sur le matériau à haute température. On parle alors d'activation physique, le gaz étant du CO_2 ou de la vapeur d'eau. Si le précurseur est organique, il peut être imprégné d'un agent qui sera à la fois déshydratant et oxydant à haute température. On parle alors d'activation chimique, l'agent activant étant NaOH ou H_3PO_4, par exemple. Les deux types d'activation ne conduisent pas au même type de porosité, d'où leur intérêt, selon le résultat souhaité. La Fig. 6 montre un modèle de structure de carbone activé, avec le classement des pores selon leurs tailles et tel que défini par l'IUPAC.

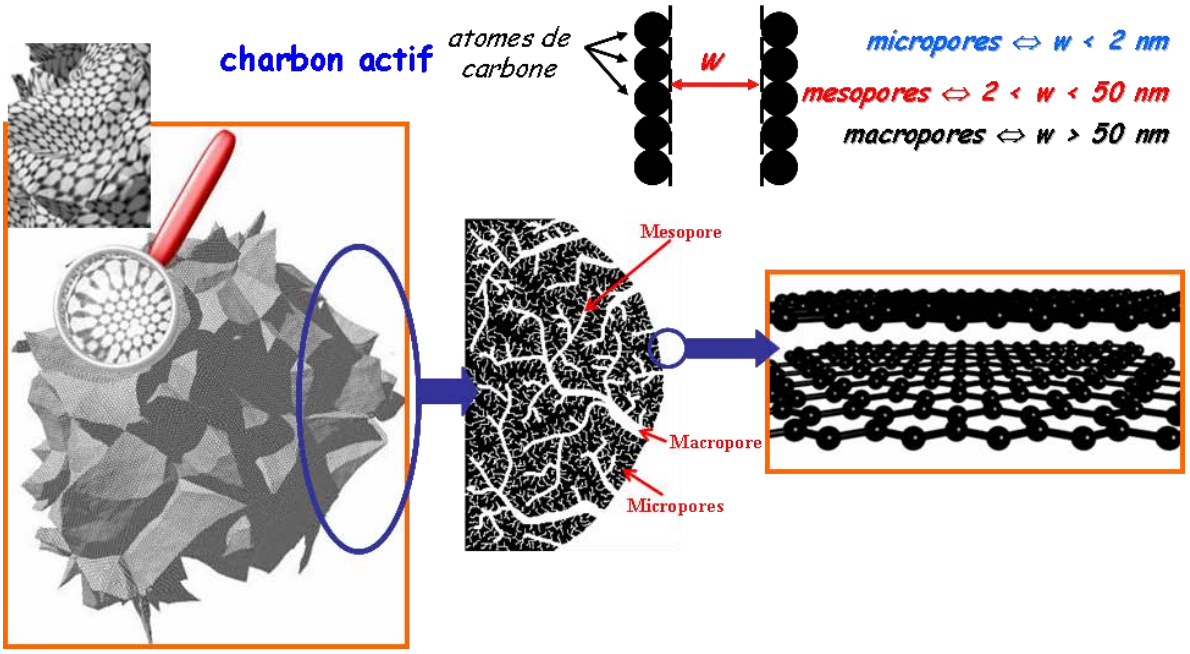

Fig. 6 : Modèle dit « du papier froissé », décrivant la structure poreuse hiérarchisée d'un charbon actif.

Clairement, une meilleure connaissance de ces systèmes aurait pu nous éviter de perdre environ six mois. Ces travaux ont néanmoins permis de nous familiariser avec les gels, leur synthèse, leur vieillissement, leur aspect, leur séchage et leur comportement en autoclave ou

en lyophilisateur. Ces études nous ont aussi familiarisés avec les techniques de caractérisation qui ont progressivement été acquises par l'IJL au cours de ces trois années de thèse : adsorption automatique et porosimétrie au mercure, puis pycnométrie à l'hélium. D'autres techniques étaient présentes au LERMAB, telles que spectroscopie FTIR, et essais mécaniques, ou sont arrivées plus tard encore à l'IJL, comme la conductivité thermique. Cependant, en raison de leur petite taille, les propriétés mécaniques et thermiques n'ont pas pu être étudiées de manière systématique. En revanche, des techniques absentes dans les deux laboratoires mais disponibles au travers de collaborations ont été utilisées chaque fois que nécessaire, notamment GC-MS, RMN et spectrométrie MALDI-ToF.

Quelques résultats originaux sur les systèmes RF ont toutefois été obtenus et valorisés par deux publications (articles n° 2 et 3 présentés dans ce mémoire). L'une (article n°2) présente les propriétés texturales de gels RF et de leurs gels de carbone dérivés obtenus par séchage supercritique dans l'acétone ou dans l'éthanol. L'eau et les sous-produits de réaction contenus dans la porosité de gels RF ont été remplacés par l'un ou l'autre de ces solvants, et séchés en autoclave par ces mêmes solvants à l'état supercritique. Le second travail sur les gels RF (article n°3) a consisté à préparer des charbons actifs à partir de ces matériaux, par activation chimique à l'acide orthophosphorique. Il était question de développer davantage la porosité de tels matériaux, dont la surface spécifique obtenue par simple pyrolyse ne permet pas aux matériaux résultants d'avoir des propriétés adsorbantes suffisantes pour nombre d'applications.

Article n°2 : **Propriétés texturales de gels RF et gels de carbone dérivés, séchés par des solvants supercritiques**

Ce travail démontre l'intérêt de se passer du CO_2 supercritique et d'utiliser à sa place de l'acétone ou de l'éthanol, deux solvants bon marché qui se laissent aisément convertir en fluides supercritiques. L'effet de ces deux fluides est identique, tant que la résistance mécanique des gels organiques à sécher est suffisamment élevée. Autrement dit, les gels doivent être assez denses. Si leur densité est faible, ces matériaux sont sujets au retrait, et une perte considérable de volume peut être observée. C'est le cas avec l'éthanol supercritique, alors que l'acétone dans le même état donne au contraire toujours une densité proche de celle que l'on peut calculer si aucun retrait n'avait lieu (Fig. 7). La pertinence de l'acétone en tant que fluide supercritique avait déjà été démontrée récemment, mais l'éthanol n'avait jamais été étudié. Compte tenu de la facilité avec laquelle des gels RF reproductibles peuvent être

obtenus, nous avions décidé de mener les études avec ce type de matériau. De manière à comparer rigoureusement les effets de l'acétone et de l'éthanol, nous avions tenu à tester nos propres échantillons dans le même autoclave. Nous avions en effet estimé qu'une comparaison avec les seuls résultats de la littérature serait insuffisante, étant dans l'impossibilité de reproduire exactement, et même de connaître, les conditions exactes utilisées auparavant par d'autres auteurs. Enfin, nous avons également pu étudier par GC-MS les produits de dégradation de ces deux fluides supercritiques et des gels eux-mêmes, ce qui n'avait jamais été fait auparavant.

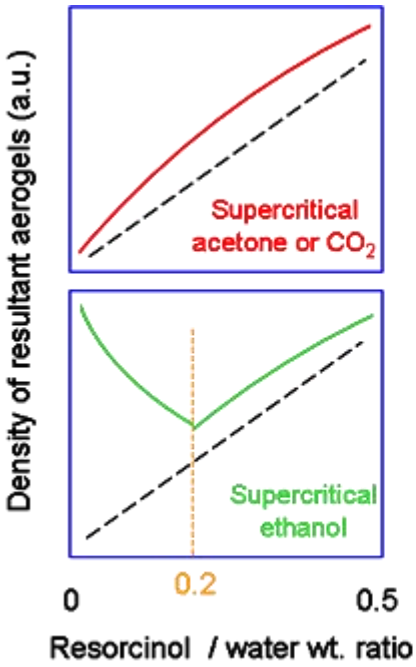

- First use of supercritical ethanol for preparing RF organic and carbon aerogels
- Exchanging water of RF hydrogels by acetone or ethanol has low effect on porosity
- Supercritical acetone and ethanol lead to similar materials only at low dilution
- At high dilution, acetone leads to much higher pore volumes than ethanol does
- Acetone is as good as CO_2 for supercritical drying of RF gels

Fig. 7: Résumé graphique et points forts du travail, tels que parus en ligne sur le site d'Elsevier. La ligne en tirets représente la densité calculée en l'absence de retrait au séchage.

Article n°3: **Charbons actifs bimodaux dérivés de cryogels RF**

En dépit de sa simplicité, l'activation chimique à l'acide orthophosphorique de cryogels à base de résine RF n'avait jamais été tentée. L'utilisation de tels précurseurs n'est pas fortuite. En effet, lors de la congélation du solvant, des cristallites très anisotropes de tert-butanol se forment, avec pour conséquence une modification assez considérable de la macroporosité. Les cryogels ne présentent ainsi pas de modification notable de surface spécifique ou même de volume mésoporeux, par rapport aux aérogels homologues, mais ont une macroporosité nettement plus développée. Grâce à cette caractéristique, on pouvait s'attendre à ce que l'activation chimique créé des micropores supplémentaires au sein d'une macroporosité déjà

largement ouverte. Le but était donc d'obtenir des charbons actifs à porosité clairement bimodale, avec une microporosité localisée à la surface de grands macropores (Fig. 8). L'intérêt de tels matériaux est d'éviter la limitation par la diffusion propre aux charbons actifs granulaires commerciaux, pour lesquels toute molécule à adsorber ou à transformer doit au préalable diffuser jusqu'au cœur des grains pour y rencontrer la microporosité. Avec les charbons ex-cryogels que nous avons préparé, ce phénomène est évité et on peut s'attendre à d'excellentes cinétiques d'adsorption. Comme la résine RF précurseur est très pure, et que les charbons sont soigneusement lavés après synthèse, des matériaux sans cendres sont obtenus. Ils sont donc utilisables en tant que supports de catalyseur pour des réactions qui sont sensibles aux impuretés, ou comme électrodes de supercondensateurs. Ces applications n'ont toutefois pas pu être testées.

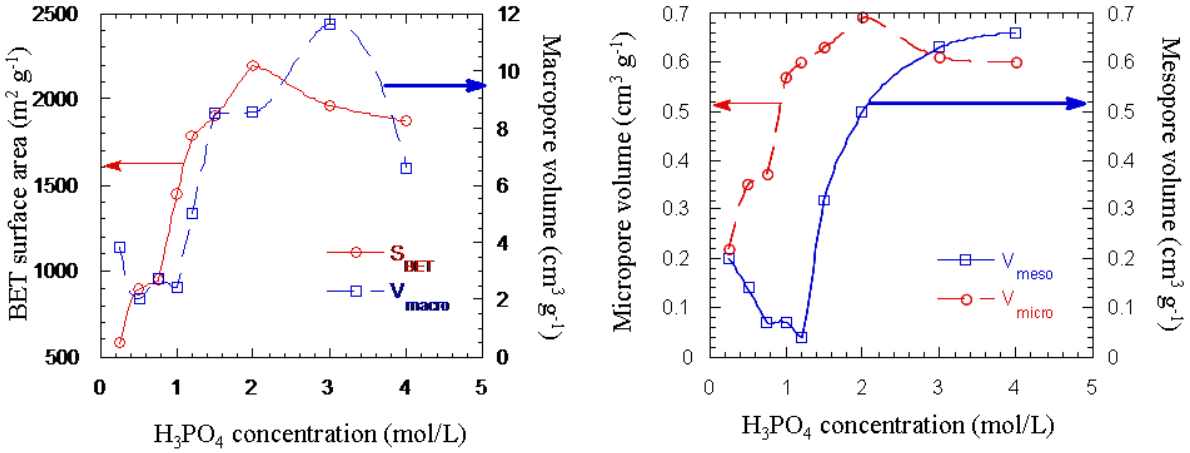

1.2 M ⇒ V_{macro} = 5 cm³/g; V_{meso} = 0.04 cm³/g; V_{micro} = 0.6 cm³/g ; BET = 1780 m²/g

2 M ⇒ V_{macro} = 8.5 cm³/g; V_{meso} = 0.5 cm³/g; V_{micro} = 0.7 cm³/g ; BET = 2195 m²/g

Fig. 8 : Surface spécifique et volumes poreux (macro, méso et micro) de charbons actifs dérivés de cryogels de carbone RF, en fonction de la concentration en acide phosphorique utilisée pour les préparer. L'échantillon préparé à 1.2M est clairement bimodal (mésoporosité ≈ nulle), alors que celui préparé à 2M présente une surface spécifique record pour ce type de matériau.

Nous avons ensuite travaillé à préparer des gels de carbone bon marché en sélectionnant à la fois un précurseur et un mode de séchage moins onéreux. Une résine phénol-formaldéhyde (PF) a ainsi été choisie et préparée, puis gélifiée dans un mélange eau/méthanol, lyophilisée et finalement carbonisée (article n°4 de ce mémoire). Outre les analyses de porosité classique, ces matériaux ont été caractérisés en tant qu'électrodes de supercondensateur. Contrairement à ce qui a été trouvé dans de nombreux autres matériaux, les meilleures capacités de stockage ont été obtenues avec les échantillons présentant la plus faible surface spécifique. Nous avons

pu l'expliquer sur la base de la caractérisation de la porosité : les matériaux les plus performants sont ceux pour lesquels le pourcentage de mésopores est le plus grand et les micropores sont les plus larges, deux caractéristiques qui permettent une meilleure accessibilité de la surface carbonée aux ions de l'électrolyte.

Article n°4 : **Cryogels de carbone dérivés de résine phénol-formaldéhyde**

La résine PF est environ cinq fois moins chère que la résine RF, et permet également la synthèse de gels organiques précurseurs de gels de carbone. Les premiers cryogels de carbone PF ont ainsi été obtenus et caractérisés complètement par adsorption d'azote (77K), pycnométrie à l'hélium et au mercure, et porosimétrie au mercure (jusqu'à 4000 bars). Concernant cette dernière technique, les courbes brutes ont été retraitées en raison de l'écrasement partiel des échantillons soumis à la pression de mercure avant leur intrusion. Des distributions de taille de pores précises ont donc pu être obtenues.

Les échantillons finement caractérisés ont ensuite été pressés en pellets en présence d'un liant (PVDF) et de noir de carbone (pour améliorer la conductivité électrique), et testés dans un dispositif à trois électrodes. Les performances en stockage d'énergie électrochimique ont été testées par plusieurs techniques : voltammétrie cyclique (Fig. 9), charge/décharge galvanostatique, impédance complexe et auto-décharge. Les résultats obtenus par ces deux dernières techniques n'ont pas été publiés. Les électrolytes utilisés ont été H_2SO_4 4M et KOH 6M, et les électrodes ont été étudiées sous la forme d'un condensateur complet, mais aussi individuellement afin d'en observer les dissymétries. Là encore, pour que la publication ne soit pas trop longue, une partie des résultats (KOH et électrodes séparées) n'ont pu être joints.

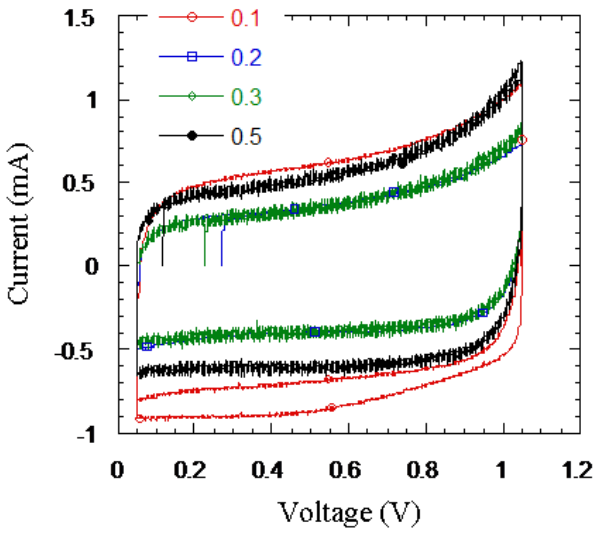

Fig. 9 : Courbes de voltammétrie cyclique à 2mV/s, pour différents rapports molaires P/F.

Nous avons montré comment la capacité est liée à la texture poreuse. Les pores plus étroits que 1 nm, principalement responsables de la valeur de surface spécifique, ne sont pas remplis par l'électrolyte, et ne participent donc pas au processus de stockage de charge. Aucune corrélation avec la surface spécifique n'a donc pu être observée, la capacité étant gouvernée par des pores plus larges. La Fig. 9 montre des voltammogrammes typiques, mettant en évidence le caractère capacitif idéal de ces matériaux (cycle rectangulaire sans pic rédox).

Ayant acquis de l'expérience dans la synthèse de gels RF, puis PF moins faciles à préparer, nous nous sommes ensuite intéressés à la réalisation de gels de tannins. Ces derniers avaient été utilisés depuis longtemps pour la préparation d'adhésifs « verts » pour le bois. Ils étaient donc potentiellement utilisables comme précurseurs d'authentiques gels organiques et donc de gels de carbone. Au même moment paraissaient en effet quelques rares articles relatant la synthèse de gels de carbone à partir du système tannin – furfural, et d'autres présentant des gels organiques tannin – formaldéhyde comme adsorbants en phase liquide. Il était donc grand temps pour nous d'étudier ces matériaux et de faire mieux que ce qui avait été publié. En effet, à la lecture de ces articles, les méthodes de synthèse nous ont paru assez inadaptées aux applications visées, et les performances rapportées en termes de capacité d'adsorption ou de texture poreuse étaient assez médiocres. Nous avons réalisé nos propres études en deux temps. Tout d'abord, sur la base des connaissances développées sur les adhésifs, nous nous sommes d'abord consacrés à préparer une résine mixte tannin – résorcinol – formaldéhyde (TRF). Une fois que le comportement des tannins a été bien compris, et nous avons pu voir que sa polymérisation était beaucoup plus délicate à contrôler que celle des résines utilisées jusqu'ici, nous avons réalisés des gels tannin – formaldéhyde (TF). Ces travaux ont fait l'objet de deux articles publiés en série, les parties I et II étant dédiées aux gels TF et TRF, respectivement (articles n°5 et 6 dans cette thèse).

Les tannins

Les tannins utilisés ont été extraits de mimosa (acacia noir : *Acacia mearnsii*, De Wild), un arbre à croissance rapide originaire d'Australie, et largement exploité dans plusieurs pays d'Afrique et au Brésil. C'est la principale source mondiale de tannins, ceux-ci représentant environ 30% en masse de matière sèche des écorces de l'arbre. Ces tannins constituent une ressource abondante (environ 220 000 tonnes/an), renouvelable et écologique dans la mesure où les arbres sont coupés après 10 ans et replantés. Les tannins sont extraits des écorces par

de l'eau circulant à contre-courant. Après enrichissement, la solution est atomisée, donnant les tannins sous forme d'une poudre fine.

Les tannins condensés dont il est question ici sont constitués par la répétition du monomère flavonoïde représenté en Figure 10. Chaque unité comporte deux anneaux phénoliques notés A et B. L'anneau A peut porter un ou deux groupements OH et s'appelle alors anneau résorcinol ou phloroglucinol, respectivement. L'anneau B peut en comporter deux ou trois, et s'appelle anneau catéchol ou pyrogallol, respectivement. Toute combinaison anneau A – anneau B est possible, conduisant à différents flavonoïdes avec différents noms et différentes réactivités. Le tannin de mimosa est majoritairement constitué de prorobinetinidine, une association d'anneau A résorcinol et d'anneau B pyrogallol. L'unité flavonoïde peut être répétée 2 à 11 fois, correspondant à un degré de polymérisation de 4 à 5. L'anneau A comporte des sites nucléophiles plus réactifs que ceux de l'anneau B et sa réactivité vis-à-vis du formaldéhyde est comparable à celle du résorcinol. En pratique, seul l'anneau A participe à la formation du réseau tridimensionnel.

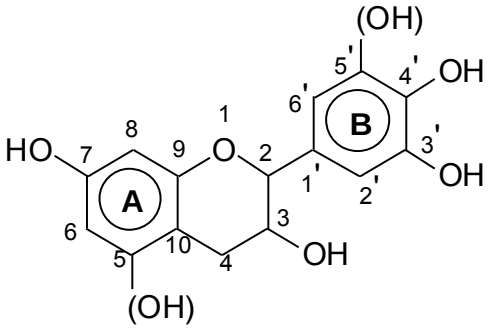

Fig. 10 : Structure chimique générale d'un flavonoïde et numérotation conventionnelle des atomes de chaque cycle. L'espèce majoritaire dans le tannin de mimosa ne possède pas de groupement OH en position 5, mais en comporte un en 5'.

Parce qu'ils ont une réactivité comparable à celle des molécules phénoliques synthétiques, onéreuses, non renouvelables et toxiques, les tannins condensés peuvent être utilisés comme substituts bon marché et écologiques pour différentes applications, comme nous avons pu le démontrer dans ce travail.

Pour des raisons de disponibilité des équipements, ce ne sont pas les mêmes types de gels qui ont été préparés : la résine TRF a été utilisée pour réaliser des cryogels de carbone, alors ce sont des aérogels qui ont été obtenus à partir de résine TF. Par conséquent, il n'est pas possible de comparer directement l'effet des résines sur la texture poreuse résultante, puisque le mode de séchage utilisé diffère, et on sait à quel point il change les résultats. Des travaux en cours, hors cette thèse, permettront d'approfondir ce point. Pour l'heure, des résultats très

intéressants ont néanmoins été obtenus ici. Tout d'abord, ce sont les premiers matériaux de leur catégorie à avoir été décrits. Dans le cas des aérogels TF, nous avons pu montrer qu'ils sont jusqu'à cinq fois moins chers à produire que leurs homologues RF. Il sera très difficile, sinon impossible, de faire mieux de ce point de vue. Tous ces matériaux présentent en outre des caractéristiques texturales qui ne permettent pas de les différencier des carbones dérivés de gels RF. On en attend donc des performances équivalentes, qui seront testées dans un futur proche.

Articles n°5 et 6 : **Aérogels et cryogels de carbone dérivés de résine TRF et TF**

Ces travaux ont indiscutablement montré la pertinence des tannins condensés comme précurseurs bon marché de gels de carbone, soit en mélange avec du résorcinol (gels TRF), soit seuls avec le formaldéhyde (gels TF). Des cryogels et des aérogels (par séchage dans l'acétone supercritique) ont pu être préparés et complètement caractérisés. Des textures poreuses bien plus diversifiées que ce que permettent les traditionnelles formulations RF ont pu être obtenues. Cette diversité est notamment due à la large plage de pH explorée que n'autorise pas la seule résine RF. Les Fig. 11 et 12 ci-dessous résument graphiquement les principaux résultats et points ports.

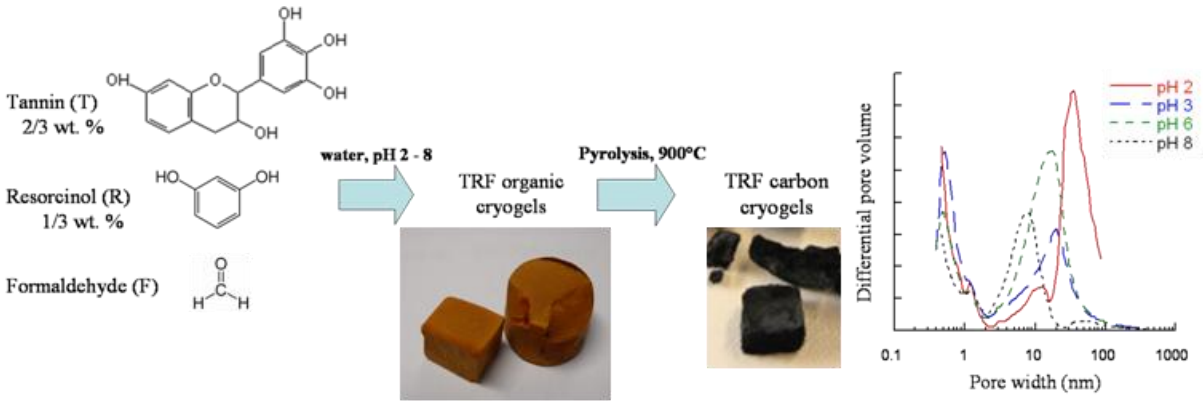

2/3 du résorcinol a été remplacé par du tannin pour préparer des cryogels de carbone à bas coût. Le tannin permet la gélation à des pH très différents, conduisant à des structures poreuses elles aussi très différentes. A pH ≤ 5, les surfaces spécifiques et les volumes de pores sont aussi élevés que ceux d'aérogels de carbone typiques dérivés de résine RF.

- 2/3 of resorcinol (R) was replaced by tannin (T) for preparing solid gels
- Low cost carbon gels were obtained from T-R-formaldehyde (F) cryogels
- Tannin allowed using an extended range of pHs during synthesis
- Due to so different pHs, very different pore structures were obtained
- At pH ≤ 5, surface areas and pore volumes are typical of costly R-F carbon aerogels

Fig. 11: Résumé graphique et points forts de l'article portant sur les cryogels de carbone TRF, tels que parus en ligne sur le site d'Elsevier.

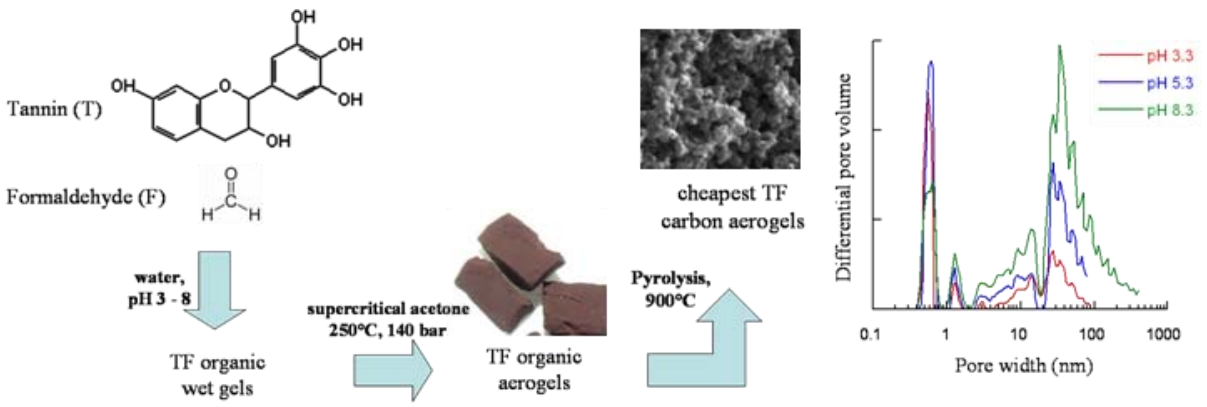

Des gels de tannin - formaldehyde (TF) préparés à différents pH et séchés par de l'acétone supercritique ont donné des aérogels de carbone très bon marché, cinq fois moins chers que leurs homologues RF, et présentant différentes fractions de mésopores. A pH 4-5, les surfaces spécifiques et les volumes poreux sont typiques de ceux des très onéreux aérogels de carbone RF.

- Formaldehyde (F) was shown to induce gelation of tannins (T) at different pHs
- Drying TF gels with supercritical acetone and pyrolysis led to carbon aerogels
- Different synthesis pHs led to mesopore fractions within the range 57 – 78 %
- Surface areas and pore volumes were as high as those of most other carbon aerogels
- TF carbon aerogels are five times cheaper than those made from resorcinol

Fig. 12: Figure équivalente à la Fig. 11, mais pour les aérogels de carbone TF.

Au moment même où ces synthèses de gels de carbone TRF et TF étaient réalisés, il nous a semblé intéressant d'étudier par spectrométrie MALDI-ToF leurs précurseurs organiques. En effet, cette technique qui permet d'identifier les oligomères présents dans un matériau solide, est à même de mettre à jour certains mécanismes réactionnels responsable de l'apparition de ces espèces chimiques. Dans le cas des résines TRF et TF, ce type d'étude n'avait jamais été réalisé, en particulier lorsqu'elles sont gélifiées dans les conditions qui président à l'obtention de matériaux hautement poreux. Deux articles (n° 7 et 8 de cette thèse) ont ainsi été produits.

Articles n°7 et 8 : **Identification des oligomères dans les gels TF et TRF**

Ce travail permet de revenir à la thématique « adhésifs » à partir des gels dont ils étaient initialement issus, tout en posant des questions d'intérêt académique. Que se passe-t-il dans le mélange TRF : le tannin coexiste-t-il avec la résine RF, ou réagit-il avec le formaldéhyde en même temps que le résorcinol ? Comment le tannin réagit-il avec le formaldéhyde dans les gels TF ? Ces questions ont trouvé réponse par l'analyse en spectrométrie MALDI-ToF des gels organiques qui ont été préparés à différents pH, et utilisés comme précurseurs des gels de carbone TRF et TF rapportés dans les articles n°5 et 6 précédents.

Dans le cas des gels TRF, l'existence d'oligomères mixtes en proportions non négligeables mais dépendantes du pH a été démontrée pour la première fois. Les pH de faible réactivité avec le formaldéhyde (pH 4 – 5) favorisent la formation d'oligomères mixtes (Fig. 13). Les oligomères RF restent toutefois prépondérants, en particulier aux pH acides et basiques, les adhésifs étant préparés à pH alcalin : 8 – 9.

Dans le cas de gels TF obtenus à pH 6, les oligomères de flavonoïde sont de faible poids moléculaire. Leur structure met en évidence à la fois des ponts méthylène formés par réaction du tannin avec le formaldéhyde, et des flavonoïdes auto-condensés. Les deux types de réaction coexistent donc. Pour la première fois à un tel pH, la participation de l'anneau B du flavonoïde aux réactions avec le formaldéhyde a été observée, probablement liée aux temps de gels très long, plusieurs jours, ayant conduit à la formation du solide.

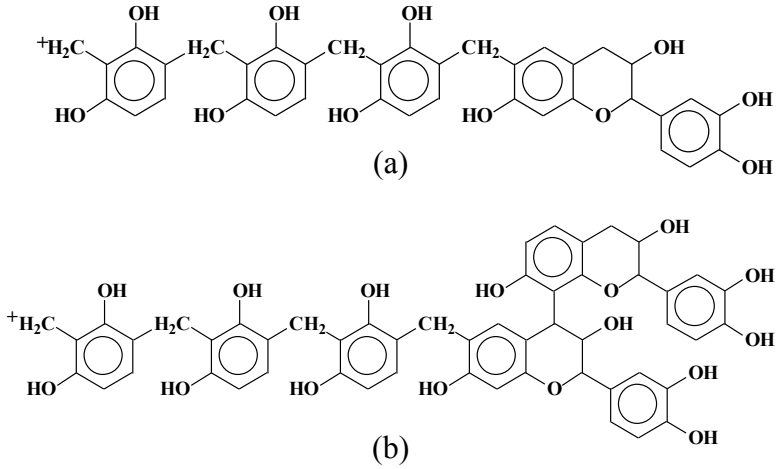

Fig. 13 : Exemples de structure possible d'oligomères mixtes détectés dans les gels organiques TRF : oligomères RF ayant réagi avec du tannin : (a) monomère ; (b) dimère.

En conclusion, cette thèse a permis dans une large mesure de sortir du schéma habituel : précurseur de gels de carbone = résine RF, et de proposer de nouvelles résines capables de gélifier en milieu solvant dilué. Des matériaux très différents : xérogels (non présentés ici pour cause de caractérisation incomplète), aérogels et xérogels, organiques et carbonés, ont pu être préparés. L'objectif initial de réduire les coûts de production des gels de carbone a été largement atteint, soit au travers de l'utilisation de précurseurs moins chers que le résorcinol, soit au travers de méthodes de séchage moins onéreuses, ne mettant pas en jeu de CO_2 supercritique, soit des deux. En particulier, les aérogels de carbone dérivés de tannin – formaldéhyde, séchés dans de l'acétone supercritique, se sont révélés au moins cinq moins chers que leurs homologues RF séchés dans du CO_2 supercritique. Tous les matériaux

préparés ont présenté des caractéristiques texturales au moins équivalentes aux gels de carbone RF, démontrant ainsi tout leur intérêt dans les applications habituellement suggérées pour de tels matériaux : adsorption, catalyse, isolation thermique, stockage électrochimique.

Les résultats obtenus au cours de ces trois ans vont bien au-delà des publications jointes à ce manuscrit. En effet, pour les obtenir, de nombreux tests, montages, mesures, ont dû être réalisés qui, au final, n'auront pas été décrits ici. Dans un mémoire de présentation plus classique, ces détails auraient été donnés, mais nous avons choisi de présenter les publications issues de cette thèse. Elles reflètent donc déjà un travail de synthèse et ne présentent que les résultats les plus marquants et les plus novateurs. Pour certaines de ces publications, éditeurs et reviewers ont même souhaité éliminer des parties afin de toujours réduire la longueur des articles. C'est ainsi, par exemple, que des spectres RMN et FTIR présentant l'évolution des échantillons de gels à différentes températures intermédiaires, ainsi que leurs interprétations correspondantes, ont été supprimés. Il en est de même de certains essais mécaniques dont, par contre, nous avons souhaité rapporter quelques résultats ci-dessous.

Exemples de propriétés mécaniques de gels de carbone

Compte tenu de leur faible taille (cf. ci-dessous) et de leurs dimensions parfois irrégulières, les résultats suivants ont été obtenus en retraitant les résultats du porosimètre au mercure, utilisé dans une gamme de pression pour laquelle aucune intrusion n'a lieu. Ces données concernent des cryogels de carbone dérivés de résine tannin – résorcinol – formaldéhyde. En absence d'intrusion, les dimensions des échantillons ont été mesurées avant et après l'expérience, de manière à déterminer le retrait induit par la pression hydrostatique de mercure. Les résultats suggèrent que les matériaux deviennent linéairement plus compressibles quand le pH de départ augmente (Fig. 14). Le module de compressibilité K, représenté aussi en Fig. 14, a été déterminé selon :

$$K = -V_0 \frac{\partial P}{\partial V}$$

où V_0 and V sont les volumes de l'échantillon avant et après application de la pression hydrostatique P, respectivement. A une exception près, K augmente avec la densité comme on pouvait s'y attendre.

Si on représente K en fonction de la densité apparente ρ_b dans un graphe double-log (non figuré ici), la loi de puissance suivante est observée :

$$K = K_0 \rho_b^{\,n}$$

dans laquelle l'exposant *n* vaut 3.5. Cette valeur est en très bon accord avec celle, 3.6, obtenue pour la compression élastique de gels de carbone et de silice[2,3].

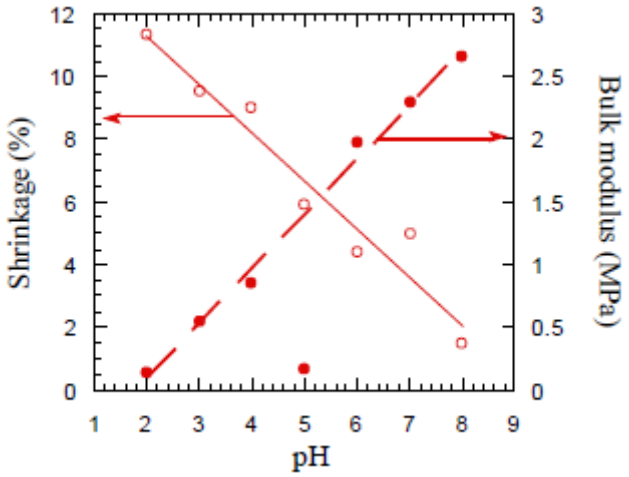

Fig. 14: Retrait de cryogels de carbone TRF soumis à une pression hydrostatique de mercure (cercles vides), et module de compressibilité correspondant (cercles pleins).

Le module élastique, *E*, des cryogels de carbone a aussi été calculé à partir de l'équation suivante:

$$E = 3K(1-2\nu)$$

dans laquelle le coefficient de Poisson, ν, a été pris égal à 0.2[3]. Nous avons ainsi obtenu des valeurs très proches de celles déjà publiées pour des aérogels de carbone RF, c'est-à-dire comprises entre 0.1 et 10 MPa, selon la densité des échantillons[2].

Dans leurs conditions actuelles de préparation, les échantillons obtenus sont de petite taille. Ce sont typiquement des cylindres de 1 cm de diamètre et de 1 cm de long, tout au plus. Ces dimensions sont idéales pour tester leurs propriétés catalytiques, études qui n'ont démarré que récemment, et leurs propriétés électrochimiques, jugées très prometteuses. Néanmoins, seuls quelques tests mécaniques ont été obtenus, et n'ont pas été publiés pour les raisons précisées plus haut. La conductivité thermique a été mesurée pour un petit nombre d'échantillons. Comme on pouvait s'y attendre, les matériaux sont isolants, mais moins que prévu. Néanmoins, ces résultats peuvent être mis en doute en raison des faibles dimensions des échantillons. Par conséquent, l'imprécision était telle que nous préférons refaire des matériaux de plus grandes dimensions avant de juger de l'intérêt de ces nouveaux matériaux en tant qu'isolants thermiques.

---

[2] V. Bock, A. Emmerling; J. Fricke. Influence of monomer and catalyst concentration on RF and carbon aerogel structure. J. Non-Cryst Solids 225 (1998) 69-73

[3] G.W. Scherer, D.M. Smith, X. Qiu, J.M. Anderson. Compression of aerogels.J Non-Cryst Solids 186 (1995) 316-320

Enfin, de nombreuses autres formulations n'ont pu être étudiées au cours de ces trois années, alors que d'autres précurseurs possibles ont bien été essayés, mais sur la base de quelques échantillons seulement. Aucune étude systématique complète autre que celles publiées jusqu'à présent et rapportées dans ce mémoire n'a donc pu aboutir. Cependant, des voies ont été ouvertes, et toutes ces nouvelles pistes sont d'ores et déjà explorées dans une seconde thèse, qui fait suite à celle-ci. Nous venons par ailleurs d'acquérir un sécheur automatique à CO_2 supercritique, qui nous servira de référence et grâce auquel les conditions de séchage que nous avons mis au point pourront être comparées. En outre, les nouveaux gels – comme ceux présentés ici – peuvent être fonctionnalisés à l'état organique comme à l'état carbone, avec différentes applications envisageables en catalyse. Ces matériaux peuvent aussi être activés, donnant autant de charbons actifs. Il reste donc de nombreuses années de travail sur cette vaste thématique des gels solides.

Chapitre 1 : Generalities about gels

1.1 Definitions and chemical background

In the literature, gels are described as three-dimensional networks of particles gathered in chains and immersed in a solution [1-4], but this is not the only one definition. According to the definition proposed by Henisch [1], a gel is a "two-component system of semisolid nature, rich in liquid". The drawback of such a definition is its inadequacy for certain types of gels, e.g. silica gels. The other definition of gels, proposed by Brinker and Scherer [2], is that gels are materials consisting of a continuous solid phase and a continuous liquid phase, both of colloidal dimensions. In other words, the gel comprises a continuous solid skeleton, consisting of chains of molecules arranged in pearl necklace structure, immersed in a continuous liquid phase. Continuity of the solid phase ensures the flexibility of gels.

The precursor molecule first undergoes hydrolysis and, depending on the amount of water and catalyst, hydrolysis may be achieved completely or not, leading to polymer chains. The latter then cross-link with each other to form a sol, i.e. a suspension of very small solid particles or polymer chains. Partially hydrolyzed particles can next assemble together through a condensation reaction. According to its definition, condensation releases small molecules such as water or alcohol. When the reaction progresses, increasingly larger particles are built. If the monomer is able to create more than two bonds, the polymerization reaction can proceed without interruption. Finally, a giant molecule of macroscopic size is formed, pervading the entire volume of the solution, and called a gel [2].

The moment at which the last bond required for forming a connected path throughout the sample volume appears is called the gel point. However, polycondensation reactions don't stop at this point. The incipient network is very tenuous, thus flexible, and different network segments can still move relatively close to each other, helping further polycondensation. It is known that such gel coexists with sol particles and smaller polymers chains, not yet connected to the network [1 – 5]. It means that fresh gels need to be aged, e.g., be treated at moderate temperature for a few days after gelation to complete the reactions. Additionally, aging significantly improves the mechanical properties of the gel. The general scheme of the sol-gel process is shown in figure 1.

Gels can also be created from particulate sols, especially when attractive dispersion forces make the particles stick together, thus forming the network.

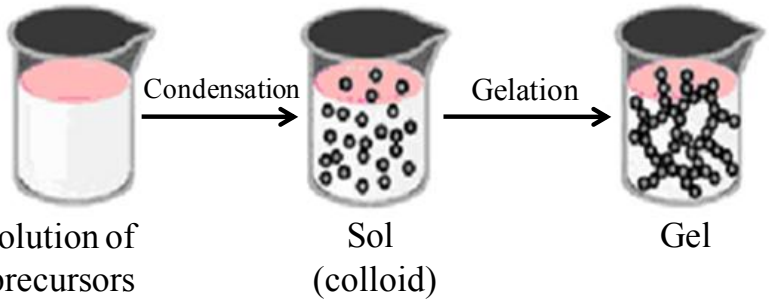

Fig. 1. Sol – gel polycondensation reaction.

Depending on the type of bonds formed in the gelation process, we can distinguish chemical gels in which covalent bonds prevail, and physical gels based on short-range van der Waals bonds, hydrogen bonds, electrostatic bonds, or entangled polymer chains. Jelly and aspic are typical examples of physical gels. Gelation may be reversible as in the case of physical gels, or not (chemical gels) [2].

1.2 Precursors of organic and carbon gels

The aforementioned sol-gel reactions have been used in the present work for preparing new gels. For that purpose, different synthetic, semi – synthetic and natural precursors are presented below and shown in figure 2. These are resorcinol, phenol and wattle (mimosa) tannin. Once organic gels are formed from such precursors, pyrolysis in inert atmosphere leads to carbon gels.

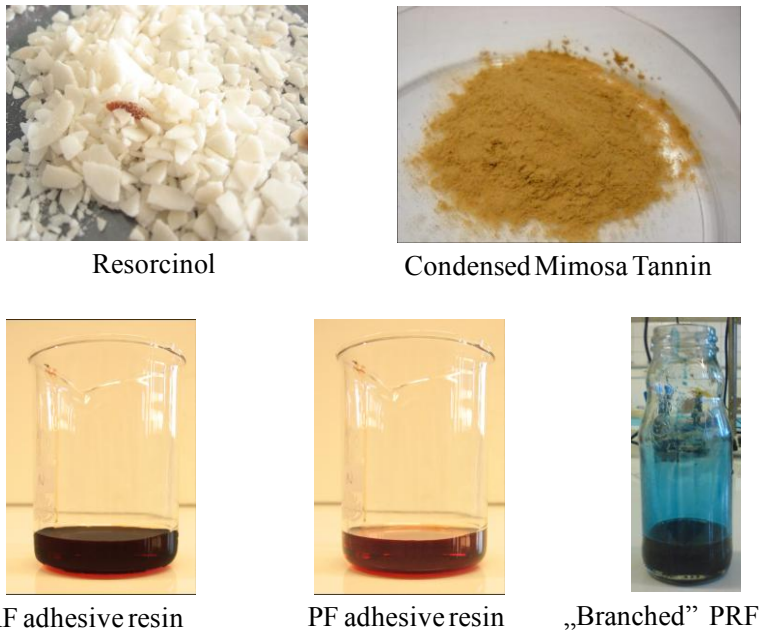

Fig. 2. Precursors of organic and carbon gels.

1.2.1 Resorcinol

The first and best known group of organic gels is RF gels. They are formed by polycondensation of resorcinol (R) with formaldehyde (F) in aqueous solution, using most of times Na_2CO_3 as a catalyst [6 – 11]. Resorcinol was selected as the gel precursor, because of its ability to react with formaldehyde at low temperatures and forming nice, reproducible, elastic gels. In suitable concentration conditions, gelation can take place at room temperature.

Resorcinol molecule has three sites capable of forming bonds, shown in positions 2, 4 and 6 in Figure 3. It is known that resorcinol is 10 - 15 times more reactive than phenol. Polycondensation reaction of resorcinol with formaldehyde may occur in both acidic and alkaline conditions, leading to a mixture of products from addition and condensation reactions. Reaction of resorcinol with formaldehyde in the presence of basic catalyst, often Na_2CO_3, leads to hydroxymethyl derivatives of resorcinol, which are next condensed to form methylene- and methylene ether-bridged compounds. The last step is disproportionation of methylene bridges plus formaldehyde as by-products [11].

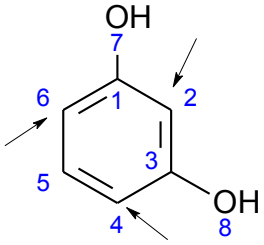

Fig. 3. Reactive sites of resorcinol.

In the case of acetic conditions of polycondensation reaction, methylene and benzylether bridges are formed, which next build a chemically cross-linked gel structure. Gelation of the initial solution occurs at elevated temperatures that accelerate the formation of the solid and increase the efficiency of the aging process [11, 12].

The main characteristics of gels, e.g. density, textural and surface properties, can be designed by changing three main parameters [8, 9, 12 ,13], which are:

- the resorcinol / catalyst molar ratio (pH),
- the resorcinol / water weight ratio (concentration of reactants, or dilution),
- the conditions of drying, by which porosity is created (see next chapter).

Sol-gel polycondensation reactions of resorcinol with formaldehyde are presented in figure 4, using Na_2CO_3 as catalyst.

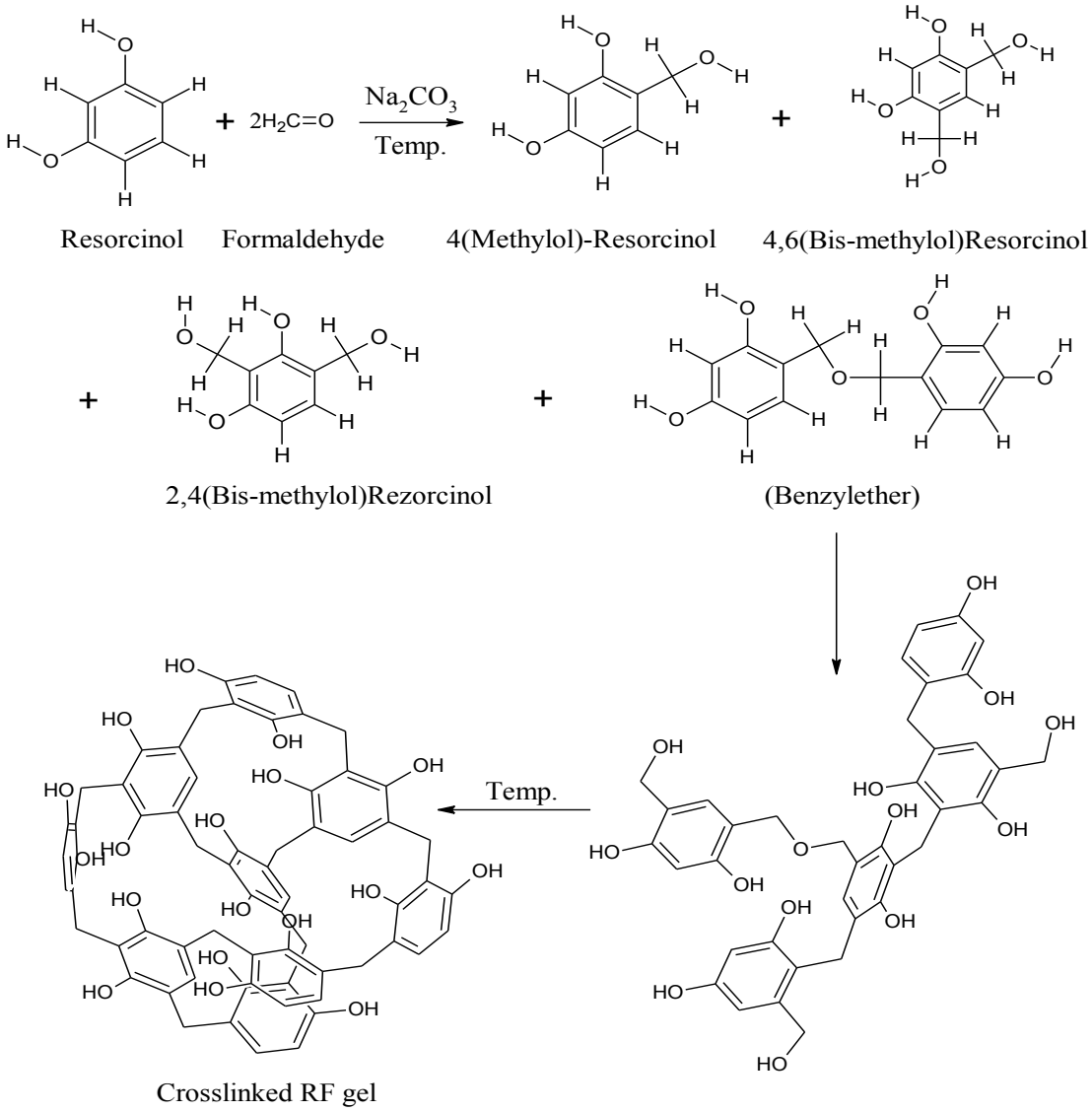

Fig. 4. Reactions of gelation and crosslinking in Resorcinol-Formaldehyde gels [11].

Resorcinol is the most common precursor in sol-gel processing of organic gels. The latter have excellent properties and can be used in many different applications, especially for their derived carbon gels (see chapter 4). However, resorcinol is one of the most expensive resins, so cheaper alternatives would be of high interest. For instance, phenol and tannin are typically 5 and 30 times cheaper than resorcinol [14].

One of the aims of our work was finding substitutes to resorcinol that would provide similar properties but at significantly lower production costs. Several precursors used in our laboratory are described below.

1.2.2 Condensed Mimosa tannin

Condensed tannins are based on nontoxic flavonoids of vegetable origin. They are mainly used for leatherwork but are also known in other fields of industry, e.g. in food industry and for manufacturing various kinds of adhesive resins used in the production of panels and particleboards [15 - 17]. They can also be used for producing rigid, insulating foams [18], and we have shown that they can also been suitable precursors in sol – gel polycondensation reactions [14,19 - 23]. The great advantages of tannins are their high availability, constant quality from the industrial extraction process, and low cost, around 1 euro per kg. On the other hand, the presence of aromatic rings bearing hydroxyl groups, having reactivity similar to synthetic and more expensive phenol and resorcinol molecules, is a good indication to use condensed tannins for the same purposes.

Commercial tannins used as gel precursors are sold with 74% guaranteed condensed tannins, and contain generally 80-82% actual phenolic flavonoid materials, 4-6% water, 1% amino acids, the remainder being monomeric and oligomeric carbohydrates derived from hemicelluloses. They are produced by spray-drying of aqueous Mimosa *(Acacia mearnsii,* formerly *Acacia mollissima* DeWild*)* barks extracts. Thus, fine, light brown, powder is obtained, consisting of flavonoid oligomers, from dimers to octamers. The predominant units are trimers and tetramers with molecular weights near 900 and 1180 Da, respectively [16].

In figure 5, the chemical structure of flavonoid units of condensed tannin is presented. Two aromatic rings are present. The first one, called A-ring, consists in one or two – OH groups, and is termed resorcinol (C7) or phloroglucinol (C5 and C7) ring, respectively. The second ring, called B-ring, can have two or three – OH groups, and is termed catechol (C3' and C4') or pyrogallol (C3', C4' and C5') ring, respectively. There is no limitation in combination of A and B rings, which leads to forming 4 different flavonoids having different names and different reactivities. The types of flavonoids are presented in table 1.

Table 1. Types of tannin flavonoids [16].

Ring A	Ring B	Flavonoid	Base element
Phloroglucinol	Pyrogallol	Prodelphinidin	Gallocatechin
Phloroglucinol	Catechol	Procyanidin	Catechin
Resorcinol	Pyrogallol	Prorobinetinidin	Robinetinidol
Resorcinol	Catechol	Profisetinidin	Fisetinidol

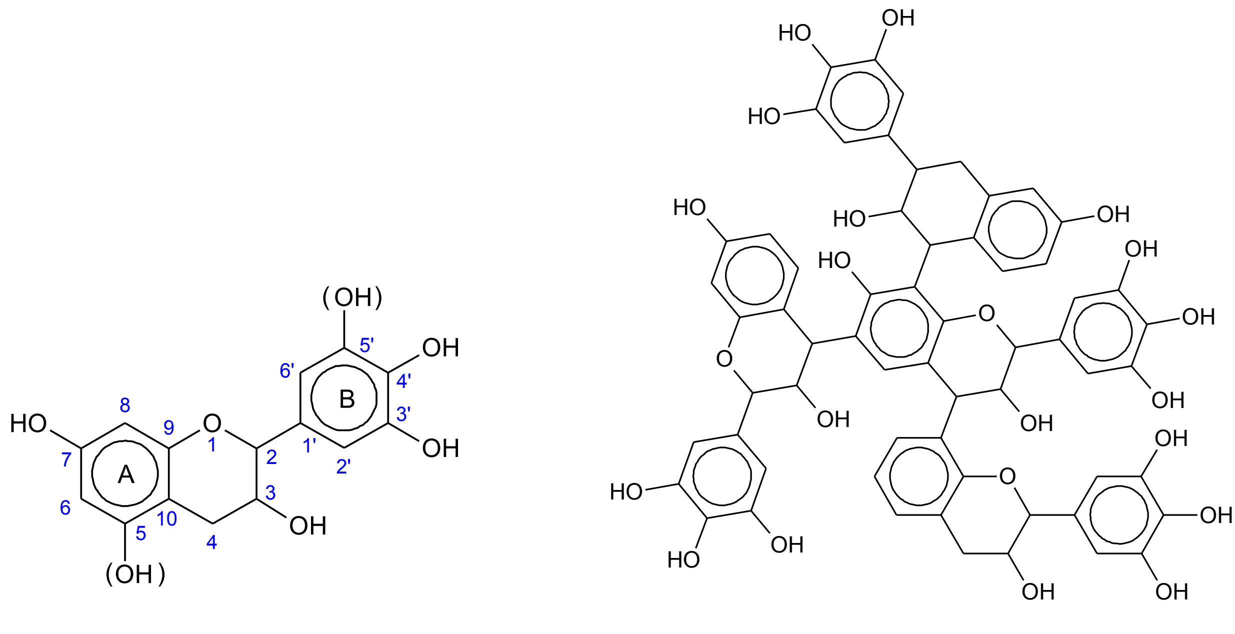

a) b)

Fig. 5. a) Chemical structure of a flavonoid monomer and usual atom numbering. b) Example of the cross-linked structure of four flavonoid tannins [16].

In the case of condensed tannins obtained from Mimosa bark extracts, the main component is prorobinetinidin, which is composed of resorcinol A – ring and pyrogallol B – ring. Such compound thus contains 5 hydroxyl groups. Prorobinetinidin represents about 70% of the total content of tannins in the extract from mimosa bark. The second most common component of condensed mimosa tannins is profisenidin, which is a combination of resorcinol A ring and catechol B ring; it represents 25% of tannins. Other components of the extract from the bark of Mimosa are "nontannins", which consist of carbohydrates, hydrocolloid gums, and small fractions of amino and imino acids. Hydrocolloid gum concentration ranges from 3 to 6% and has a significant effect on the viscosity in spite of its low concentration.

Knowing the frequency of phloroglucinol A – rings versus resorcinol A – rings allows determining the reactivity of tannins towards aldehydes and predicting the degree and quality of the resultant cross-linked compounds. In the case of B – ring, frequency of pyrogallol versus catechol affects the opening of the heterocyclic pyrane and specifies the type of arrangement in consideration of the structure in alkaline conditions.

Specific flavonoid units constituting tannin can be identified by ^{13}C NMR. However, the limitation of this method is the impossibility of distinguishing prodelphinidin from procyanidin on one hand, and prorobinetinidin from profisetinidin on the other hand. Nevertheless, comparison of (prodelphinidin + procyanidin) and (prorobinetinidin + profisetinidin) is possible. In condensed mimosa tannin, the repeating units (Fig. 5) are mostly 4, 6-linked and sometimes 4, 8-linked. Flavonoid units are repeated 2 – 10 times to produce

tannin with a number-average degree of polymerization of 4 – 5. In the first step of the condensation reaction, proanthocyanidin dimers sometimes called biflavonoids are formed.

Condensed mimosa tannins are natural phenolic compounds, so they react as phenol does, both in acidic and alkaline conditions. Increasing the pH increases the phenol nucleophilicity, especially at pH = 8, for which phenolic ions are created. Nucleophilic sites on A-ring of any flavonoid exhibit a greater reactivity than those of B-ring. This phenomenon is due to the nearness of hydroxyl groups, leading to activation of the whole B-ring without localization of reactivity, as it is in the case for A-ring.

Formaldehyde is the most commonly used aldehyde in the preparation, setting and hardening of tannin-based resins. It is also widely used as a cross-linking agent in the sol-gel polycondensation of most organic gels. The reaction of formaldehyde with tannin occurs through the creation of methylol bridges between reactive sites of flavonoids, mainly on A-ring and formaldehyde. In practice, only A-rings are involved in the formation of the three-dimensional network. Figure 6 shows the typical reactive sites of flavonoids on the A-ring. Formaldehyde can be connected in position 6 or 8 (depending on the type of tannin) of the flavonoids, or simultaneously in positions 6 and 8 for the larger units of flavonoids.

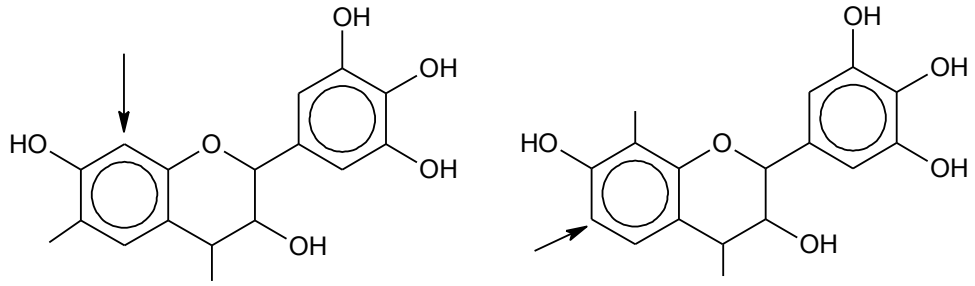

Fig. 6. Attachment sites of formaldehyde to flavonoids: a) resorcinol ring, b) phloroglucinol ring.

A – rings of condensed tannins present a reactivity with formaldehyde which is comparable or slightly lower than that of resorcinol. Assuming that the reactivity of phenol and resorcinol is 1 and 10, respectively, the A - ring is characterized by a reactivity of 8-9. However, molecular size and conformation of tannins cause that they can already not move at low degrees of polymerization with formaldehyde. Thus, possible reaction sites are quickly too far apart for building additional methylol bridges. Such behaviour leads to an incomplete polymerization which in turn weakens the reaction product. In the case of gels synthesis, this

problem can be ignored and is even favourable, since low density and high porosity are looked for.

Gels are prepared by sol-gel polycondensation of tannin with formaldehyde in aqueous solution with certain concentration of reactants, but mixtures of condensed Mimosa tannins with furfural have been first described in the literature. Tannin – formaldehyde (TF) gels can be prepared at different initial pH ranging from 3 to 10, and we have shown that pH has a great influence on textural and surface properties of dried and carbonized gels.

1.2.3 Tannin – Resorcinol – Formaldehyde resin

Tannin-Resorcinol-Formaldehyde (TRF) resins are used as cold – setting exterior-grade wood adhesives, mainly in the production of panels and particleboards [15 – 16]. They are synthesized by copolymerization of resorcinol with resorcinol A–ring polyflavonoids of condensed tannins. Several different compositions are known for these resins:

1) Grafting of Resorcinol on a Tannin-Formaldehyde resole

The synthesis of this type of resin consists in adding an aqueous solution of resorcinol to tannin–formaldehyde resole. Moreover, fusion reaction can be controlled by adding alcohol to the mixture of reactants, such as methanol. Alcohol stabilizes part of the formaldehyde attached to the compound, called hemiacetal [$CH_2(OH)(OCH_3)$]. Carrying out the reaction at elevated temperature causes the alcohol to be driven off at a fairly constant rate. The formaldehyde is thus gradually released from the hemiacetal. This treatment hinders the evaporation of formaldehyde when the reactants reach their reaction temperature, thus the pot-life of the resin is prolonged.

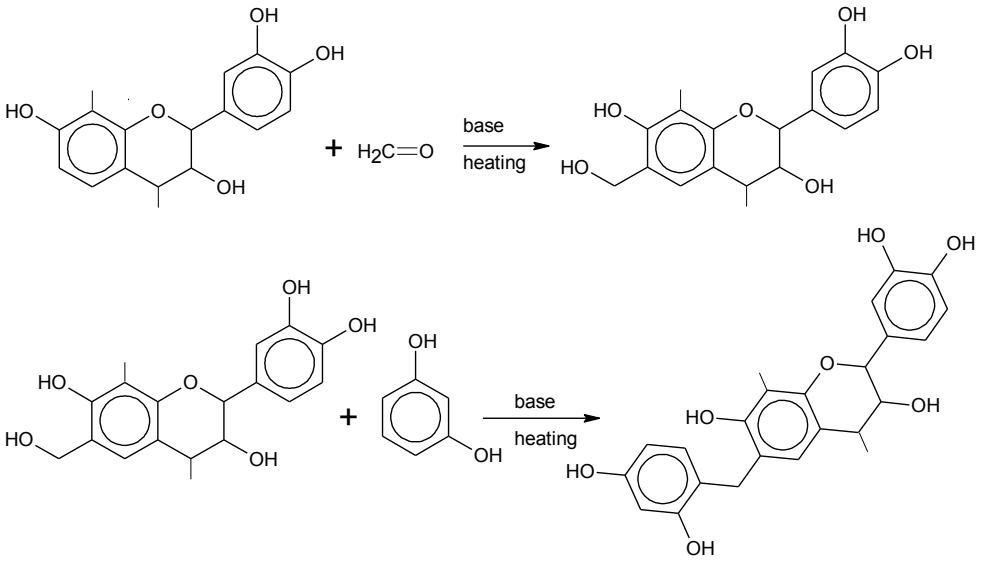

Fig. 7. Polycondensation of Tannin-Resorcinol-Formaldehyde adhesives [15].

2) Simultaneous synthesis of Resorcinol – Formaldehyde and Flavonoid – Formaldehyde condensates

In this type synthesis, Resorcinol, Tannin and Formaldehyde are mixed in an aqueous medium to obtain a homogeneous, brown, solution which is next heated up to the curing temperature. Reaction of polymerization is shown in figure 8.

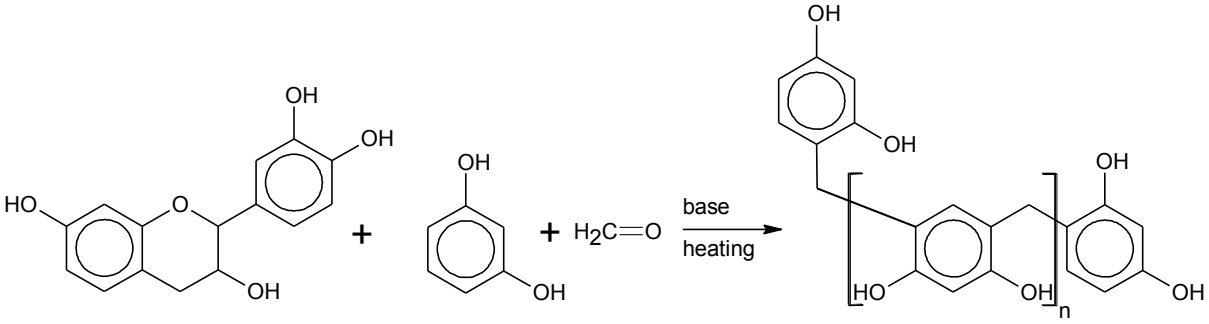

Fig. 8. Simultaneous polycondensation of Resorcinol – Formaldehyde and Flavonoid – Formaldehyde condensates [15].

In the case of gel preparation, both kinds of TRF adhesives can be used as precursors, but in our case only TRF adhesive resin prepared by simultaneous synthesis of Resorcinol – Formaldehyde and Flavonoid – Formaldehyde condensates was used. This resin was mixed in certain weight ratios with formaldehyde. The pH of the as-prepared solutions was adjusted from 2 to 10. In this way, two independent conditions of polycondensation were investigated: TRF/Formaldehyde weight ratio on one hand, and pH of initial mixture TRF/F on the other hand. The results show that changes of pH have an influence on density, textural and surface properties of dried and carbonized gels. The great advantage of such composition is the very short gelation time, which also depends on the pH of the initial solution, see figure 9.

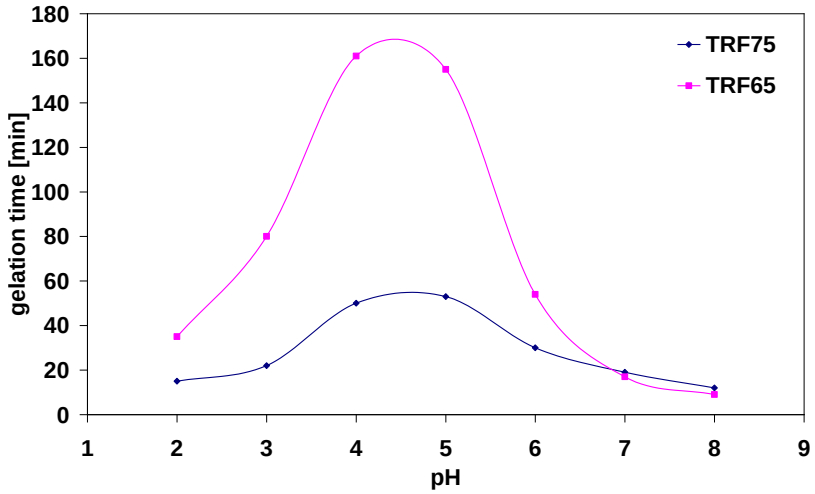

Fig. 9. Influence of the pH of the initial solution on the gelation time [14].

Gelation time varies from 10 to 50 minutes for samples TRF75, for which the concentration of formaldehyde as a cross-linking agent was higher than that of samples TRF65, which have gelation times ranging from 35 to 175 minutes. For both types of gels, the longest gelation time were obtained for pH 4-5. The same behaviour has already been reported in the literature. For example, Job et al. examined the influence of the initial pH of resorcinol-formaldehyde solutions on textural and porous properties [13]. In another paper, the highest gelation time of Resorcinol-Formaldehyde gels was also obtained for samples prepared at pH 4 [24]. These similarities arise from the presence of resorcinol in both types of gels. Benefits of gels prepared from TRF precursor are much shorter gelation time and lower amount of resorcinol, hence a lower production cost of organic and resultant carbon gels [14].

1.2.4 Phenol – Formaldehyde resin

Phenol-formaldehyde resins are polycondensation products of phenols with aldehydes, especially formaldehyde [16, 25]. In the industry, a wide range of different reaction products of polycondensation of phenol and its counterparts (cresols, xylenols, polyhydroxy phenols) with aqueous solutions of formaldehyde can be obtained. During synthesis of PF resins, oligomers whose molecular weights range from 1500 to 2000 Da are formed, and macromolecular compounds are formed directly in the moulding process. Oligomeric phenol-formaldehyde resins are used for the production of moulded, laminated materials, adhesives and coatings. Raw materials for the preparation of phenol-formaldehyde resins are, of course, phenol and formaldehyde, but other phenolic molecules are possibly used as well as furfural instead of formaldehyde. Through polycondensation reactions of phenols with aldehydes, both thermoplastic products (novolacs) as well as thermosetting products (resoles) can be formed. Key factors determining the structure and the properties of phenol-formaldehyde resins are [16, 25, 26]:

- Phenol functionality
- Phenol / formaldehyde molar ratio
- pH of the reaction

Phenols exhibit different functionalities depending on the number of hydrogen atoms capable of reacting with aldehydes. Figure 10 shows the main phenolic molecules and their functionality. Tri-functional phenols reacting with aldehydes can lead to both novolacs and resoles, whereas bi-functional phenols only lead to novolacs. Most important, only formaldehyde and furfural are able to lead to both resoles and novolacs. Other aldehydes, as a

result of their lower reactivity and inadequate conformation, can't produce resoles. Figure 11 shows the conditions in which resoles and novolacs can be formed [26].

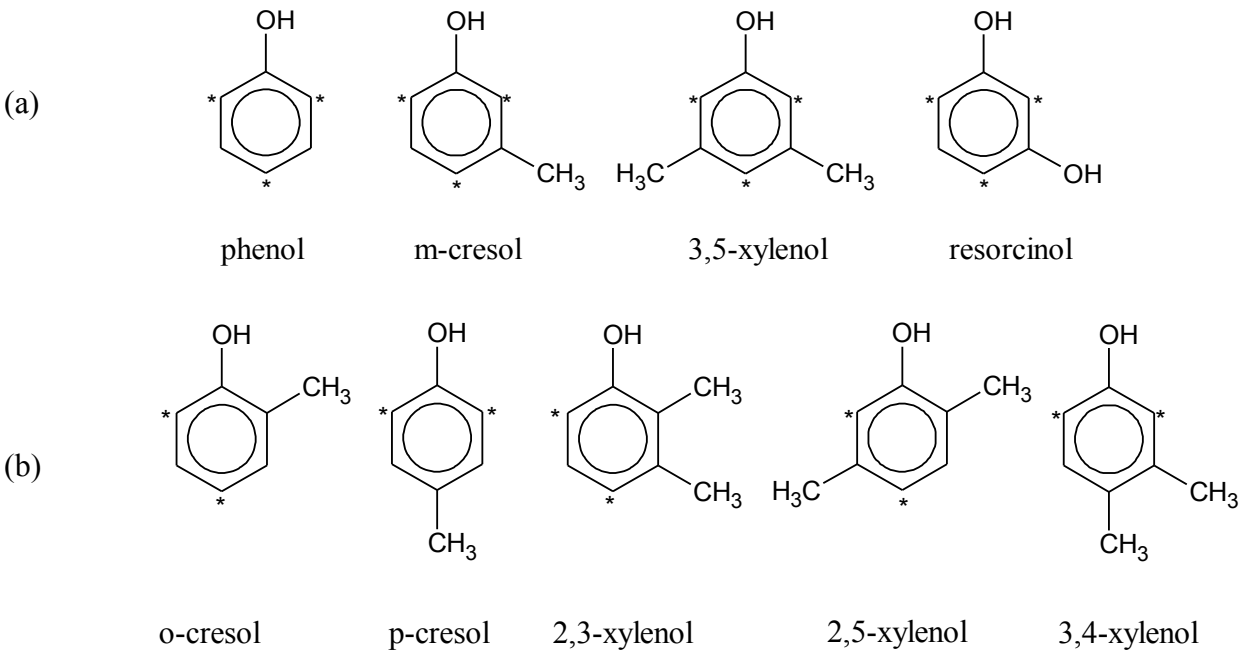

Fig. 10. (a) Tri-functional and (b) bi-functional phenols and their counterparts [26].

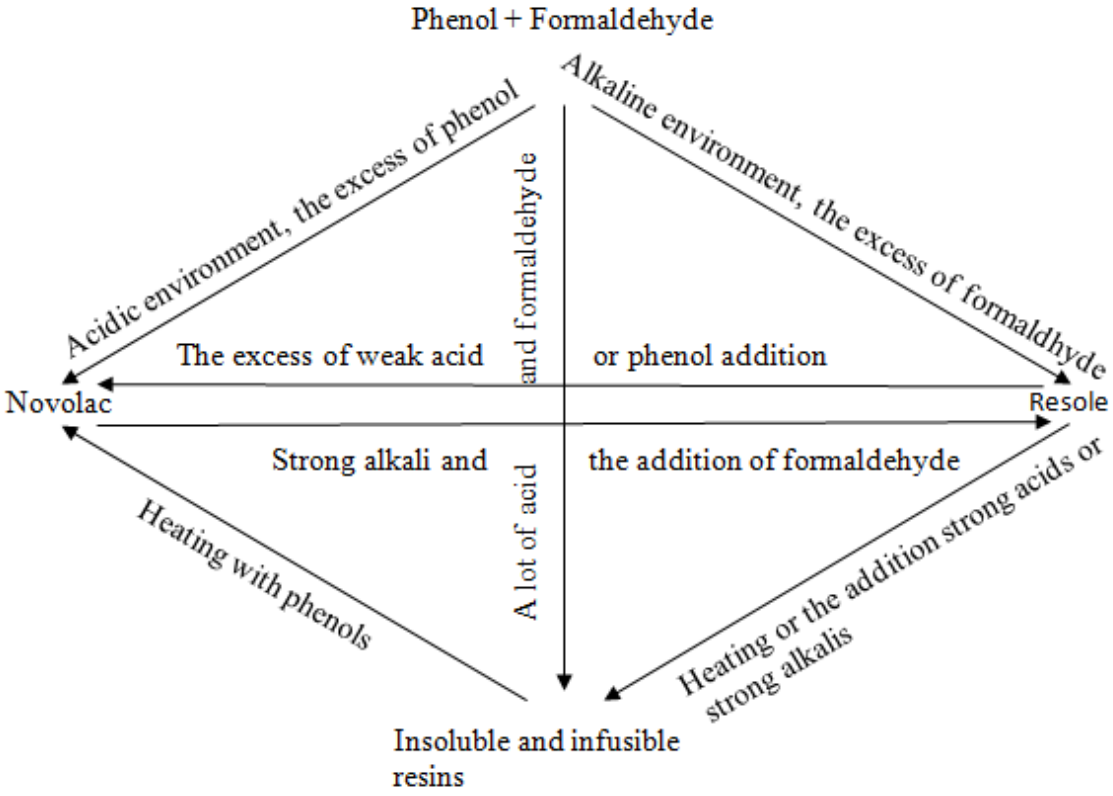

Fig. 11. Pathways of Phenol-Formaldehyde adhesives preparation [26].

Polycondensation of phenol with formaldehyde occurs through successive and parallel addition and condensation reactions. As a result of addition reactions, hydroxymethylphenols (methylphenols) are formed, which are the initial products of condensation of resoles and novolacs. Importantly, the addition reactions, which don't release by-products contrary to condensation reactions for which the by-product is water, are practically irreversible and can be carried out in aqueous solution.

Phenol - formaldehyde (PF) resins were already used in the past for the synthesis of organic gels. The most common gel precursors are novolacs PF resins using furfural as a cross-linking agent [27, 28]. Pekala [27], who first used this type of resin in the formation of organic gels, gave several reasons justifying its use as a precursor of organic gels and as an alternative to RF:

1) Time of process preparation of gels and dried gels can be reduced through the use of alcohol, like methanol, as a reaction environment of gelation. Thus, solvent exchange step may be omitted, and the gels can be dried immediately after gelation.
2) The price of the resin is relatively low compared to that of resorcinol.
3) Texture and surface of dried and carbonized gels are similar to those of other gels.

The main difference between gels prepared from novolac phenolic resin and from resorcinol, is the shape of their constitutive particles, looking irregular and somewhat flat in the case of PF dried gels.

Phenol-Formaldehyde resoles can also be used as a precursor of gels. In this case, PF resoles can be mixed with formaldehyde and furfural. The polycondensation of such resin with formaldehyde can be carried out in aqueous solution or in alcohol like methanol. The advantage of using alcohol as a solvent is reducing the gel preparation time since the solvent exchange step can be omitted, and samples can be dried in supercritical methanol.

We have shown [30] that carbon gels prepared from phenolic resole with formaldehyde have very good textural properties, e.g. BET surface area ranging from 300 to 600 m^2/g. These results are similar to other gels prepared from novolac resin, mimosa tannin and in some case from RF resins.

1.2.5 Phenol – Resorcinol – Formaldehyde adhesives

Phenol – Resorcinol – Formaldehyde (PRF) resins are known as cold-setting adhesives for wood. Similarly to the case of Tannin-Resorcinol-Formaldehyde and phenol resins, PRF is prepared by grafting the resorcinol to the active groups of poorly condensed methylol resoles that are the polycondensation products of phenol with formaldehyde [16, 31, 32]. The addition of resorcinol to phenol-formaldehyde resin ensures acceleration and improvement of cross-linking at room temperature. Resorcinol is also a component in the PRF resin that provides its characteristic cold-setting behaviour. Traditional PRF resins are prepared by polycondensation of phenol and formaldehyde in an alkaline environment. The reaction products are phenol-formaldehyde resoles having a linear structure. Resorcinol is usually added in excess to the methylol groups of PF resin, and then can be attached via methylol bridges to the backbone PF resin. PRF resin can be written schematically as follows:

$$\text{Resorcinol} - CH_2 - [\text{phenol} - CH_2]_n - \text{Resorcinol}$$

Each PF oligomers is terminated by resorcinol groups.

The main limitation of the use of these resins is the high production cost, given that resorcinol is an expensive chemical. Ways of reducing the content of resorcinol in the resin, while maintaining similar properties, were thus looked for. Using a branching agent in the liquid PRF resin during its preparation can help decreasing the content of resorcinol. Experiments showed that the increased branching in the resin solution during polycondensation resulted in a significant reduction in the resorcinol content without loss of properties of the traditional PRF resin. Introduction of a branching agent allows using only the half of resorcinol compared to traditional resins. Typical branching agents are melamine, urea, and aniline, whereas other substances also showed good properties for the same purpose.

If a molecule capable of branching (three or more effective sites with an aldehyde) is used during or after the PF resin preparation, a branched PF, and consequently a branched PRF resin, is formed. This reaction can be schematically presented as shown below [32]. Another result of the use of a branching agent is the significant increase in the degree of polymerization of the resins, which is associated to an increase of the viscosity of adhesives. PRF resins being used in a quite narrow range of viscosity, it is necessary to decrease the content of solids [31, 32]. Doing this further lowers the production costs while maintaining the resin properties.

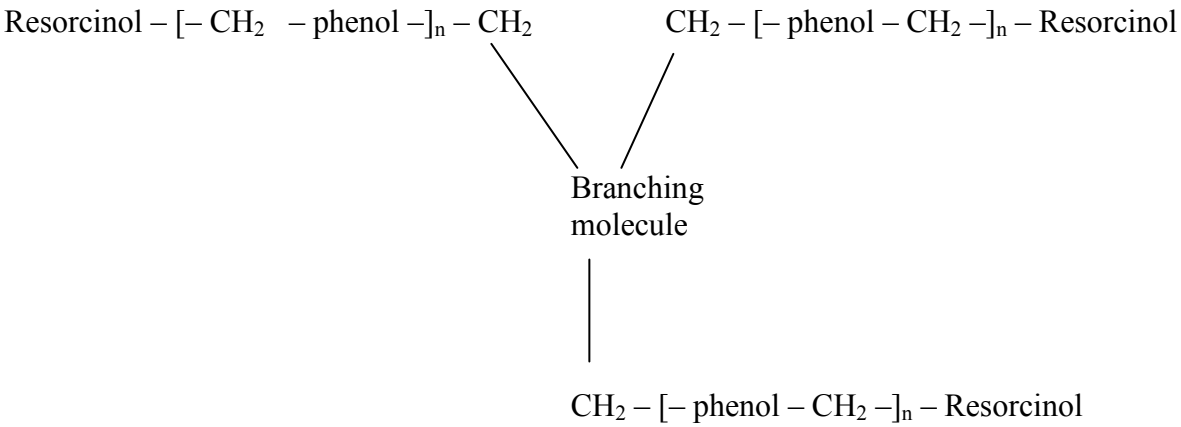

Additional studies have shown that the three-dimensional branching has very little impact on the properties of branched resins containing resorcinol. The mechanical resistance is only decreased by 8 - 9%. In practice, the urea that has been added cross-links PRF resin chains, not in three branching sites as shown above, but in only two points of the branching agent. In other words, most of the resin doubles its linear molecular weight and degree of polymerization. As a result, despite half of the resorcinol is present, good properties are maintained. Decreasing the content of the resorcinol is thus possible, but 90 - 100% of the polymer is still linear [31].

Urea-branched PRF resins were used as precursors in the production of organic gels. This resin has a characteristic dark blue colour and a very high viscosity, which can be very easily reduced by the addition of methanol or alcohol to the resin. Gels were prepared by polycondensation of furfural and PR resin, and methanol was used as reaction medium. The pH of the reaction mixture was fixed at appropriate values (8 – 10). Gelation took place at 85°C after several days. As a result, the gel lost the original blue colour of the resin and became black or brown, depending on the initial pH of the solution. These results are not described in the present manuscript, but the resultant carbon gels presented good textural properties, similar to those obtained with classical expensive RF precursors.

Chapitre 2: Drying of wet gels

In the first chapter, the typical precursors and their reactions with aldehydes leading to the formation of gels were discussed. As-prepared, wet, gels can only have applications in the liquid phase, e.g. adsorption or catalysis. Indeed, as soon as transferred to atmosphere, evaporation of the solvent trapped between the polymer chains begins. Therefore, formerly flexible and occasionally transparent gels become very hard, most of times broken and opaque solids. Drying is indeed one of the most important steps in the preparation of gels, crucial for their final physical, mechanical and porous properties. Due to capillary forces, which are extremely strong at the nanometre scale, spontaneous and uncontrolled drying can lead to cracks, and can destroy the structure of the porous gel. In order to avoid this and prepare materials whose pore structure is more or less maintained after removal of the solvent, other drying modes need to be considered, as shown in Fig. 12. Each way of drying has a different impact on the resultant pore structure of the dry material.

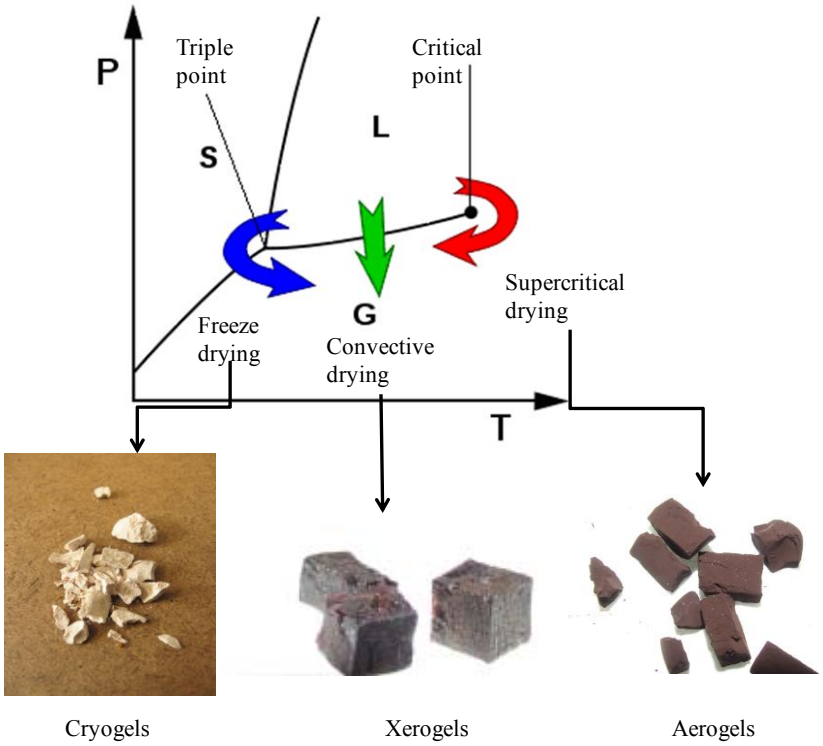

Fig. 12. Phase diagram of a solvent contained in the pores of a wet gels, different drying modes and related resultant materials.

Literature reports three main drying modes. Traditional, i.e. subcritical, drying under atmospheric conditions leads to the formation of xerogels. Such a drying can be carried out through different ways: evaporative, convective and even microwave drying. Supercritical drying leads to the formation of aerogels, whereas freeze-drying leads to cryogels.

2.1 Subcritical drying

According to Brinker and Scherer [2], the formation of xerogels can be decomposed into three main stages presented in figure 13 and described below.

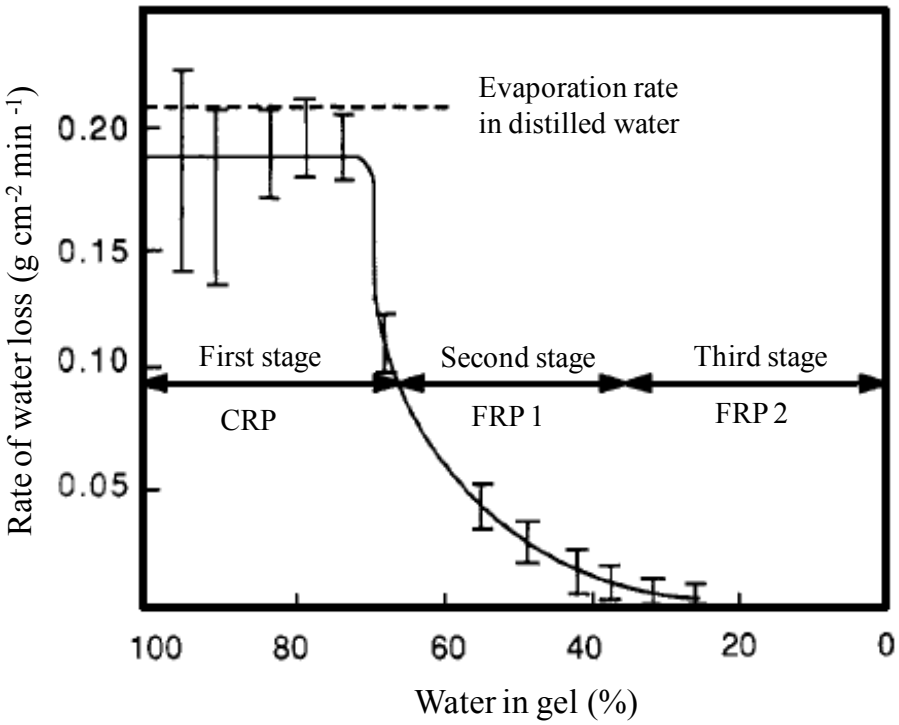

Fig. 13. Illustration of the three classical steps of subcritical drying [2].

2.1.1 Constant rate period (CRP), the first stage of drying

In the first stage, called constant rate period, the rate of evaporation per unit area of the drying body is independent of time [2, 3]. Researches carried out on alumina gels have shown that the rate of evaporation is similar to that in an open vessel filled with pure liquid. However, the rate of evaporation can differ slightly and depend on the texture of the drying solid surface. For example, gels built from grains and clusters have higher wetted area than gels having smooth surfaces, resulting in a correspondingly higher evaporation rate.

In figure 14, a typical illustration of the evaporation process is presented. The liquid creates a thin film at the surface of the solid. It has been proved that the chemical potential of the film is equal to the one beneath the concave meniscus. The reason of such phenomenon lies in the stability of liquid that could otherwise flow for balancing the potential. On the other hand, the surface of the gel is covered by a thin liquid film because, if drying took place at menisci only, shrinkage of the solid would decrease the rate of evaporation.

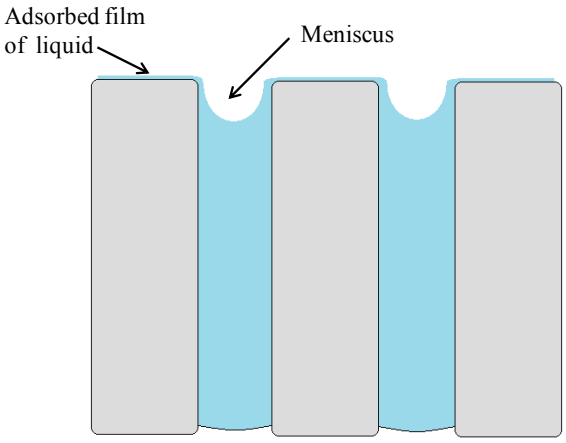

Fig.14. Illustration of meniscus creation at the outer surface of the pores.

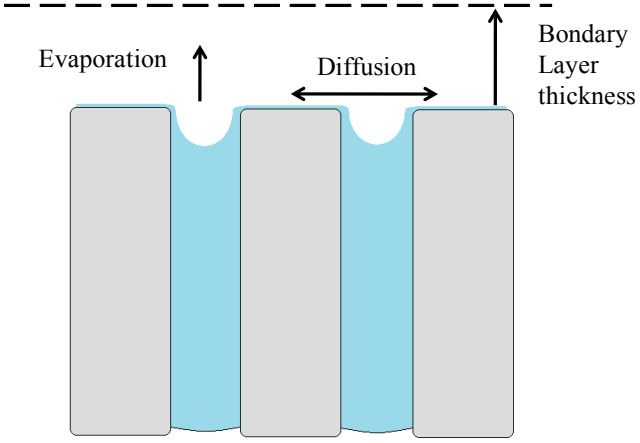

Fig. 15. Boundary layer at the equilibrium concentration of vapour.

It has been also proved that the evaporation rate can remain constant even if dry areas form at the surface of the solid during drying. Stagnant or slowly flowing boundary layer of vapour indeed exists at the solid surface. When the extent of such dry area is small compared to the thickness of the layer, diffusion parallel to the surface makes uniform the boundary layer at the equilibrium concentration of vapour [2,3]. This phenomenon is illustrated in figure 15.

As mentioned above, the liquid phase evaporates from the surface of the solid phase in the form of a thin film. The liquid remaining inside the pores flows along the pore walls in order to fill the newly exposed dry surface, but the liquid remaining after partial evaporation from the pores can't do so without developing concave menisci. According to eq. 1, pressure (P) in the liquid is related to the radius of curvature of the meniscus (r) and to the liquid – vapour interfacial energy (γ_{LV}) :

$$P = -2\frac{\gamma_{LV}}{r} \qquad (1)$$

In the case of cylindrical pores of radius *a*, the radius of curvature of the meniscus obeys equation 2:

$$r = -\frac{a}{\cos(\theta)} \qquad (2)$$

where θ is the contact angle. If the contact angle is equal to 90°, than the liquid doesn't wet the solid and the liquid – vapour interface is flat. This occurs because $r \rightarrow -\infty$, so P = 0. When the contact angle θ = 0°, than liquid completely covers the surface of the drying solid.

The solid phase is submitted to the pressure of the liquid, and more exactly to the suction of liquid (hence corresponding to a "negative pressure" [2]), inducing deformation and

shrinkage of the compliant network of gels, as pictured in figure 16. Such capillary forces don't need to be too large for drastically reducing the volume of the solid, the radius of the menisci being much larger than that of the pores.

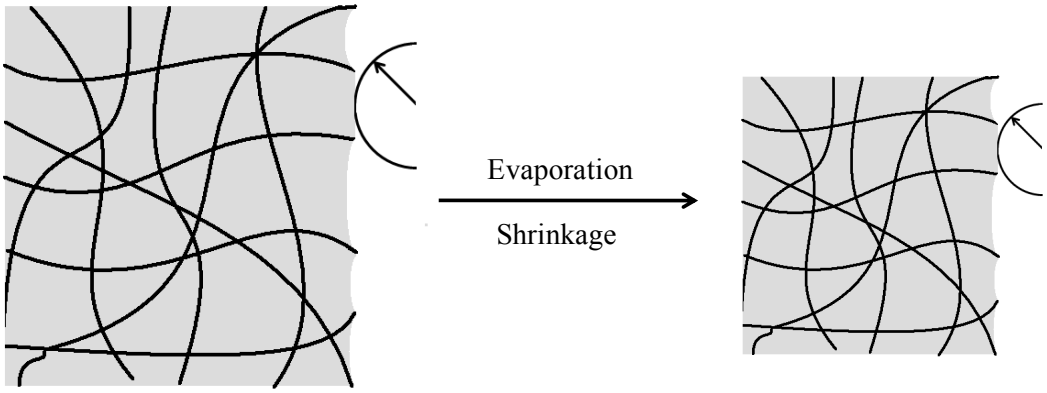

Fig. 16. Illustration of CRP, the first step of drying.

Progressive drying makes the polymer particles be closer to each other, leading to the formation of new bonds and increasing the cross-linking of the gel. As a result of this process, the network becomes stiffer and stronger. Other consequences are the decrease of the porosity and the corresponding increase of suction in the liquid. Finally, there is a moment at which the suction in the liquid reaches its maximum value when the radius of the menisci becomes equal to the radius of pores, which is equivalent to the completion of the first step of drying. Beyond this point called the *Critical point*, the suction in the liquid is not able to overcome the further stiffening of the network, leading to empty pores near the surface of the gel (see next subsection). In other words, the first step of drying induces a shrinkage which is equal to the evaporated volume of the liquid, during which the centre of the meniscus, whose radius decreases continuously, remains at the outer surface of the drying solid.

Although the first stage of drying is in the line with the classical theory of drying, it is adequate only for materials whose pores are wider than 20 nm. Hench and Wilson [3, 33, 34] have indeed demonstrated that, for materials with pores smaller than 20 nm, the kinetics of the first stage of drying decrease substantially, even though the meniscus remains at the surface as required by the definition of the CRP stage. These authors indicate that such differences are related to the effect of pores radius on the rate of evaporation. The evaporation rate from the gel is dictated by the difference between the vapour pressure at the evaporating surface, $\boldsymbol{P_s}$, and the vapour pressure in the ambient atmosphere, $\boldsymbol{P_a}$. Evaporation goes on as long as $\boldsymbol{P_s} > \boldsymbol{P_a}$ at a rate $\boldsymbol{V_e}$ according to equation 3:

$$V_e = K_e(P_s - P_a) \qquad (3)$$

where K_e is a constant. The vapour pressure of a surface comprising a large number of very small pores, $\boldsymbol{P_v}$, is influenced by the radii of the pores, as described by the Gibbs-Kelvin equation 4:

$$\ln \frac{P_V}{P_0} = \frac{V_m \gamma_{LV}}{RT} \frac{2}{r} \tag{4}$$

in which P_V and P_0 are vapour pressures over the meniscus of the pore and over a flat surface, respectively, V_m is the molar volume of the liquid, R is the ideal gas constant, and T the temperature.

2.1.2. First Falling Rate Period (FRP1), the second stage of drying

The second stage of drying begins at the critical point, at which the shrinkage of the network stops. This step is also known as "first falling rate period" because evaporation rate decreases during it. It coincides to the first entry of the meniscus into the pores, leaving behind empty pores as shown in figure 17.

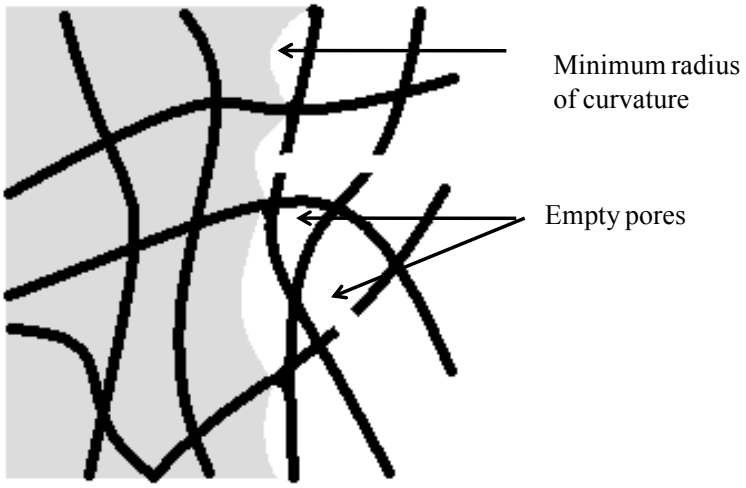

Fig. 17. Entry of meniscus into pores [2].

The liquid in the pores located near the surface of the solid remains in funicular conditions[2] [2], thus liquid can continuously migrate to the outer surface. The outer surface remains below the ambient temperature. Now, the rate of evaporation is sensitive to ambient

[2] In this context, the term "funicular" is related to continuous thin film of liquid and hence to continuous flow of liquid, just like a transport by train on railway. In contrast, pendular regions (as shown in the next Fig. 18), are those of non-continuous flow of liquid, first evaporating from closed pocket and next evacuated by diffusion from pores. This behaviour thus looks like the pendulum in old clocks.

temperature and vapour pressure. Evaporation induces cooling of the wet solid, hence the correspondingly lower temperature decreases the rate of evaporation and slows down the cooling. The surface temperature may only increase after the evaporation rate decreased, as it happens in FRP1. Originally, it was claimed that the liquid flow in FRP1 stage occurred by diffusion. However, more recent studies have shown that the driving force is the existence of a gradient of capillary stress [2, 3]. Just like in the case of the CRP stage, evaporation takes place at the outer surface of the drying solid, since the local vapour pressure is lower than that inside the partially wet pores. Confirmation of this is provided by equation 5,

$$P_v = P_0 \exp\left(\frac{PV_m}{RT}\right) \quad (5)$$

where and P_V and P_0 have the same meaning as in eq. (4). As already mentioned, the liquid flows from inside the pores to the outer surface, where evaporation occurs because the vapour pressure is lower there than inside the pores partially filled with liquid. Therefore, the funicular liquid migrates to the outer surface, where the suction is the greatest. This flow takes place according to Darcy's law, which states that the flux of liquid, J, is proportional to the gradient of pressure in the liquid ∇P_L:

$$J = \frac{D}{\eta_L} \nabla P_L \quad (6)$$

where ∇P_L is the pressure gradient (Pa m^{-1}), η_L is the viscosity of the liquid, and D is the permeability of the unsaturated solid. Transport of liquid is dominated by the flow, as long as the flow of liquid along the pore walls is continuous.

The capillary pressure gradient is influenced by the gradient of temperature because vapour pressure and surface tension both depend on temperature. High vapour pressure and low surface tension favour the flow toward the outer surface by increasing the suction in the liquid. The cooler outer surface will have lower P_v, giving consequently lower r, and higher interfacial energy, γ_{LV}. This behaviour is shown in figure 18 a) [2]. The flow rate may also depend on the adsorption forces. In such a case, the surface of the drying solid retains a thick layer of adsorbed fluid, which contributes to the flow of the film. This mechanism occurs only when the contact angle, θ, is equal to 0° and is most likely to be important when the vapour pressure at the surface is very low.

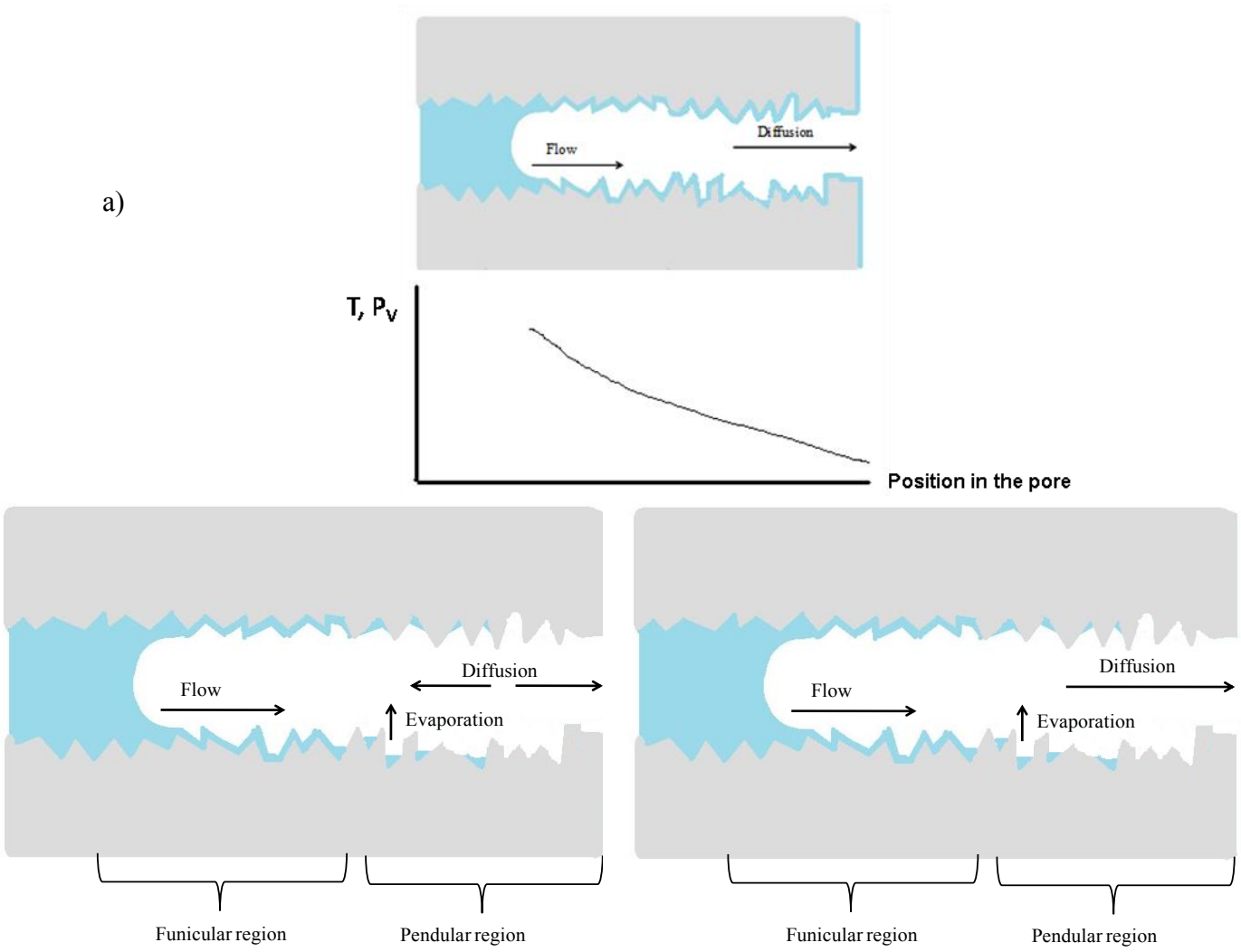

Fig 18. Above: a) Funicular transport throughout the pores. Below: illustration of FRP 2, the last step of drying: b) convective drying, c) microwave drying.

For some gels, a characteristic feature of this stage is the matting observed during the progressive drying of the solid. There are several theories explaining this phenomenon, such as phase separation in the pores and release of gas from the liquid during drying. The most probable explanation of this phenomenon has been proposed by Show, who suggested that the gels become opaque due to scattering of light by isolated pores or groups of pores having dimensions able to scatter light, during their emptying process. Wilson and Hench proved this assertion by examining in stage II the changes of open porosity of drying gels [3]. Their results confirmed that the open porosity increased during the transparent to opaque transition.

2.1.3. Second Falling Rate Period, the third stage of drying

The beginning of the stage III of drying is the most difficult to identify. Therefore it is widely accepted that it begins at the end of the opaque phase. Scherer and Brinker describe stage III as the "second falling rate period". In this step, evaporation occurs inside the porous solid. The temperature of the outer surface approaches the ambient temperature. Thus, the evaporation rate becomes less sensitive to external conditions, such us temperature, humidity, drying rate, etc. [2].

The liquid meniscus is moving into the pores along a drying front, thus the distance between the latter and the outer surface increases with time. As a result, capillary pressure and hence flow of liquid both decrease. If the sample is thick enough, the flow becomes so slow that the liquid is retained in isolated pockets. The continuous flow of liquid towards the surface stops and the liquid is removed only by diffusion of its vapour. The drying front is drained by flow of funicular liquid whose evaporation takes place at the boundary of funicular – pendular regions. The vapour in pendular region is in equilibrium with isolated pockets of liquid and with adsorbed film, and vapour pressure significantly depends on the adsorption forces [2].

Two different behaviours can be observed. It was demonstrated that, during convective drying of sandstone and when the temperature of the outer surface is higher than that of the interior, diffusion exists from partially emptied pores toward outer, dry, surface. However, diffusion also takes place in the opposite direction, see Fig. 18(b). In contrast, microwave drying makes the temperature inside the drying, porous, solid be higher than that of the exterior, so the vapour always flows toward the outer surface, see Fig. 18(c). In general, pores of gels are so small that vapour flows via Knudsen diffusion, meaning that molecules more frequently collide with pore walls than with each other.

During drying, the saturated region moves inside the porous solid, consequently leading to a slight expansion as the total stress on the network is relieved. In the meantime, a differential strain occurs because the network is more compressed in the saturated region than near the surface of the body. This phenomenon can lead to warping in the sample dried from one side, as faster contraction of the wet side makes the sample convex toward the drying side. Interestingly, warping is permanent which suggests that the unsaturated zones in drying solid retain some plasticity during FRP2. In this stage, cracks can occur, associated to the increasing tension of the network in saturated region. It was proved that cracks in drying gels often appear near the inner surface still saturated by liquid.

All the stages described above: CRP (constant rate period), FRP1 (first falling rate period), and FRP2 (second falling rate period), are parts of the classical theory of drying. The latter was described on the basis of inorganic gels, so application to organic gels may be questioned. Job et al. [35] investigated convective drying of resorcinol – based gels, and found that drying rate depends on aging time. This means that samples dried directly after gelation (i.e., without aging) are materials difficult to dry because polycondensation is not completed yet. Therefore, part of the water is trapped via hydroxyl groups of methylol derivatives. In this case, polycondensation takes place during drying, and hence the rate of evaporation becomes dependent on the rate of reaction. Water accumulated in gel structure thus needs a longer time for evaporation. Samples dried just after gelation presented higher shrinkage than those submitted to aging. The former were indeed more fragile, with a softer structure, than the latter, a structure not strong enough for resisting to the capillary forces. Moreover, evaporation of the water involved in methylol bridges partly destroyed the polymer network, further helping the development of cracks in the samples during drying.

Non-aged materials thus lost 20 – 30% of their initial weight at the beginning of drying (0 – 1h). The rate of weight loss then slowed down, but constant mass could not be reached even after a long time. Samples cured longer than 24h showed no influence of aging time on drying process. For example, samples cured for 24, 48 and 72h presented drying curves having the same slopes, and in all cases around 90% of the mass was lost at the beginning of drying (0 – 2h). The drying then slowed down and the mass of samples became constant after 6 – 7 h. In another work about the production of carbon xerogels, the influence of different drying conditions on the final properties of RF xerogels was investigated. The degree of final shrinkage was found to increase when the resorcinol/catalyst (R/C) molar ratio decreased. For example, for samples with R/C = 1000, the shrinkage was around 15% whereas samples with ratios 500 and 300 presented shrinkages of 45 and 60%, respectively. It was also found that the extent of shrinkage is independent of drying temperature, however higher temperature of drying leads to cracks in the samples, especially at low R/C ratios. The other parameter measured by Job et al. [35] was the drying time. They found that drying time depends on both R/C ratio and drying conditions. Increasing R/C produced faster drying. At constant R/C, the drying time was mostly influenced by temperature, so that higher temperature accelerated the drying and consequently shortened the drying time. Moreover, the effect of temperature was more pronounced at low R/C values. When R/C was low, it was very difficult to have both a fast drying and the preservation of the monolithic structure: temperature had to be reduced to

30°C at an air velocity at 2 m/s, in order to avoid the cracking of the samples. The other parameter having an influence on drying time is air velocity. The higher is the air velocity, the higher is the drying flux and consequently the lower is the drying time [35]. This phenomenon is presented in figure 19, wherein the curves exhibit a constant drying flux period, followed by a long decreasing drying flux period. These results show that convective drying of organic gels is in agreement with classical theory of drying, which graphical presentation has been presented in figure 13.

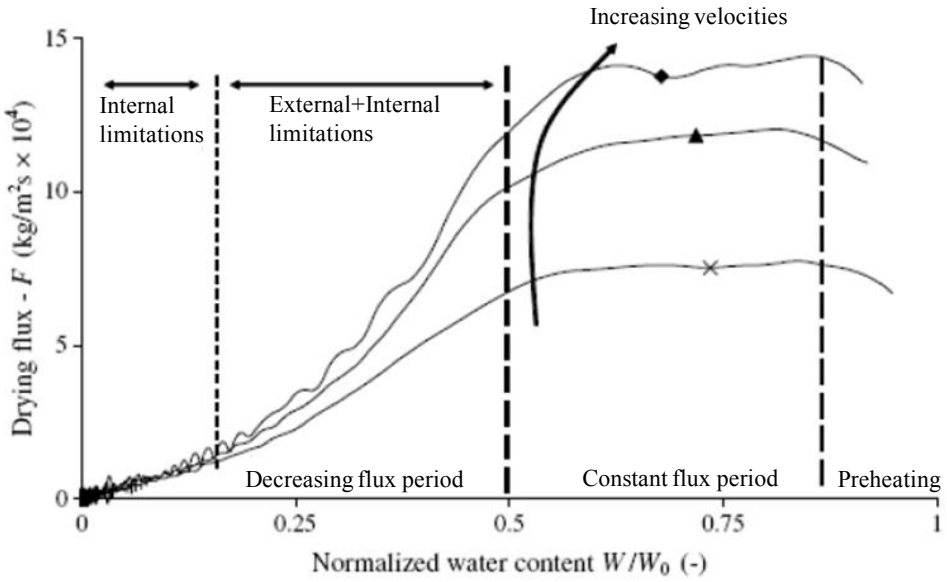

Fig. 19. Kirscher's drying curves for resorcinol-formaldehyde gels [35].

2.2 Supercritical drying

Convective drying can be a good and cheap method for drying inorganic and organic gels. However, large shrinkage, cracking of samples during drying, and insufficient textural properties are generally obtained. For example, xerogels usually have rather low surface areas and low total pore volumes.

One drying method which strongly reduces shrinkage and eliminates cracks is supercritical drying in some supercritical solvents. Supercritical drying in liquid CO_2 was proposed by Kistler in 1931 as a result of a bet with Charles Learned about the replacement of the liquid in jellies by a gas without causing shrinkage [36]. Kistler claimed that the problem of capillary forces between solid network and solvent can be solved by removing the solvent from the pores above its critical point (red arrow in Figure 12), beyond which differences between liquid and vapour phases vanish. When transformed into a supercritical fluid, liquid-

vapour interface and thus capillary pressure disappear. These conditions allow to dry samples without collapsing pore structure, and thus allow obtaining a very low shrinkage.

The first proposed supercritical fluid was CO_2 because of its low critical temperature and relatively low critical pressure. However liquid CO_2 is not the only fluid used for supercritical drying. The most commonly used supercritical solvents are given in table 2.

Table 2. Critical temperatures and pressures of common solvents [2].

Solvent	Formula	T_c (^oC)	P_c (MPa)
Freon 116	CF_3CF_3	19.7	2.97
Carbon dioxide	CO_2	31.2	7.37
Acetone	C_3H_6O	235	4.6
1 - propanol	C_3H_8O	265	5.1
Ethanol	C_2H_6O	240	6.3
Methanol	CH_4O	240	7.9
Water	H_2O	375	22.0

As was shown in table 2, water has a rather high critical point, so it can not be used as a practical and attractive supercritical drying agent. It should thus be exchanged by a more suitable drying agent. The best drying agents appear to be CO_2 and Freon 116, since they have the lowest critical temperature and pressure. However Freon 116 has very negative ozone depletion potential, whereas liquid CO_2 is very expensive and requires several steps before it can be used. Indeed, the water contained in the sample must first be exchanged by a solvent in which CO_2 is soluble, e.g., ethanol, then such solvent must be exchanged by liquid CO_2 before the latter is transformed into a supercritical fluid. An alternative to these two agents may be 1 – propanol [37], acetone [23, 38 – 39], as well as ethanol itself [39]. Even though they have higher critical temperature and pressure than CO_2, they can lead to comparable textural properties as we have shown in the present thesis.

Before drying, water and by-products of polycondensation have to be replaced by a suitable solvent for supercritical drying. The exchange step is also necessary because, as Kistler noticed in the case of silica, wet gels could dissolve if submitted to supercritical conditions when pores contain water [2]. After the exchange step, samples can be dried in supercritical conditions. Figure 20 presents typical conditions and pathway of supercritical drying in acetone. At the beginning, the wet gel is placed in an autoclave containing an additional amount of solvent, and is heated and pressurized above critical temperature and critical pressure of solvent (step I). Temperature and pressure are increased simultaneously in such a

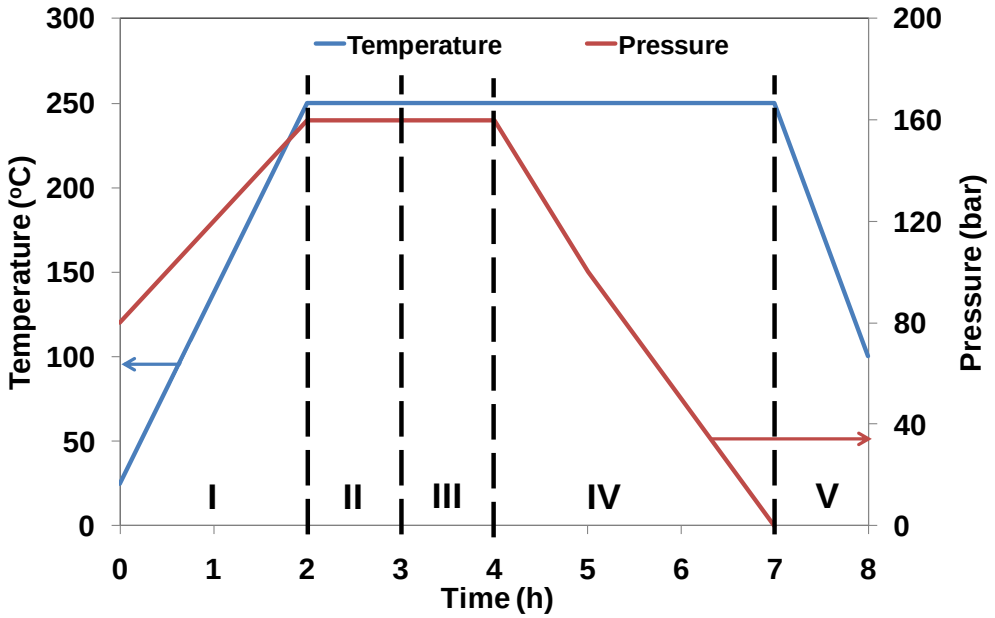

Fig. 20. Pathway of supercritical drying in supercritical acetone.

Once the critical point is by-passed, samples are maintained inside the supercritical fluid for a certain period of time (II), and next the autoclave is vented with Nitrogen or Argon flowing at the same pressure and at constant temperature (III), both being higher than the critical point (this step is required for supercritical fluids different than CO_2). Next, the autoclave is slowly depressurized to ambient pressure at constant temperature (IV), and finally it is cooled down to room temperature (V). The resultant materials of supercritical drying are aerogels, i.e. solids having similar volume to that of the original wet gels. Aerogels are monolithic, often transparent or semitransparent, low-density, highly porous, dry gels. Figure 21 presents the devices we used for doing supercritical drying in acetone (or other organic solvent) and in CO_2.

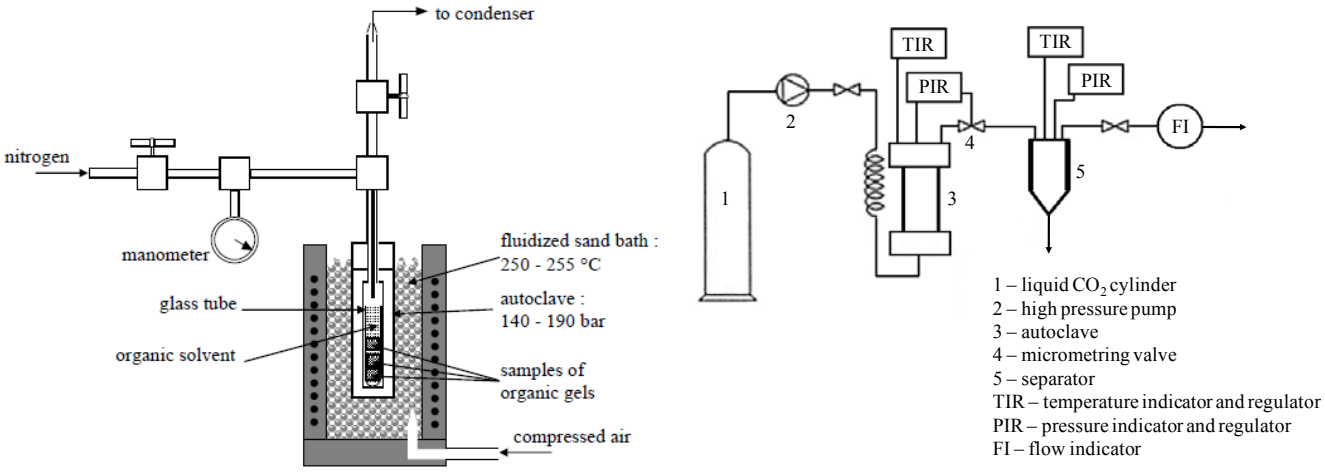

a) b)

Fig. 21. a) Acetone (or other organic solvent) supercritical drying device; CO_2 critical point drier.

The first organic aerogels were obtained by Pekala [6] in 1989 using resorcinol as a polymeric precursor and formaldehyde as a cross-linking agent. For that purpose, sol-gel polycondensation was carried out in water with Na_2CO_3 as catalyst. The solution was gelled and cured for 5 days and next wet gels were placed in ethanol for solvent exchange and were finally dried in supercritical CO_2. As-obtained aerogels were brown, transparent and low-density materials which can be next carbonized and used in many different applications (see Chapter 4). As shown by these experiments, it is possible to obtain crack-free materials with low shrinkage, in some cases 5 – 10%. Organic aerogels are characterized by extremely low densities, ranging from 0.03 to 0.1 g cm^{-3}, and by a micro and mesoporous structure with high surface area varying from 100 - 500 m^2 g^{-1}. The resultant properties of such organic aerogels strongly depend on the conditions of polycondensation, e.g., R/C ratio and solid content (dilution) [6, 9, 13].

2.3. Freeze – drying

The last known method for drying gels is freeze drying. In this case, the interfacial tension and capillary forces are almost completely eliminated by solvent freezing and sublimation under vacuum (see blue arrow in figure 12). Freeze drying, also named lyophilisation, is widely used in food industry, wherein it is carried out for preparing instant soups or instant coffee. Some authors claimed that freeze drying doesn't allow preparing monolithic gels, the

main limitation being the growth of crystals of solvent ice which may lead to cracks in the gel network [2, 40]. Crystals nucleated in liquid confined in pores can indeed grow up to a size a few millimetres. This phenomenon is known in the case of inorganic gels, for which freeze drying leads of flake – like or translucent solids with large pores that are the templates of the crystals. The crystal growth is illustrated in figure 22.

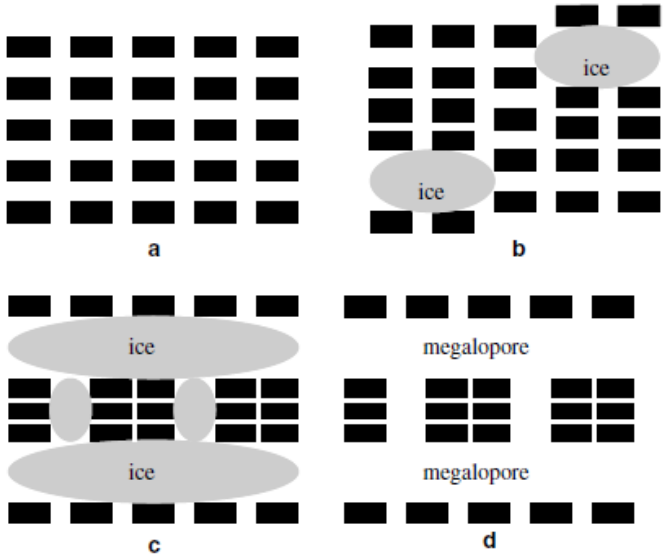

Fig. 22. Growing of ice crystals during freeze drying [40].

After the formation of an organic gel, its pores are filled by water and other by-products of sol – gel polycondensation. Just like for supercritical drying, this complex liquid needs to be exchanged by pure solvent before freeze drying. In order to minimize the effects presented in Fig. 22, a solvent having a moderate volume change upon freezing should be preferred. Table 3 presents differences of density between liquid and solid phase and vapour pressure of two solvents.

Table 3. Differences of density between liquid and solid phase, vapour pressures and freezing points of water and tert – butanol.

Solvent	**$\Delta\rho$ by freezing (g cm^{-1})**	**P_0 at 273 K (Pa)**	**Freezing point (K)**
Tert – butanol	-3.4×10^{-4}	821	299
Water	-7.5×10^{-2}	61	273

The most known and widely used solvent for freeze drying is tert – butanol (2-methyl-2-propanol). As shown in table 3, the volume change of *t*-butanol upon freezing is much smaller

than that of water, and the vapour pressure of *t*-butanol is also much larger than that of water. *t*-butanol is thus also useful for shortening the drying time [7,41]. Besides, past works have shown that cryogels washed and dried in *t*-butanol had higher BET surface area and pore volume than samples freeze-dried without exchange step. Using *t* – butanol also strongly helped developing the mesoporous structure of the resultant cryogels [41].

At room temperature, *t* – butanol is a crystalline solid which melts at 26^{o}C, thus samples have to be kept above the melting point. Tamon et al. [41] examined the influence of repetitive rinsing with *t*-butanol and observed that the largest differences in pore size distributions were observed for samples rinsed once and twice. Additional rinsing (3rd, 4th, 5th etc.) had no influence on pore size distribution of the resultant cryogels, suggesting that rinsing twice with *t*-butanol is enough for a complete solvent exchange.

After exchanging water by *t* – butanol, samples are frozen in deep – freezer (–24°C) and next freeze dried at -48°C under 1 mbar, thus providing optimal conditions for fast sublimation of *t* – butanol from the porosity of the gels. Monolithic, crack – free and opaque cryogels can thus be produced, whose properties strongly depend on the initial conditions of gel preparation [41]. In this thesis, such experimental conditions have been used.

Chapitre 3: Carbon gels, products of carbonization of organic gels

3.1. Characterization of Carbon

Carbon is a chemical element with atomic number 6 and molecular weight 12.011. As a member of group 14 in the periodic table, it is non-metallic and tetravalent, so it has four electrons available for making covalent bonds. There are three naturally occurring isotopes of carbon: ^{12}C and ^{13}C being stable, and ^{14}C which is radioactive with a half-life of 5730 years [42, 43]. The carbon atom has the unique ability to form bonds with other carbon atoms, as well as with other elements, leading to an infinite number of chemical compounds which are the basis of organic chemistry and the basis of life on Earth.

The Carbon ($[(ls^2)(2s^22p^2)]$) aptitude of creating such diverse and unlimited number of chemical components can be related to its ability to form sp^3, sp^2 and sp^1 hybrid bonds as a result of promotion and hybridization. In the first type of hybridization, sp^3, four equivalent $2sp^3$ hybrid orbitals occur that are tetrahedrally oriented around the carbon atom. They can create four equivalent tetrahedral σ bonds by overlapping with orbitals of other atoms. Such type of hybridization is present in the molecule of ethane C_2H_6, for example, where Csp^3 – Csp^3 σ bond is created between two atoms of carbon through the overlap of sp^3 orbitals. Moreover, three Csp^3 – H1s σ bonds are formed on each atom of carbon, as presented in figure 23a.

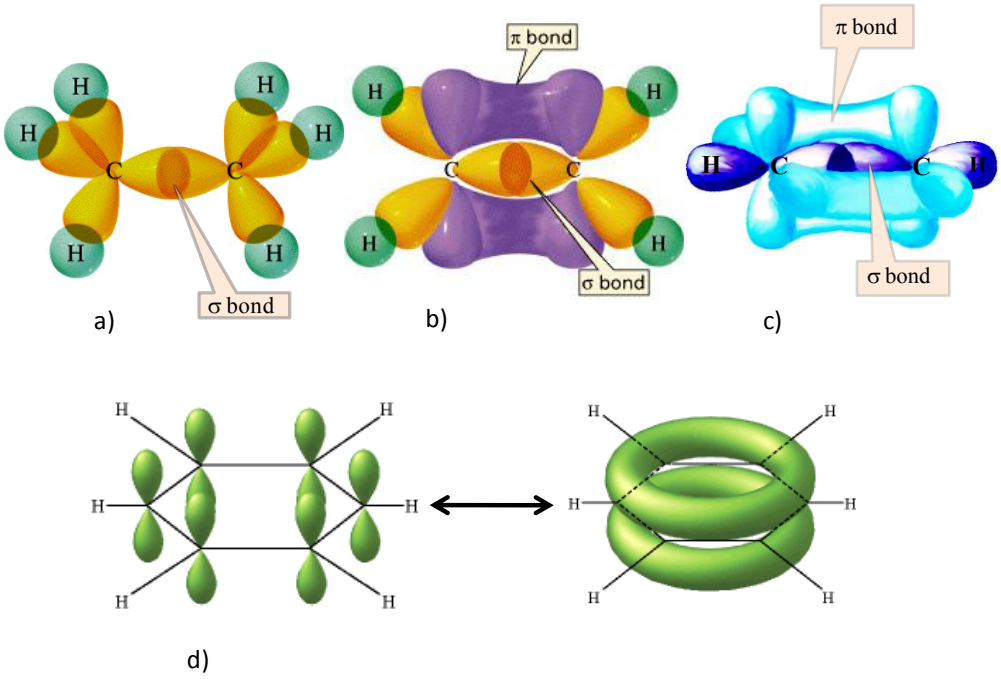

Fig. 23. Types of carbon hybridization: a) sp^3; b) sp^2; c) sp; d) hybridization of aromatic rings: example of benzene [44].

In the second type of hybridization of valence electrons in carbon atoms, three hybrid orbitals 2s2 and one unhybridized 2p orbital are involved. The sp^2 orbitals are equivalent, coplanar and oriented at 120° to each other and form σ bonds by overlapping with orbitals of neighbouring atoms, whereas the p orbital of each carbon atom forms a π bond by overlapping with the p orbital of neighbouring carbon atoms. The bonds formed between two atoms of carbon can be represented as $Csp^2 = Csp^2$, or C=C. This type of hybridization is shown for ethylene taken as example, C_2H_4, in figure 23b.

The hybridization sp^1 is a third type of hybridization. In this case, two linear $2sp^1$ orbitals and two non hybridised 2p orbitals are present. Linear σ bond is created via overlapping of sp hybrid orbitals with orbitals of neighbouring atoms, while the non hybridised p orbitals of the carbon atoms overlap to form two π bonds. The bonds formed between two atoms of carbon in this way are represented as Csp≡Csp, or simply as C≡C. This type of hybridization is shown for acetylene taken as example, C_2H_2, in figure 23c.

Most of precursors of organic gels are phenolic compounds possessing aromatic carbon-carbon bonds in their structure, exemplified by the prototypical aromatic benzene molecule, C_6H_6. In the case of benzene, the carbon atoms are arranged in a regular hexagon which is ideal for the formation of strain-free sp σ bonds. The ground state π orbitals in benzene are all fully occupied, bonding orbitals, and there is a large delocalisation energy that contributes to the stability of the compound. The aromatic carbon-carbon bond is denoted as $C_{ar}=C_{ar}$ [43]. This type of hybridization is shown for benzene in figure 23d.

Carbon in the solid state presents several allotropes, from which the best known are diamond and graphite. These two familiar examples show how the physical properties of solid carbon strongly depend on the structure. Thus, diamond is the hardest material and is a transparent, colourless crystal, while graphite is black, soft, and has lubricating properties. Most forms of solid carbon are chemically stable, requiring sometimes high temperature to react, even with oxygen. Carbon has the highest melting and sublimation points among all other chemical elements. In general, at atmospheric pressure, melting of carbon doesn't occur, and the triple point exists at 10 MPa, therefore it sublimates above 4000K. When used as an electrode, carbon sublimates in an electric arc at a temperature of about 5800K. Thus, irrespective to its allotropes, carbon remains solid at higher temperatures than the most refractory metals (tungsten and rhenium). However, thermodynamically speaking, carbon is very easily oxidized, much more than iron or copper which behave as weak reducing agents at room temperature [45]. Other intensively studied carbon forms are fullerenes, nanotubes, and

graphene, having different crystalline structures and hence different physical properties. Comparison of a few properties of graphite and diamond is given in table 4, and structures of some carbons allotropes are shown in figure 24.

Table 4. Properties of two common allotropic forms of carbon: diamond and graphite.

Properties	**Diamond**	**Graphite**
Hardness	The hardest known material (10 in Mohs scale)	Very soft material (0,5 – 2 in Mohs scale)
Transmittance	Highly transparent	Opaque
Colour	Depends on lattice defects and impurities	Black
Electrical properties	Isolator	Conductor
Thermal conductivity	Excellent ≈ 2000$Wm^{-1}K^{-1}$	Poor thermal conductor

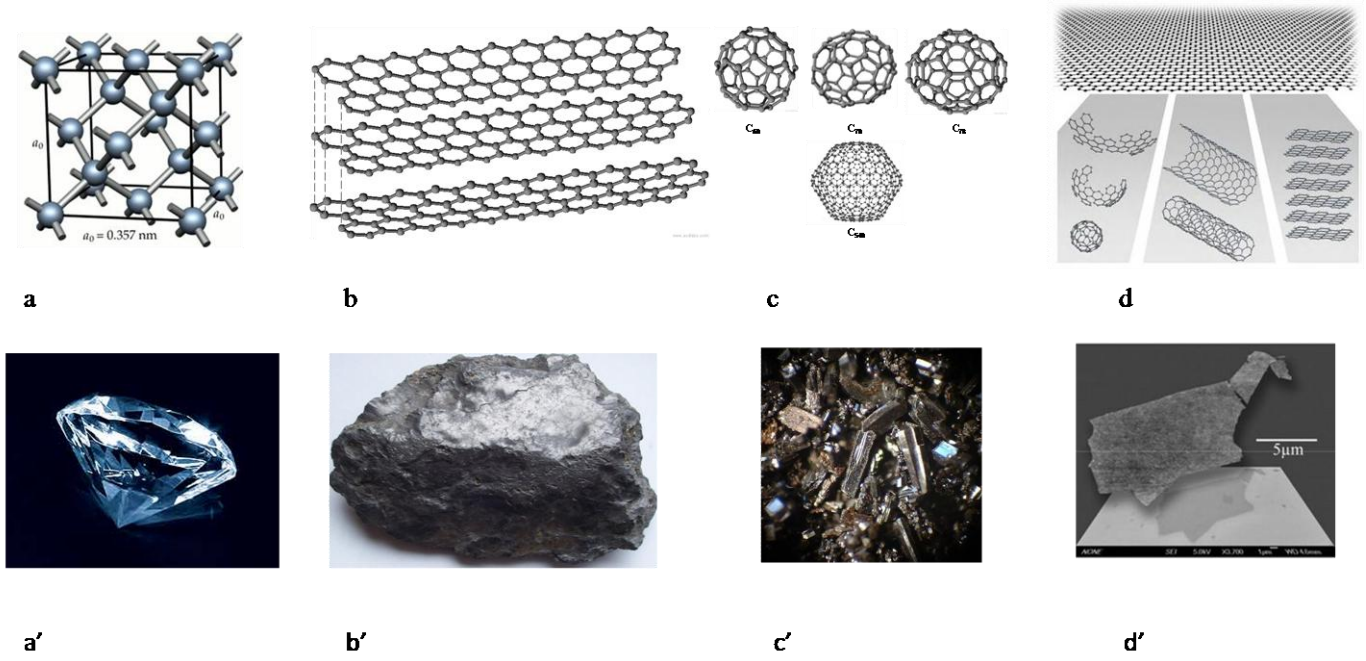

Fig. 24. Allotropes of carbon: a,a') diamond; b,b') graphite; c,c') fullerenes; d,d') graphene.

The situation is even more complex due to the possibility of carbon of doing more or less disordered phases, such as soot, anthracite, glasslike carbon, chars and activated carbons for example. Many of these carbon forms are porous, such as carbon gels, obtained by simple pyrolysis of infusible organic gels (see below).

3.2. Carbonization

Carbonization, also called pyrolysis, is the process by which organic compounds are converted into a carbon. Carbonization must be carried out in inert atmosphere, nitrogen or argon for example, otherwise combustion prevails. Samples are heated at a given heating rate up to a temperature ranging from 450 to 1000°C and even above. The higher is the temperature, the higher is the purity of the resultant carbon. Materials prepared below 800°C, typically, indeed still contain a significant amount of heteroatoms, especially oxygen, and should not be called “carbons”, but “chars” instead.

During carbonization, tarry substances and volatiles are released. This process leads to an enrichment of solid in elementary carbon and, depending on the composition of the precursor, to the formation of a more or less developed porous structure. In figure 25, examples of the mechanisms occurring during the carbonisation of a model precursor, *Acenaphthylene,* are shown [43].

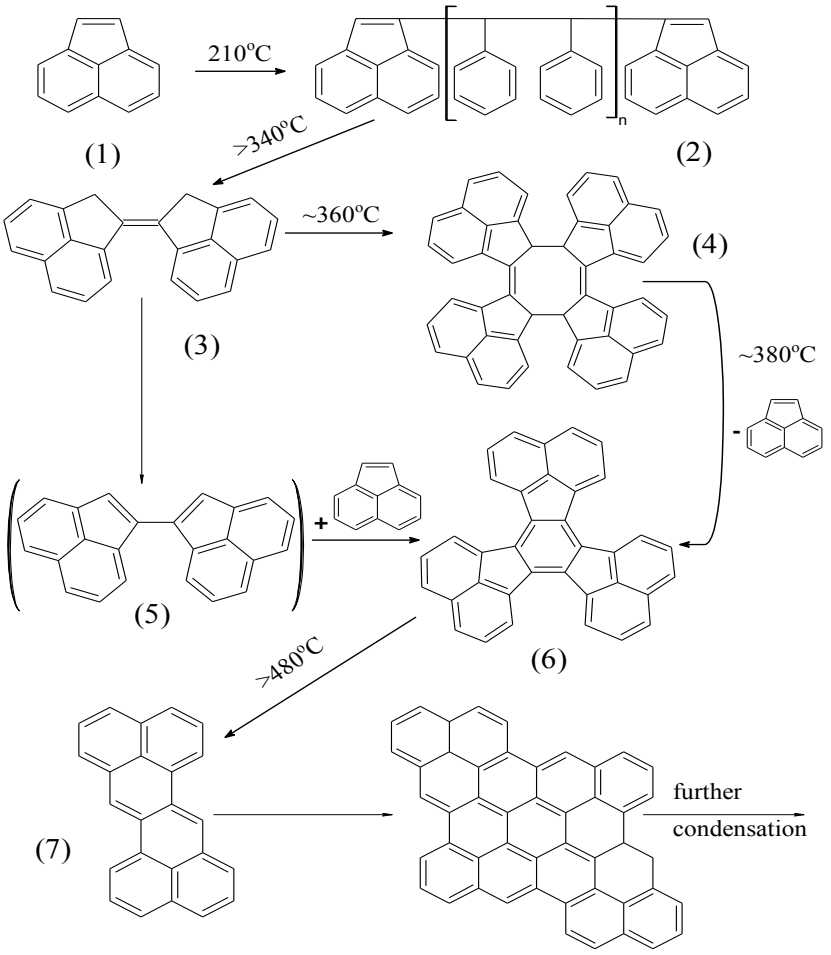

Fig. 25. Pathway of carbonization. (1) acenaphthylene; (2) polyacenaphthylene; (3) biacenaphthylidene; (4) fluorocyclene; (5), dinaphthylenebutadiene; (6), decacyclene; (7), zethrene.

The final properties and structure of the carbon materials depend on those of their precursors, and on the conditions of the pyrolysis: final temperature, time, heating rate and atmosphere.

3.2.1 Carbon materials

Carbonaceous materials, or "carbons", are solids in which carbon is the main (but not necessarily the unique) component. Table 5 presents the most common solid, liquid and gaseous organic precursors of carbon materials. It can be seen that some of the volatilisation products of carbonisation can be used as secondary precursors in carbon production.

Table 5. Typical precursors of carbonaceous materials [43].

Primary precursor	Secondary precursor	Final carbon materials
Hydrocarbon gases		Pyrocarbons, carbon blacks, vapour grown carbon fibers, matrix carbons
Petroleum		Delayed coke, calcined coke
	Petroleum pitch	Needle coke carbon fibres, binder and matrix carbons
	Mesophase pitch	Mesocarbon, microbreads, carbon fibres
Coals	Coal chars	Semi-coke, calcined coke, activated carbons
	Coal pitch	Premium cokes, carbon fibres, binder and matrix carbons
Polymers	Mesophase pitch	Mesocarbon, microbeads, carbon fibres,
	Polyacrylonitrile (PAN)	PAN – based carbon fibres
	Phenolic and furan resins	Glassy carbons, binder and matrix carbons
	Polyimides	Graphite films and monoliths
Biomass		Activated carbons

Most of carbons have a structure based on the hexagonal, lamellar, structure of graphite. However, the structure of real carbon materials can differ strongly because graphitic layers may contain defects in the form of gaps, five-membered rings, interstitial atoms or heteroatoms in substitution. The number of defects depends on the composition and structure of the raw material, as well as the methods and the conditions for preparing the carbonaceous

material. This phenomenon was observed for the first time by Hoffman and Wilm [47] in 1936. During an X-ray diffraction study of a carbon black, they noticed that only (hk0) graphite reflections instead of typical graphitic (hkl) reflections were observed. This observation allowed them to suggest a structure consisting of graphitic carbon layers still parallel but disordered along the plane. They also noted from the position of the (002) peak that the interlayer spacing, **d**, was greater than that of graphite crystal (d = 0.3354 nm).

A few years later, Biscoe and Warren proposed the term "turbostratic" to characterize parallel stacks of carbon layers with random translation along a – axis and rotation with respect to c – axis. Turbostratic carbon therefore doesn't present three-dimensional order, and the turbostratic value of the interlayer spacing is greater than that of graphite. Franklin [48] proposed the following classification of turbostratic carbon materials, depending on their ability to graphitize:

- Graphitizable carbons, see figure 26a, develop three-dimensional graphitic order on heat-treatment above 2000°C. In this case, the turbostratic carbon units are organized in a near-parallel (pre-graphitic) array. Graphitizable carbon layers contain a few defects only, and the bonds between them are rare and weak. In addition, the porosity of such materials is poorly developed.
- Non – graphitizable carbons, see figure 26b, don't develop 3D graphitic order during carbonization, even above 2000°C. They comprise turbostratic units in a random array that are cross-linked by disorganised carbon. Such kind of carbon is characterised by a well-developed porous structure, a low skeletal density and a significant hardness.

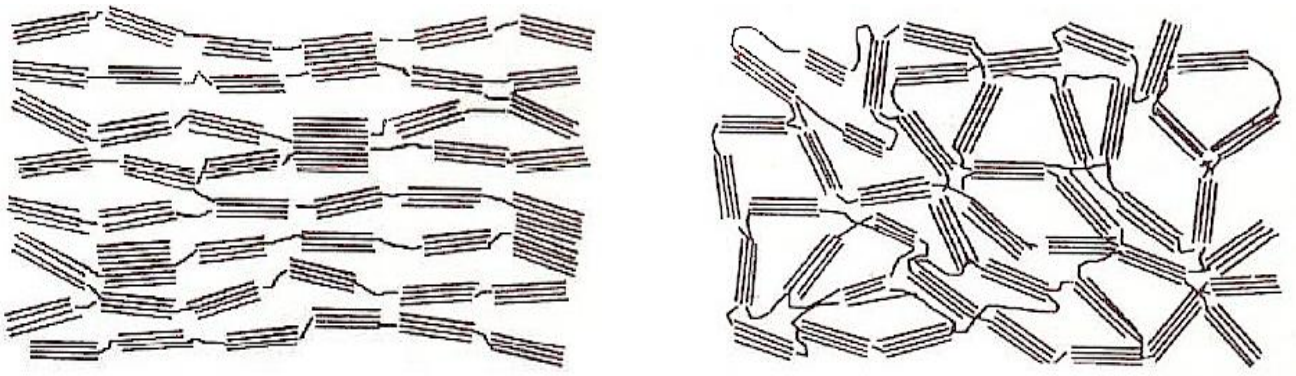

a) b)

Fig. 26. Illustration of: a) graphitizable carbons; b) non-graphitizable carbons [43, 46].

3.2.2 Carbonization of organic gels and related characterization

Organic gels are made from the agglomeration of spherical nodules, themselves based on cross-linked macromolecules. Consequently, gels are porous three-dimensional networks, whose porosity is both inside and between the polymer nodules. Because of the considerable disorder of such a structure, but also because of the initial composition, organic gels lead do non-graphitisable carbon after pyrolysis. The presence of large amounts of oxygen, just like in the present case, is indeed known to be in favour of non-graphitizable carbons.

3.2.2.1. Thermogravimetric and calorimetric studies

In the case of organic gels, two main transitions during carbonization can be distinguished. Job et al. [13], basing on thermogravimetric analysis (TGA) of Resorcinol – Formaldehyde xerogels, found that a first transition takes place within a temperature range of 150 – 200°C corresponding to the release of the remaining solvent and/or to the elimination of H_2O formed by condensation of –OH groups. The second transition occurs at temperatures ranging from 400 to 500°C, at which hydrogen and oxygen atoms included in the polymer network are eliminated as CO, CO_2, CH_4 or other volatile organic molecules. Carbon monoxide is formed during the decomposition of bonds formed in water elimination reactions, while methane is produced from methylene groups that don't participate to dehydration reactions. Desorption of adsorbed organic compounds may also be invoked. On the other hand, Kuhn et al. [49] observed transition of RF aerogels during pyrolysis. Two characteristic TGA peaks were also found: in the range of temperature 50 – 100°C, corresponding to desorption of adsorbed water, and around 280°C due to the release of organic groups. Additionally, basing on DSC analysis, Kuhn et al. have shown that endothermic reactions can be observed in temperature regions varying from room temperature up to 250°C, and from 250 to 600°C. The first DSC peak is due to the release of adsorbed water and the second one, very pronounced, corresponds to the release of organic matters. At a constant temperature of 250°C, no changes in DSC signal were observed. At temperature equal or higher than 600°C, the DSC slope presents additional small endothermic and exothermic effects. Similar curves and transition regions can be also found for different precursors of organic and carbon gels. Guilminot et al. [50] thus found similar behaviour for their cellulose-based aerogels. As in the previous cases, two main temperature regions of gels transition could be observed. The first transformation of gels took place within the temperature range 40 – 180°C, and corresponded to evaporation of water from gel structure.

The second one occurred at temperatures varying from 180 to 330°C and could be related to the formation of volatile species such as CO, CO_2 and formaldehyde produced during the pyrolysis of cellulose. The same conclusions were drawn for organic gels prepared from chitin [51], cresol [52] or polybenzoxazine [53].

3.2.2.2. Infrared spectroscopy

TGA or DSC are not enough for investigating in detail transformations occurring during pyrolysis. This is the reason of the frequent use of Fourier-Transform InfraRed (FTIR) spectroscopy. FTIR technique reveals many details of the carbonisation process which cannot be obtained so easily by other methods. Pyrolysis can be separated into release of water and organic groups on one hand, and formation of carbonaceous solid followed by rearrangement of the incipient carbon structure. The phenomena are likely to occur simultaneously.

Many publications present FTIR analysis of organic and carbon gels, showing changes of chemical structure during carbonization. Job et al. [13] and Kuhn et al. [49] investigated thermal transformation of Resorcinol – Formaldehyde xerogels and aerogels, respectively. In our own work, the transformation of Tannin – Formaldehyde aerogels into carbonaceous material was investigated as well [23]. The transformation process of organic aerogels into carbon gels can be explained from the example of cresol – formaldehyde aerogels [52]. In this case, samples were carbonized at different temperatures varying from 250 to 900°C and next investigated by FTIR spectroscopy. Spectra of heat-treated Cresol – Formaldehyde aerogels are given in figure 27.

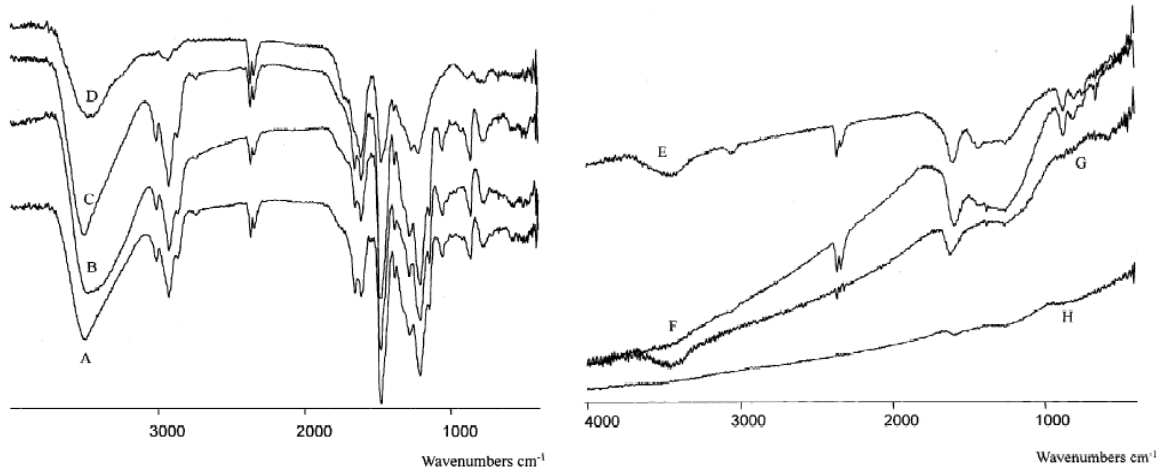

Fig. 27. FTIR spectra of cresol – formaldehyde aerogels carbonized at different temperatures and with different times of heat-treatment. A: raw material; B : 250°C, t=0'; C : 250°C, t=60'; D, 400°C, t=60'; E 600°C, t=0'; F 600°C, t=60'; G 700°C, t=60'; H 900°C, t=60' [52].

Within the temperature range 25 – 250°C, no significant change was observed, except the gradual decrease of intensity of hydroxyl groups (3472 cm^{-1}), related to the evolution of adsorbed water. This phenomenon became more significant at 400°C, before completely disappearing at 600°C. The authors claimed that water elimination is associated to condensation reactions between hydroxyl and methylene groups and also between two hydroxyl groups. The other characteristic groups for many organic gels are seen at wavelengths near 2921 cm^{-1}, attributed to CH_2 – stretching vibration, and at 1429 – 1479 cm^{-1}, corresponding to CH_2 – scissor vibration. The CH_2 – bond is a cross-linking bridge formed by the condensation of hydroxymethyl derivatives. Both peaks remained stable in the temperature range 25 – 250°C, and the significant degradation of these groups started at 400°C and continued at higher temperatures. Basing on this observation, it can be concluded that during pyrolysis the CH_2 bridges between the aromatic rings are broken, leaving aromatic structures with dangling bonds which recombine into larger entities. These aromatic multi-ring structures are the bases of the following carbonisation and local graphitisation. Li, and also Kuhn [49] observed at 1590 – 1607 cm^{-1} the C–C stretching bond of the carbon ring in cresol and resorcinol systems during the carbonization process. Furthermore, aromatic carbon structures occurred as shown by the emergence of a C–C vibration around 1607 cm^{-1}. These bonds interfere with the C–C bonds from the aromatic carbon rings of carbonizing gels that are the origin of the graphite-like structure observed at the end of the pyrolysis process.

In the range of wavelengths from 1145 to 1052 cm^{-1}, the methylene – ether bridge CH_2 – O – CH_2 can be evidenced. Methylene – ether bridges are formed between aromatic rings due to polycondensation. They are stable up to 250°C, and the progressive decrease of their intensity starts at 400°C before complete disappearance at 600°C. This is the first chemical reaction that happens during the pyrolysis process, leading to a higher mobility of the more or less tightly bound carbon rings. Thus, this rearrangement of aromatic rings can be regarded as the starting point of a long-range aromatisation, characteristic of most carbonaceous materials.

The occurrence of the IR-active vibrational states of graphite-like structures can be clearly observed at 400 – 600°C at a wavelength of 874 cm^{-1}. It was shown that the intensity of this peak gradually increases with pyrolysis temperature. Within the range of temperature 750 – 900°C, only this kind of vibration and also C – C vibration of aromatic rings bonds were observed, suggesting that the long-range aromatisation process started at 400 – 600°C, although it was not yet completed at 900°C. This finding is obvious given that, if graphitization was possible, temperatures at least as high as 2000°C would be required.

3.2.2.3. Transmission electron microscopy

Carbon gels have the same structure as that of their organic precursors, i.e. they are made up of aggregates of nanoparticles between which mesopores and macropores exist. The particles of gels carbonized at 800 – 1000°C have typical average diameters ranging from 8 to 50 nm. However, these values depend on the kind of precursor used in the sol - gel reaction and on the experimental conditions, especially the pH [54]. TEM images of Hanzawa et al. for carbon aerogels derived from Resorcinol - Formaldehyde and prepared at 1000 and 2800°C show that the stacking of graphitic layers is improved at higher temperature, see figure 28.

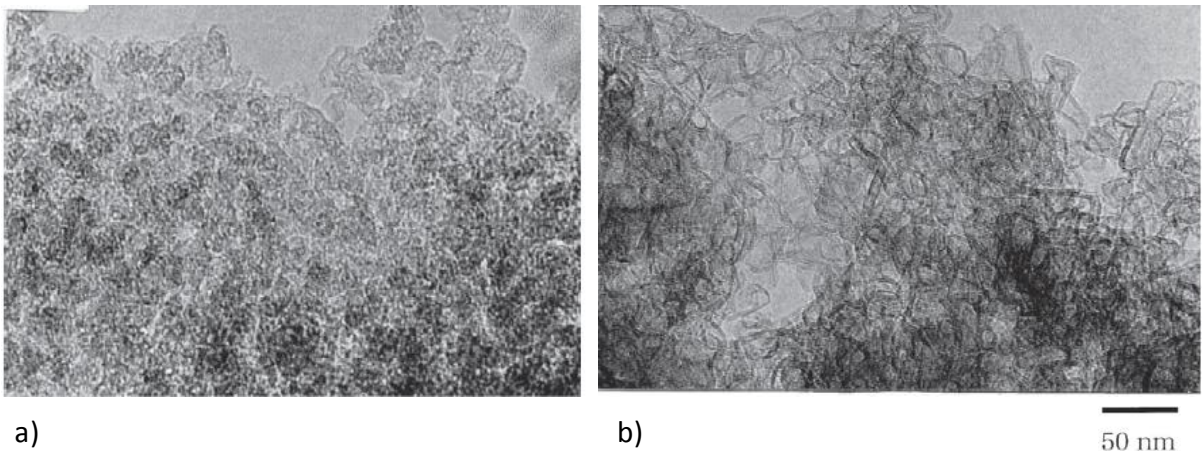

Fig. 28. TEM images of RF carbon aerogels heat-treated at: a) 1000°C; b) 2800°C.

However, and as expected, carbon aerogels heat-treated at 2800°C have the typical microstructure of non-graphitized carbons. The length of the coherent domains along the direction of the carbon layers increased up to 5 – 10 nm in the sample cured at 2800°C, higher than the size of the particles constituting the sample treated at 1000°C. As a result, the shape and the size of the original particles could not be distinguished in the sample heat-treated at 2800°C. Additionally, the boundary between particles became unclear due to the merging of the nodules and the improvement of carbon sheets packing. TEM micrographs indicate that carbon aerogels treated at 2800°C possess cage-like structures also known as “bubble structures” according to Kipling et al. [55].

Influence of pyrolysis temperature on the structure of Resorcinol – Formaldehyde aerogels was investigated by Thery during his PhD thesis [56]. Thery and his group have pyrolysed aerogels at different temperatures ranging from 800°C to 2600°C and next observed the corresponding changes using High-Resolution Transmission Electron Microscopy (HRTEM). Aerogels pyrolysed at 800°C and 1050°C did not presented significant differences: they were

disordered and comprised single carbon sheets. Organization of carbon sheets became more visible when samples were carbonized above 2000°C, and was very clear in samples prepared at 2600°C. The latter were characterized by longer and more organized sheets, and thus the greater number of sheets formed larger coherent domains. However, the number of packed sheets resembling graphite crystallites is still small compared to the extent of disordered areas. TEM micrographs allow concluding that the number of ordered carbon sheets increases with heat-treatment temperature, and that the growth of coherent domains is easier for gels having initially larger nodules. Thery also noticed that the greatest contribution to coherent domains are stacks consisting of 2 or 3 layers, having lengths not exceeding 6 nm. These values are similar to those obtained by Hanzawa's group. The dimensions of the graphitic sheets obtained at 2600°C were limited by the shapes and by the sizes of the pores of their precursors first obtained at 1000°C, and hence depended on their initial organic gels.

Calculation of the interlayer distance D between stacked sheets is also possible. X – Ray Diffraction (XRD) measurements of carbon aerogels prepared at high temperature confirmed that D decreased at increasingly high pyrolysis temperatures, and reached minimum values of 0.35 - 0.37nm above 2000°C. Such values remained always higher than those of graphite (0.335nm), further proving the non-graphitizable character of carbon gels derived from phenolic precursors.

3.2.2.4. Adsorption studies

Results of nitrogen adsorption – desorption measurements are reported in many publications related to carbon gels. These methods are indeed the most important ones for probing the narrow porosity of porous materials and determining their specific surface area. The influence of preparation conditions was investigated for many carbon gels obtained from different precursors such as resorcinol, cresol, polyurethane or cellulose. Interestingly, two different behaviours depending on heat-treatment temperature can be observed, typically below and above 1000°C.

First, basing for example on the results of Li et al. [52], who prepared organic aerogels by sol – gel polycondensation of Cresol with Formaldehyde, N_2 adsorption measurements clearly showed that surface and porosity can be developed by carbonization up to 900°C. Organic CF gels had typical mesoporous structure with high mesopore volume and high surface area: 1.7 cm3 g-1 and 400 m2 g-1, respectively. During carbonization, BET surface area increased due to the development of micropores. Moreover, organic samples presented a broad pore size

distribution, whereas the thermal treatment made the pores become narrower, with a decreased average width.

On the other hand, Job et al. [13] examined structural changes during pyrolysis of organic xerogels prepared from polycondensation of Resorcinol and Formaldehyde, and found that BET specific surface area and microporous volume increased with carbonization temperature as long as the latter did not exceed 700°C. Above this temperature, the specific surface area began to decrease, and 10% of the microporosity was lost between 700 and 800°C. The hysteresis adsorption/desorption loop was shifted towards smaller relative pressure, indicating the narrowing of the pore size distribution at increasingly high carbonization temperatures. Nitrogen adsorption also showed that pyrolysis developed microporosity by creation of new micropores or opening and widening of existing ones, related to the elimination of carbon, oxygen and hydrogen. The whole processes took place at 400 – 600°C.

For both CF and RF gels, the results are very similar, and can be extrapolated to most other phenolic precursors and other conditions of gel preparation. Thus, for other carbon gels prepared form cellulose, phenol and other phenolic resins including tannins (our own work), development of porosity of carbon gels during carbonization was also observed.

On the other hand, the experiments of Thery and Li [52, 56] have shown that carbonization at temperatures higher than 1000°C led to decreasing both BET specific surface area and total pore volume. The reason of this behaviour was attributed to the closure of microporosity because of the enhanced organisation of sheet packing into coherent domains. At the same time, polygonization of mesopores clearly appeared at 2600°C for the same reason, i.e. parallelisation and growth of formerly disordered stacked carbon sheets.

3.3 Control of carbon gels properties

3.3.1 Concentration of precursors

The concentration of precursors in the solvent used in sol – gel synthesis plays a very important role with respect to the properties of resultant organic and carbon gels. Increasing concentrations of reactants led to an almost linear increase of bulk density of gels after drying and pyrolysis. The same behaviour can be found for many different precursors such as resorcinol [39, 40], phenol [29], tannin [19, 20] or phenolic novolac resin [57].

Job et al. [40] have shown that samples dried in supercritical conditions or freeze dried are not free of shrinkage, as expected from theoretical assumptions. Shrinkage after drying strongly depends on the concentration of reactants, C. The higher is the concentration, the lower is the shrinkage, which can be as low as a few %. On the other hand, samples dried by evaporation under vacuum present much higher shrinkage, also dependent on the initial concentration, ranging from 50 to 80% for high and low concentrations, respectively. Pyrolysis of these samples caused additional shrinkage of the resultant carbon gels. The shrinkage of carbon aerogels and carbon cryogels is comparable, but the one obtained for samples dried by evaporation under vacuum (xerogels) is always higher [40].

It is also remarkable that, in the case of carbon xerogels, shrinkage mainly occurred during the drying treatment, whereas the shrinkage was more marked during the pyrolysis of aerogels. Depending on their composition, cryogels could shrink mainly during drying or during pyrolysis. Similar observations were found in our own work, in the case of RF aerogels prepared via supercritical drying in acetone and supercritical drying in ethanol. In both cases, shrinkage after drying decreased when the initial concentration of resorcinol in the solution was increased [39]. Pyrolysis induced further shrinkage. For samples supercritically dried in ethanol, high shrinkages were obtained only for gels having a very low initial concentration, whereas very low shrinkages were always obtained for aerogels dried in supercritical acetone, whatever the initial concentration. At concentrations higher than 10 wt%, comparable values of shrinkage were obtained whether the aerogels were obtained in supercritical ethanol or in supercritical acetone.

The influence of the precursor concentration on the porous properties was reported by Babić et al. [9] for carbon cryogels prepared from resorcinol and formaldehyde. Porous characteristics such as BET surface area, micropores surface area and total pore volume changed with the concentration of resorcinol. Increase of resorcinol concentration caused the decrease of micropore volume and related surface area. On the other hand, changes of BET surface area not systematically occurred, the maximum BET surface being obtained for the sample at 10 wt% resorcinol concentration. Higher concentrations led to lower surface areas. The pore size distribution presented a sharp single peak, and the values of the pore radius at the maximum of the distribution depended on resorcinol concentration and varied from 2 and 4.0 nm. Such samples are thus mostly mesoporous according to IUPAC classification [91].

Samples prepared in the same conditions, e.g. with the same molar resorcinol/catalyst (R/C) and weight resorcinol/water (R/W) ratios, but dried in supercritical acetone and ethanol

(our own work), presented quite different porous properties [39]. Samples dried in supercritical acetone reached the maximum BET surface area when prepared with the lowest concentration of resorcinol. BET surface areas and micro- and mesopore volumes systematically decreased at increasingly high resorcinol concentration. On the other hand, samples prepared by supercritical drying in ethanol (our own work) reached their maximum of BET surface area and micro- and mesopore volumes for resorcinol concentration of 20% [39].

However, results obtained for phenolic novolac-furfural carbon aerogels indicate that shrinkage and also porous properties can strongly depend on precursor and conditions of synthesis, drying and carbonization. In this case, no correlation between concentration and shrinkage or porous properties could be clearly evidenced [57].

3.3.2 Nature and amount of catalyst

3.3.2.1 Influence of catalyst nature on carbon gels properties

The role of catalyst in sol – gel reaction is not clearly known, but many researches have concluded that the amount and the kind of catalyst has an important contribution in the final textural properties of organic and carbon gels [12,13,58]. It was found that the acidic or basic character of the catalyst has an influence on gelation time in the sol – gel process. For example, using acidic catalyst may divide the gel time by a factor 2. However, for gels synthesized with the same concentrations of resin, the density of samples prepared under acidic conditions was two or three times higher than that of samples prepared using alkaline carbonates as catalysts. This may result from a larger aggregation of clusters formed during the polymerization reaction under acidic conditions, leading to lower void spaces between the clusters. Most of the carbon aerogels were mesoporous with narrow pore size distributions. Moreover, samples prepared in acidic conditions are characterized by lower BET surface areas and lower micropore volumes in comparison to carbon gels prepared with basic catalysts. It was observed that the nature of the acidic catalyst had only an influence on the meso- and macropore volumes but did not affect the micropore texture. These results suggest that the nature of the acid used in the preparation of these aerogels only affected the gelation process [12, 13].

The impact of various basic catalysts, such as Na_2CO_3, K_2CO_3, $NaHCO_3$, $KHCO_3$ and also NaOH and $Ca(OH)_2$, on the final properties of carbon gels was also studied [59]. It was

noticed that samples prepared with Na_2CO_3 (R/C = 50) were denser; they had higher BET surface areas and micro- and mesopore volumes, and narrower pore widths values than those prepared with K_2CO_3 as a catalyst. Potassium and sodium carbonates are commonly used catalysts in gel preparation. However, the porous properties of carbon gels can be improved by using $NaHCO_3$ or $KHCO_3$ as catalysts. Only small differences of BET surface area and micropore volume of carbon gels were observed for different kinds of catalyst. However, the mesopore volume was strongly dependent on catalyst species. In some cases, the mesopore volume of samples prepared with $NaHCO_3$ or $KHCO_3$ was two times higher than that of samples prepared with Na_2CO_3 or K_2CO_3. Pore widths of samples prepared with bicarbonates were also shifted towards higher values, and pore size distributions of such samples were broader than samples made with carbonates.

Using hydroxides (NaOH, $Ca(OH)_2$) [56] instead of carbonates also gave interesting results, especially when comparing sodium carbonate with sodium hydroxide. The results obtained by Thery [56] have shown that samples prepared at 800°C with NaOH, R/C = 45 had comparable density, but higher BET surface area and micropore volume and lower mesopore volume, than samples prepared with Na_2CO_3 in the same conditions.

3.3.2.2 Influence of catalyst amount on carbon gel properties

Reported investigations have also shown that the amount of catalyst used in the sol – gel process had a strong impact on the final properties of carbon gels. Decreasing the precursor/catalyst molar ratio and consequently increasing the pH of initial solution (given that most catalysts have a basic nature), caused an increase of bulk density of carbon gels, whatever the drying method. Job et al. [13, 40] observed that the bulk density of carbon RF xerogels was increased from 0.53 g cm^{-3} for samples prepared at pH = 5.45 (R/C ~ 1000) up to 1.32 g cm^{-3} for samples prepared at pH = 7.35 (R/C ~ 50). The bulk densities of carbon aerogels and carbon cryogels prepared in the same conditions were significantly smaller and were in the ranges 0.38 – 0.95 g cm^{-3} and 0.36 – 1.02 g cm^{-3}, respectively [13,40].

Job et al. [40] also investigated the changes of porous properties of carbon aerogels, cryogels and xerogels prepared at different R/C ratios changing from 50 to 1000. From nitrogen adsorption measurements, it could be concluded that samples prepared at high R/C ratios had high BET surface areas, within the range 500 – 700 m^2 g^{-1}, and high micropore and total pore volumes, whatever the method of drying. For samples prepared at low R/C ratios, only carbon aerogels presented high surface area, 535 m^2 g^{-1}, whereas cryogels and xerogels

had relatively low BET surface areas. These materials even become non-porous when prepared at high pH. The same trend was found for micropore volume, given that BET surface area is always strongly related to micropores. The total pore volume and consequently mesopores volume decreased with decreasing R/C ratios (i.e. with increasing pH). This trend was clearly shown for carbon xerogels, whose total pore volume decreased from 1.4 cm^3 g^{-1} (pH = 5.45) to less than 0.10cm^3 g^{-1} (pH = 7.35).

In general, the texture of carbon material can be easily controlled through the precursor/catalyst ratio (or through the initial pH of the solution), but it also depends on the type of precursor, catalyst and synthesis conditions, for example. Tannin-based carbon aerogels, and even more carbon xerogels, exhibited quite different behaviour from RF carbon aerogels [12,40]. In the case of tannin carbon aerogels, total pore and also mesopore volumes increased with pH, whereas maxima of surface area and micropore volume were observed at pH 4 – 5 [23]. On the other hand, Horikawa [59] noticed also for RF carbon aerogels that total pore and mesopore volumes can increase when increasing the pH of the initial solution.

TEM micrographs of RF carbon gels have shown that the size of the carbon nodules decreases when the initial pH of the precursor solution increases. Diameters were estimated from the micrographs: the nodule size decreases from about 25–30 nm to 5–10 nm when R/C decreases from 1000 to 50 [40]. At such a high magnification, cryogels cannot be distinguished from aerogels of the same composition. The size of carbon xerogels nodules is rather similar that of the corresponding aerogel, xerogels just having a higher density [40].

3.3.3 Additional treatments

As emphasized above, carbon gels obtained by pyrolysis of organic aero-, cryo- or xerogels are micro and mesoporous materials with easily controllable porous properties through the change of different synthesis parameters. After pyrolysis, most carbon gels present BET surface area within the range 500 – 800 m^2 g^{-1}, and easily accessible mesopores throughout a connected network of macropores. Such characteristics may lead interesting applications to carbon gels such as adsorbents, electrodes of supercapacitor or catalyst supports. Although the obtained results are satisfactory, they cannot always compete with other carbonaceous materials, such as activated carbons, whose surface area can be as high as 3000 m2 g-1 due to their highly developed microporous structure. Therefore, the properties of porous carbon gels can be improved by additional treatments, such as activation and doping.

3.3.3.1 Activation process

Activation is the process by which the porosity of a carbonaceous material is both open and developed. In general, two different types of activation are distinguished, called physical and chemical activation. In physical activation, the porosity is progressively developed by gasification of the carbon through the use of slightly oxidizing gases at high temperatures, such as CO_2 or steam, or even air. This is a two-steps process: organic precursors first require a preliminary pyrolysis for being converted into carbon, next the resultant carbon is activated. Activated carbon gels prepared by physical activation via CO_2 are materials having a highly developed micropore structure without any alteration of the mesoporosity formed during the sol – gel processing [60, 61]. The development of microporosity depends linearly on the weight loss obtained during gasification, called burn-off, provided that the latter is not too high. It is thus possible to control the surface area development rather easily. Roughly, burn – offs lower than 50% lead to microporous material, with increasingly high surface area and micropore volumes. But higher burn-offs lead to materials whose porosity is so widened that their BET surface area decreases due to the prevalence of meso and macropores. In other words, physical activation both opens and widens the pores. For avoiding this, and even though some residues may remain in the final product, chemical activation should be preferred. Besides, this is a one-step process requiring lower temperatures [60,61].

Chemical activation is one of the most common techniques used to prepare activated carbons from any kind of organic precursor. The precursor is first impregnated by an activating agent, such as orthophosphoric acid, a Lewis acid ($ZnCl_2$), or a strong alkaline hydroxide such as NaOH or KOH [62, 63], and the mixture is directly pyrolysed at temperatures ranging from 450 to 900°C. Disadvantages may be the corrosiveness of the chemical activation process, and the need of a subsequent washing step. However, depending on precursor, amount of activating agent, temperature, etc., almost purely microporous or purely mesoporous carbons can be obtained, whereas both kinds of pores generally coexist after physical activation. By changing the activation conditions, it should be possible to control the development of micropores in carbon gels having an already controlled mesopore/macropore network.

3.3.3.2 Metal doping of carbon gels

As it is well known, carbon gels are micro- and mesoporous materials with very good and controllable structural properties such as low density, high surface area, and connected

porosity. Therefore, they offer the possibility of incorporating metallic species in the carbon framework. Carbon gels doped with metals or metallic compounds can be used as electrodes for electric double-layer capacitors [64, 65] and as catalysts for different reactions [67], including fuel cells [66, 67]. Metal-doped carbon gels have also been prepared in order to modify structure, conductivity, and adsorption behaviour of carbon gels. It was proved that transition metals incorporated into the carbon aerogels structure seem to be the best catalysts for graphitizing them at very high temperatures [67].

Three different methods are possible for introducing metal species into carbon gels:

1) Dissolving the metal precursor into the initial liquid solution
2) Introducing a functionalized moiety with binding sites for the metal ions into the initial mixture or in the organic gel
3) Depositing the metal precursor on the organic or carbon gel by different methods.

A number of metal-containing carbon gels have already been prepared and characterized. For example, carbon aerogels and xerogels have been successfully doped with metals such as Na, K, Mg, Zr, Cr, Mo, W, Mn, Fe, Ru, Co, Ni, Pd, Pt, Cu, Ag, Ce and Eu [67]. Depending on required properties and applications of metal – doped carbon materials, the metal must remain accessible to gases or liquids. In catalysis or electrochemistry for instance, the metal surface should be easily reached by reactants. Accessible metal nanoparticles can be dispersed on pre-existing carbon supports by impregnation, electrodeposition or ion exchange. On the other hand, some applications require the metal to be isolated from the outside for avoiding its leaching or oxidation. For example, carbon-encapsulated metal particles are of great interest for magnetic recording media, magnetic toner in xerography, or contrast agent in magnetic resonance imaging [68, 69]. Typical metal dispersion in pores of carbon gels is presented in figure 29.

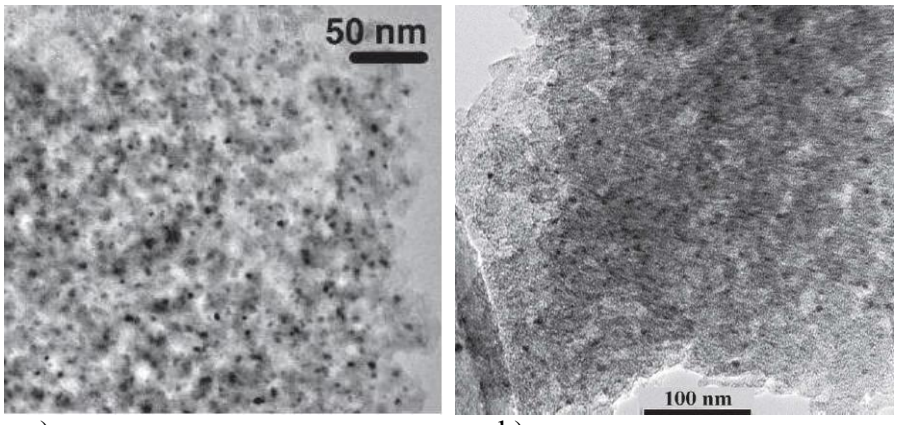

a) b)

Fig. 29. TEM images of (a) Ni – doped carbon xerogel [71]; b) Co – doped carbon aerogels [70].

Chapitre 4: Applications of carbon gels

Due to their unique porous properties and very low density, carbon gels may have a number of useful applications. Carbon gels can be used as highly efficient adsorbents of volatile or liquid contaminants, or as catalyst supports. Many studies have also confirmed that they can be used as electrodes in Electric Double-Layer Capacitors (EDLC), and even for storing hydrogen or methane. Before carbonisation, the organic precursor hydrogels can also be used as heat insulators, or for drug delivery in medicine. In this chapter, the most promising applications of carbon gels are briefly described.

4.1 Carbon gels as adsorbents

4.1.1 VOCs adsorption

Volatile organic compounds (VOCs) are a group of chemicals having the following properties: they easily pass from the liquid to the vapour state due to their high vapour pressure, they have a low solubility into water, and their boiling point is usually within the range 50 – 250°C at normal pressure. VOCs are by-products of many industrial processes and represent a source of environmental pollution. Therefore, standards of emission control exist in many countries, by specifying the maximum acceptable VOC content in the environment. Such VOC content determines the mass of volatile organic compounds that can be released by a given industrial product ready for use, and is expressed, in the case of liquids, in grams per litre (g L-1) of this product [72].

Carbon gels are known as very good adsorbents in Solid – Phase Extraction (SPE), which is an efficient method of concentrating dilute pollutants from the environment. Experiments carried out with RF carbon cryogels microspheres have shown that such mesoporous carbon gels are much better adsorbents than typical microporous commercial granular activated carbons (GAC). This finding has been explained by the presence of both micropores, which give a high specific surface area, and mesopores, which enhance intraparticle diffusion and then shorten the adsorption time. In contrast, GAC is a typical microporous material having a huge specific surface area, sometimes higher than 2000 m^2 g^{-1}, but with a low mesopore volume. It was also proved that the amount of adsorbed VOCs on the carbon microspheres could be tuned depending on the size of mesopores or the volume of micropores. Studies have also shown that carbon microspheres had better adsorption properties than GAC for VOC removal in the presence of humidity. It was indeed observed that adsorption performances of

a VOC adsorption module prepared from carbon gel microspheres were hardly influenced by moisture [72, 74].

4.1.2. Adsorption of halides from water

In addition to the problems associated to air pollution by VOCs, an important concern is the presence of halide ions in drinking water. The presence of bromide (Br^-) and iodide (I^-) in water resources can result in the formation of undesired inorganic and organic bromine- and/or iodine-containing by-products if an oxidative treatment is applied during drinking water production. During chlorination, a large variety of brominated and iodinated organic by-products can be formed which may be potentially harmful. Some of them, such as iodoform and brominated phenols, have a very low taste and odor thresholds in water, and should absolutely be removed. The main limitation of ozonation process of bromide-containing waters is the formation of bromate, because it is potentially carcinogenic. The investigations carried out by Sanchez-Polo et al. [73, 75] have shown that Ag – doped carbon aerogels can successfully be used in the removal of halide ions from drinking water. Silver – doped materials had slightly lower BET surface areas, within the range 428 – 845 $m^2 g^{-1}$, than non-doped, carbon aerogels. However, their surface area, micro – and mesopore volumes could be controlled by physical activation. Activation processes have indeed increased the surface area and micropore volume of Ag – doped materials, while mesopore and macropore volumes decreased. The influence of activation on adsorption capacity and affinity of the anion for the adsorbent was also evidenced.

An increase of the adsorption capacity was observed with an increase in the concentration of Ag(I) at the aerogel surface, whatever the anion considered. Moreover, it was shown that the aerogel sample prepared in absence of Ag had no appreciable capacity to remove halide from water. This suggests that adsorption of halides took place as a result of specific Ag(I) – halide interactions at the carbon surface. Ag – doped aerogels presented high adsorption capacity (3.01 μmol g^{-1}) and quite high affinity of the anion for the adsorbent (257 g L^{-1}). Carbonization and activation of aerogels considerably increased, even twice, its capacity to adsorb halide anions from water. This was caused by a higher concentration of Ag – adsorption sites and an increase of the basicity of the carbon surface. These facts can also be explained by presence of other chemisorption interactions involved in halide adsorption. There are indeed attractive electrostatic interactions between the positively charged carbon

surface at the working pH and the negatively charged halide anions, thus favouring the halide adsorption process.

Based on the adsorption isotherms of halide onto Ag-doped carbon aerogels, it can be concluded that the adsorption capacity of the adsorbent and the affinity for anions increase when the latter are smaller and more polarized [73]. Moreover, the presence of chloride and dissolved organic matter in the water decreases the adsorption capacity of other halides onto the carbon surface. It was observed that halide adsorption onto commercial activated carbon (Sorbo-Norit) is much lower than that of Ag-doped carbon aerogels. Based on this, it can be concluded that the adsorption of halide ions on doped aerogels is controlled by a chemical interaction with Ag(I) surface site [73, 75].

4.1.3 Sulphured organic compounds adsorption

In this subsection, the adsorption of sulphured organic compounds, such as thiophenes, benzothiophenes, and dibenzothiophenes on carbon gels is addressed, in relation to supply of fuel cells. Fuel cells are considered as one of the most interesting alternative to the present power sources for both mobile and stationary applications. Fuel cells are indeed able to convert chemical energy directly into electrical energy with high efficiency and low emission of pollutants. The most extensively investigated fuel cells are hydrogen-powered fuel cells (e.g. polymer electrolyte membrane fuel cells). However, the lack of infrastructure for hydrogen distribution and storage necessitates the development of technologies for producing hydrogen from various sources such as methanol, gasoline, and diesel [76,77].

Gasoline and diesel seem to be the best fuel for hydrogen production due to their high energy densities, ready availability, and proved safety for transportation and storage. Nevertheless, the great disadvantage of such fuels is their content of sulphured organic compounds, whose typical level currently ranges from 0.5 to 3000 parts per million in weight (ppmw). In contrast, the sulphur content of hydrocarbon fuels has to be reduced to less than 0.1 ppmw for fuel cell applications, because it has a detrimental effect on the performances of catalysts used in reforming, water gas shift reactors, and fuel cell stacks. However, reducing the amount of sulphured compounds in gasoline and diesel to required level is extremely difficult using traditional methods, which don't produce satisfactory results. Therefore, Haji et al. [76] proposed the selective adsorption of sulphured compounds on RF-based carbon aerogel (CA). Adsorption measurements have shown that carbon aerogels displayed suitable

adsorption capacity for refractory sulphured compounds such as dibenzothiophene (DBT) and 4,6-dimethyldibenzothiophene (4,6-DMDBT). Application of Langmuir's equation led to an adsorption capacity of 11.2 and 15.1 mg S/g of dry CA for carbon aerogels having average pore sizes of 4 and 20 nm, respectively. In comparison, the capacity of undisclosed transition metal compound (5 wt%) supported on silica gel is 1.1 mg S/g of adsorbent, as calculated by integration of the breakthrough curves [76, 77], whereas a Cu-doped Y zeolite designed for the adsorption of sulphured compounds from commercial diesel presented an adsorption capacity of 18.9 mg S/g.

DBT was more easily and more quickly adsorbed on carbon aerogels having higher average pore size than was 4,6-DMDBT. This may be due to steric effects caused by the two-methyl groups of 4,6-DMDBT. Furthermore, the faster adsorption rate can be related to the lower internal mass transfer resistance due to the larger pore size. The higher capacity can be explained by the changes in the physical and chemical properties of the RF carbon aerogels surface, which depends on the initial dilution of the gel. The selectivity in the adsorption by carbon aerogels of DBT in the presence of naphthalene was also investigated. The obtained results were comparable for both average pore sizes. However, the presence of naphthalene had a negative impact on the amount of DBT adsorbed on the carbon surface.

4.2 Carbon gels for energy storage

4.2.1 Carbon gels for hydrogen storage

Hydrogen storage is an intensively explored domain of science due to the expected application of hydrogen as the energy vector of the future. During recent years, the amount of studies on carbon materials as hydrogen storage systems has increased, because carbon is a potentially good adsorbent, combining low density and high adsorption/desorption kinetics. It was found that carbons having highly developed microporous structure and a narrow micropores size distribution centred on around 0.7 nm are the most suitable for this purpose.

Although a significant part of researches focus on hydrogen storage on activated carbons presenting such characteristics, carbon gels are also of interest. They can indeed also present an ensemble of favourable properties, such as high specific surface area, microporosity, low weight and thus good adsorption capacity. There are many papers reporting good storage properties of modified carbon gels. Raw carbon aerogels prepared from resorcinol and furfural, and carbon xerogels prepared from resorcinol and formaldehyde, didn't present

attractive storage properties: 2.2wt% at 77K and 1.7 MPa and 1.83 wt% at 77K and 2 MPa, respectively. However, such storage properties could be improved by additional treatment such as activation and doping. Tian et al. have examined hydrogen storage on resorcinol – furfural carbon aerogels prepared with the use of KOH [78] or acetic acid [79] as catalysts, and next activated with CO_2. Their results have shown that hydrogen storage of carbon aerogels catalysed with KOH reached 5.2 wt% at 77K and 2.5 MPa after activation at 1000°C, and 3.1 wt% at 77K and 2.8 MPa after activation at 900°C. In contrast, non-catalysed samples only reached 4.2 wt% at 77K and 2.7MPa and 2.9 wt% at 77K and 2.7 MPa after activation at 1000 and 900°C, respectively. The authors concluded that the basic catalyst KOH was beneficial for creating micropores, which is a practical method to increase hydrogen storage capacity of carbon aerogels. Moreover, for the catalysed samples, the heat-treatment at high temperatures caused an increase of pore volume and a shift of the pore-size distribution towards wider pores.

Similar values of hydrogen uptake were obtained for carbon aerogels and carbon xerogels catalysed with acetic acid and activated with CO_2. For these samples, the maximum hydrogen uptake at 77K was 5.4 wt% at 4.6 MPa and 4.9 wt.% at 4.6 MPa for aerogels and xerogels, respectively. As expected, the authors observed that the method of drying had an influence on the textural properties. Carbon aerogels had surface areas 19% higher, and micropore volumes 12% higher, than those of carbon xerogels, resulting in a 10% higher hydrogen uptake [79].

In addition to the choice of a suitable catalyst and activation, doping is another method of improving hydrogen storage properties of carbon gels. Many different elements can be used as doping agents, such as cobalt [70], nickel [71] or nitrogen [80]. Carbon xerogels doped with nitrogen were prepared by carbonization of samples in argon atmosphere and submitting the samples to an atmosphere of pure ammonia at different temperatures. The presence of nitrogen was shown to have a significant influence on surface area and pore volume development. Increasing the time spent in ammonia during the carbonization of RF xerogels systematically led to higher BET surface area and micropore volume than those of samples only carbonized at the same temperature. Now, hydrogen uptake generally increases linearly with micropore volume and surface area of carbon gels. This trend was also observed in the case of N – doped carbon xerogels. The hydrogen uptake of raw carbon gels carbonized within the temperature range 650 – 950°C varied from 1.83 to 1.88 wt% (77K, 2 MPa), whereas samples doped with nitrogen had hydrogen uptake within the range 1.91 – 2.93 wt% (77K, 2MPa), depending of the final temperature of carbonization. Samples heat-treated in

NH_3 at temperature of carbonization presented higher hydrogen uptakes: 2.53 wt% - 3.24 wt% (77K, 2MPa).

However, though encouraging, these hydrogen storage capacities remain rather far from the target of 6 wt. % H_2 established for 2010 by the US Department of Energy (US-DOE). However, values of 5.3 wt. % were reported at 77K for some carbon gels [78], which is close to the aforementioned target.

4.2.2 Carbon gels as electrodes for Electric Double Layer Capacitors (EDLC)

Electrochemical energy storage, especially as electrodes of supercapacitors, is an application that has been suggested since the first carbon gels have been prepared and characterized. Supercapacitors are new and promising booster power supplies, which are able to meet the growing demand of mobile energy storage devices. The growing interest in this type of systems is due to their much lower energy density, higher power and much longer shelf and cycle life than secondary batteries. EDLC electrodes have been fabricated using activated carbon, carbon black, carbon aerogel and carbon cloth. Currently, many researches focus on carbon gels because of their attractive properties such as high electrical conductivity (25–100 Scm^{-1}), high porosity (80–98%), controllable pore structure and high surface area (up to 1100 m^2g^{-1}). Their monolithic form also allows their use as such, no binder being required for making electrodes.

Carbon gels prepared from different precursors, such as resorcinol (R), cresol, phenolic resin and tannin (our work), used in different synthesis conditions and dried by different methods have been tested as electrodes for EDLC. The role of the precursor in the final electrochemical properties of carbon gels it not significant, since carbon gels prepared from different chemicals can present comparable values of specific capacitance, ranging from 26 to 150 F g^{-1}. More important are the conditions of synthesis, such as precursor/catalyst molar ratio or precursor/water weight ratio. The resultant specific capacitance changes with the amount of catalyst (C) used. For example, increasing the R/C ratio led to an increase of specific capacitance of carbon electrodes, as shown by cyclic voltammetry whatever the scan rate. Moreover, the amount of catalyst has no influence on the shape of the voltammograms, which are almost similar for all samples prepared with different R/C [81]. Babic et al. [9] have shown that the concentration of resin in the initial solution strongly influenced the specific capacitance of carbon cryogels prepared from Resorcinol – Formaldehyde: increasing

the concentration decreased the specific capacitance, whatever the scan rate. However, in this case, only one sample, prepared with R/W = 20 presented rectangular-like cyclic voltammograms which were reproducible and very symmetric, ensuring that the electric double-layer charging/discharging process was reversible. The voltammograms did not present significant peaks revealing the presence of redox processes, and contribution of surface functional groups (pseudocapacitance) was found to be negligible. In contrast, cyclic voltammograms of other samples were not symmetric, and the capacitance increased with the potential, especially for the sample of R/W = 50. This feature shows that the charging process was slow, probably due to a high internal resistance related to too narrow pores. These results show how the electrochemical performances are related to pore structure, and hence to synthesis parameters. Examples of cyclic voltammograms are presented in figure 30.

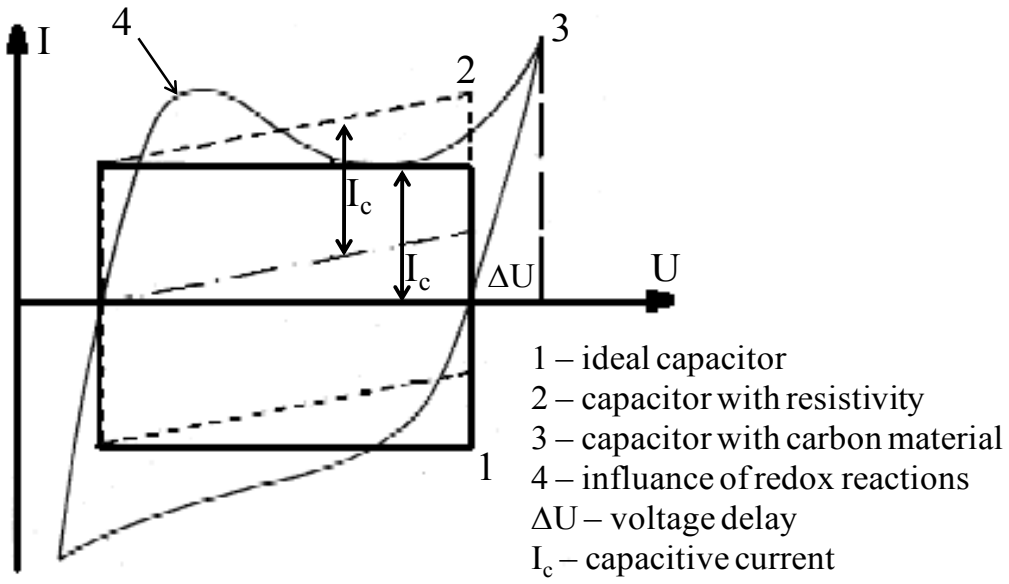

Fig. 30. Typical cyclic voltammograms and main quantities of interest that can be derived [82].

Our own work on electrochemical properties of phenol-formaldehyde – based carbon cryogels [30] concluded that specific capacitance can differ with micro/mesopore fraction in carbon gels. It was proved that samples possessing high mesopore fractions had also high specific capacitances. In contrast, the lowest specific capacitance was obtained for samples having the highest micropores fraction, see figure 31.

Interestingly, no clear influence of BET surface area on electrochemical performances of carbon gels could be found. A lower specific capacitance at comparable or even higher BET surface area may be explained by a lower accessibility of the electrode surface to the ions of the electrolyte, especially the micropore surface [83]. How micropores contribute to the

capacitance is a question that has been debated for a long time. Some authors suggested that electrical double-layer formation could not occur in aqueous electrolytes for micropores [85], while others claimed that micropores wider than 0.5 nm could be accessible to aqueous electrolytes [82, 85]. Anyway, a number of studies already concluded to the lack of correlation between capacitance and BET surface area. This finding is due to the fact that the surface area measured by adsorption of nitrogen at 77K is not representative of the actual electrode/electrolyte interface area [30].

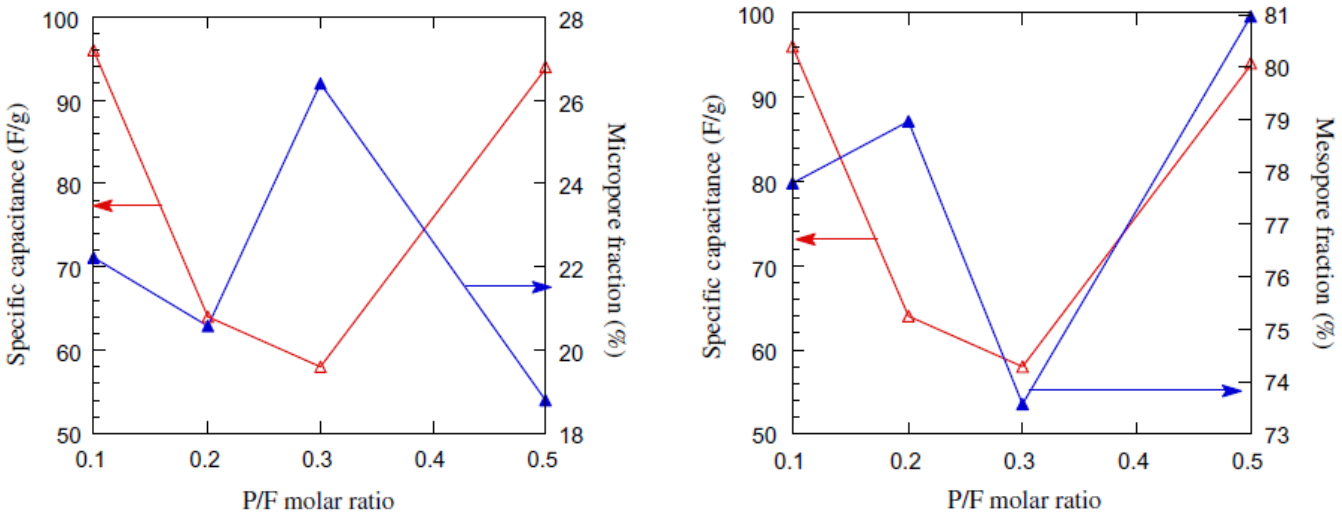

a) b)

Fig. 31. Influence of the type of porosity on the specific capacitance: a) micropore fraction; b) mesopore fraction [30].

4.3 Carbon gels as catalyst supports

Carbon gels and their metal – doped derivatives can also be used as catalyst supports and as catalysts, respectively. Examples of reactions catalyzed by metal-doped carbon aerogels and xerogels are environmental and fuel cell applications, C=C double-bond hydrogenation, skeletal isomerization, hydrodechlorination, and other reactions, including synthesis of methyl *tert*-butyl ether, Knoevenagel condensation, Mizoroki–Heck coupling reaction, and Michael addition [67]. In this section, only environmental and fuel cells applications, taken as examples, are discussed.

4.3.1 Environmental applications

In the case of environmental applications, metal – doped carbon gels have been used for treating both gaseous and liquid phases. The first group of reactions, in the gas phase, included volatile organic compound (VOC) oxidation (e.g., toluene and xylene oxidation) and NO reduction. It was proved that in the case of Pt – doped carbon aerogels, the combustion of VOCs can take place at a temperature lower than 473 K, a temperature reported for some Pt/Al_2O_3 catalysts. Additionally, the VOCs combustion curves can be very steep and shifted towards lower temperatures when increasing the Pt particle size. Surprisingly, larger Pt particles were more active than smaller ones in xylene combustion. This finding suggested that VOC combustion is a Pt-structure-sensitive reaction, as already described for benzene combustion on Pt/Al_2O_3 [87,88]. Smaller Pt particles formed strong Pt–O bonds in xylene combustion, explaining their lower combustion activity compared to that of larger particles deposited on the same support.

Metal – doped carbon aerogels can also work as reducing agents, as catalyst or catalyst support for the removal of nitrogen oxides. Basing on the investigations of Liu et al. [86], it has been shown that carbon in Co – and Cu – doped carbon xerogels can play a double role as a support for the metal and as a reducing agent for NO. The authors have also shown that the method of doping can have an influence on the resultant reduction properties. For example, Cu – doped carbon xerogels obtained by dissolving Cu nitrate in the initial RF mixture led to about 90% of NO conversion to N_2 at 773 K, wherein this rate was maintained for 1000 minutes onstream. In contrast, the same materials prepared by impregnation were led to 85% of NO conversion to N_2 at 773 K, and the conversion rate decreased gradually with time onstream. The reaction of combustion reads:

$$2NO + C \rightarrow N_2 + CO_2$$

The same reaction made with raw, non-doped, carbon xerogels led to about 10% of NO conversion, clearly indicating the catalytic effect of the metal. Co-doped carbon xerogels showed the same behaviour as that of Cu-doped carbon xerogels.

The second type of reactions takes place in the liquid phase and includes the catalytic wet air oxidation (CWAO) of aniline solutions and advanced oxidation processes (AOPs) (e.g., catalytic ozonation and photo-oxidation of pollutants).

The removal of aniline was carried out over Pt – doped carbon xerogels comprising 1 wt% of Pt. A large percentage of mesopores contributed to the surface area (around 70% of

$724 m^2 g^{-1}$). It was proved that the mesoporous character of the carbon gels and their concentration of surface oxygen complexes facilitated aniline adsorption onto the support and subsequent reaction on the Pt active sites. A high mesoporous surface area, like that of the carbon xerogels, allowed higher diffusion rates than those corresponding to a purely microporous material. In addition, the basicity of aniline favoured its adsorption onto acidic supports [89].

4.3.2 Fuel cells

Carbon gels are also known as supports for Pt-based electrocatalysts for proton-exchange membrane fuel cells (PEMFCs), also named polymer–electrolyte fuel cells. These fuel cells are convenient and environmentally acceptable power sources for portable and stationary devices and electric vehicle applications [106]. PEMFC systems can use H_2 or methanol as fuel. This last type of fuel cell is sometimes called DMFC (direct methanol fuel cell). In comparison to other carbonaceous materials commonly used as supports of electrocatalysts, such as carbon blacks, Pt – doped carbon aerogels (Pt content = 20 wt%) present lower electrically active Pt surface: less than 25 % against around 50 % for carbon black. It was suggested that some Pt nanoparticles were buried in pores and were partially wetted by the liquid electrolyte. However, Pt – doped carbon aerogels presented two or three times higher catalytic activity than catalysts supported on carbon blacks, indicating that oxygenated species introduced during the air treatment enhanced the catalytic oxygen reduction reaction (ORR).

Other investigations have shown that Pt supported on carbon aerogels can also be used as cathodic catalysts in PEMFC at ambient pressure. Platinum catalysts indeed present rather high open-circuit voltages and larger electrochemical surface areas than those of commercial catalysts. Catalyst loading ranged from 0.06 to 0.6 mg cm^{-2}. Additionally, increasing the average pore size of the aerogel from 16 to 20 nm caused an increase of the cell's performance in terms of power density. Moreover, Pt particles located in the pores of carbon aerogels had a low tendency to agglomeration and sintering during cell operation. Pt-doped carbon aerogels with a Pt loading of 0.1 mg cm^{-2} presented high power densities, up to $0.8 mW cm^{-2}$, under fuel cell operation conditions in air at ambient pressure.

The method of preparation, e.g. the nature of the metallic precursor, has an influence on the final properties of Pt-based catalysts. Some authors claimed that catalysts prepared with $H_2[PtCl_6]$ presented the best ORR specific activity, whereas the activity of catalysts prepared

from $[Pt(NH_3)_4](OH)_2$ was low, despite the higher dispersion of Pt. This fact can be explained by the size of Pt particles which can affect the ORR activity. Pt particles with smaller size presented lower activity. The influence of pore texture of carbon aerogels on the Pt surface area (dispersion) and ORR activity was also examined. It has been shown that the pore texture affected neither the dispersion of Pt nor the ORR activity. However, the latter increased when the mean mesopore size increased, so that the highest ORR performances were obtained for a mesopore size of 18.5 nm [107].

In the case of DMFC systems, Pt-based catalysts (Pt, Pt–Ni, and Pt–Ru) were used as an anodic catalyst, because of the ability of Pt to activate the C–H bond cleavage in the temperature range of fuel cell operation (298 to 403 K). Experimental results have shown that Pt catalysts based on carbon xerogels (Pt content = 10%) were characterized by a mean particle size of around 2 nm. The activity of the catalyst for methanol electro-oxidation was higher in alkaline than in acidic solution. Moreover, the surface Pt slowly developed more favourable sites during cycling in alkaline solution. Pt supported on carbon xerogels showed better performances in methanol electro-oxidation than Pt supported on carbon black such as Vulcan XC-72R at identical metal content. In this case, pore texture presented an influence on catalytic properties. The large mesopore fraction of carbon xerogels significantly enhanced the metal dispersion, favouring methanol electro-oxidation. In some cases, the properties of Pt – doped carbon gel catalysts used in methanol electro-oxidation could be improved by using bimetallic systems such as Pt – Ni or Pt – Ru, which presented a significantly higher activity [108 – 111].

Chapitre 5: Analytical methods used in the present work

5.1 Assessment of porosity

Pores play a major role in the properties of carbonaceous materials, allowing chemicals (gases and vapours) to be retained or to go throughout the porous structure. Porosity in carbons is generally considered as a series of tubes or slits that might be interconnected in an arborescent way. However, some researchers claim that such models of porosity may be misleading. A more realistic approach considers that carbon atoms form a covalently bonded three-dimensional network within which turbostratic arrangements of graphene sheets exist but present gaps giving rise to the porous structure [90 and refs therein].

Porosity in carbon gels can be investigated with several methods such as adsorption – desorption of gases, mercury porosimetry, mercury or helium pycnometry, X-ray or neutron small-angle scattering, optical or electron microscopy, etc. Each method provides information on some types of porosity (open or closed), having a given width range (from mm to nm and below), and has its own limitations. In the present work, only N_2 adsorption, Hg porosimetry and pycnometry, and He pycnometry have been used. Adsorption and porosimetry give information about surface area, pore volumes and pore size distribution, whereas true and bulk densities are determined by He and Hg pycnometry, respectively.

Pores have been categorized according to their widths by IUPAC [91], which gives a guideline applicable to all kinds of porosity:

- Micropores: < 2 nm, among which micropores can also be separated as:
  - Ultramicropores: < 0.7 nm
  - Supermicropores 0.7 - 2.0 nm
- Mesopores: 2 – 50 nm
- Macropores > 50 nm

Carbon gels may comprise all classes of pores, and the three types of pores are formed in different ways. Micropores are present inside the nodules of the gels, i.e. between the polymer chains, and are developed during the pyrolysis of the precursor organic gels. Meso- and macropores are located between the nodules. The hierarchical porosity present in carbon materials may be illustrated as shown in figure 32.

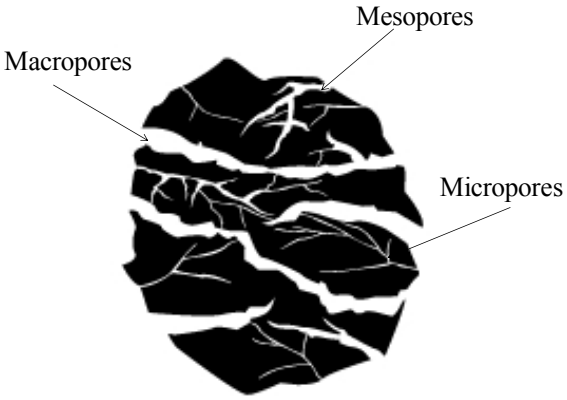

Fig 32. Porosity in carbon

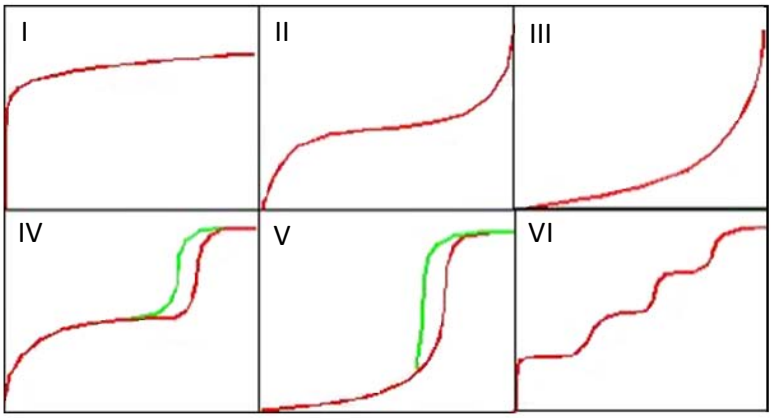

Fig 33. Types of adsorption isotherms

Isotherms of gases adsorbed onto the surface of a solid provide a significant amount of information about this solid and about the gas-solid interaction, including [90]:

- assessment of the surface chemistry and fundamentals involved in the adsorption process;
- estimation of surface area, pore volume and pore-size distribution;
- Performances of carbons used in industrial processes.

All adsorption isotherms should fit at least one, or at least a combination of two or more, of the six recognised types classified by Brunauer, Deming, Deming and Teller (BDDT system) [92] . Figure 33 presents the possible types of isotherms.

Type I: Typical isotherm of adsorbents having a predominantly microporous structure, such as activated carbons or activated carbon gels. As the majority of micropore filling occurs at relative pressures below 0.1, the adsorption process is usually complete at a relative pressure of ~ 0.5. This isotherm is known as Langmuir-type.

Type II: It is a typical isotherm for carbons having both micro- and mesoporosity, such as carbon gels. It may also describe physical adsorption of gases by non-porous solids.

Type III: This class of isotherm is characteristic of weak adsorbate-adsorbent interactions and is most commonly associated with both non-porous and microporous adsorbents. The adsorption of water molecules on carbon, wherein the primary adsorption sites are based on oxygen moieties, can be described by this type of isotherm.

Type IV: A hysteresis loop, which is commonly associated to the presence of mesoporosity, is a common feature of Type IV isotherms, the shape of which is unique to each adsorption system. Capillary condensation gives rise to a hysteresis loop and these isotherms also exhibit a limited uptake at high relative pressures.

Type V: This isotherm is characteristic of weak adsorbate-adsorbent interactions, and is indicative of microporous or mesoporous solids. The reasons behind the shape of this class of isotherm are the same as those of Type III, i.e. weak interactions between the adsorbate and the adsorbent, leading to low uptakes at low relative pressures. However, once a molecule has been adsorbed at a primary adsorption site, the adsorbate-adsorbate interaction, which is much stronger, becomes the driving force of the adsorption process, resulting in accelerated uptakes at higher relative pressure. Again, water adsorption on carbon may exhibit a Type V isotherm [90 and refs therein].

Type VI: This isotherm arises from adsorption on highly homogeneous, non-porous surfaces, and for which the monolayer capacity corresponds to the step height. One example is the adsorption of krypton at 90 K on graphitised carbon black or on exfoliated graphite [90 and refs therein].

5.2 N_2 adsorption – desorption analysis

The basic parameters of porous structure of carbon gels, detailed below, were determined through the treatment of nitrogen adsorption – desorption isotherms obtained at 77K with an automatic analyzer ASAP 2020 (Micromeritics, USA).

- S_{BET} : specific surface area, calculated from the Brunauer – Emmett – Teller (BET) equation [93] at a relative pressure of $p/p_0 \approx 0.2$,
- V_T : total pore volume measurable by adsorption techniques (hence much lower than the true, total, pore volume of the porous solid considered), calculated on the basis of the maximum adsorption of nitrogen at $p/p_0 = 0.99$ [95],
- V_{DR} : volume of micropores calculated from the Dubinin-Radushkevich (DR) equation [94] at $p/p_0 \approx 0.015$,
- L_0 : average micropore width determined according to Stoeckli's equation [96],
- Pore-size distribution (in the range of micropores and narrow mesopores), calculated by application of the Density Function Theory (DFT) [97],
- V_{meso} : mesopore volume, calculated as the difference $V_T - V_{DR}$.

Nitrogen adsorption – desorption measurements at 77K thus allow determining the most important pore texture parameters, but only deal with open pores wider than 0.7 nm up to narrow mesopores, typically 20 – 30 nm wide.

5.3 Hg porosimetry

Mercury porosimetry is a characterization method of pore texture which gives access to both mesopore- and macropore-size distribution. Depending on the pressure of mercury that can be reached for intruding the porosity, the narrowest pores possibly studied corresponds to narrow mesopores. In our case, using an AutoPore IV 9500 (Micrometrics, USA), the highest pressure was 400 MPa, so the pores accessible with this method were wider than 3.6 nm. The experiments were performed in two steps: low- (0.001– 0.24 MPa) and high-pressure (0.24–414 MPa) steps. Pore-size distribution was calculated by using Washburn equation 7:

$$L = -\frac{4\gamma cos\theta}{P} \quad (7)$$

where L is the pore width (nm), γ is the surface tension of mercury (0.48N/m), θ is the contact angle between mercury and the material, usually fixed at 140°, and P is the intrusion pressure (MPa).

However, application of Washburn's equation is limited to solids which are only intruded by mercury, and not deformed by the pressure necessarily applied. Some materials, such as mesoporous silica but also organic and carbon gels, present a low compressive strength and may undergo a preliminary densification without any intrusion. After such pressure-induced shrinkage, intrusion may occur abruptly. In these conditions, Washburn's equation should be used straightforwardly [98]. When pressure-induced compression of the samples occurs, equation 8 relating the pore width to the applied pressure needs to be applied:

$$L = \frac{k_f}{P^{0.25}} \quad (8)$$

where k_f is a constant to be determined experimentally, and characterizing the material stiffness. Equation (8) stands for the usual collapse mechanism of gels submitted to isostatic pressure [98]. Such pore collapse occurs at pressures lower than a critical value P_c, which is determined experimentally for each sample, as well as the constant k_f. Above P_c, mercury intrudes the porosity, and the well known Washburn' equation (7) can be applied. At the critical pressure at which intrusion finally occurs, identification of eqs. (7) and (8) allows determining the constant k_f (nm $MPa^{0.25}$):

$$k_f = \frac{4\gamma cos\theta}{P_c^{0.75}} \quad (9)$$

5.4 He and Hg pycnometry

Helium pycnometry was used for determining the true density of organic and carbon gels. The true density, ρ_s, sometimes called skeletal density, is the density of the solid from which the investigated material is made. In our case, the true density was measured by He pycnometry with an Accupyc II 1340 device (Micromeritics). For that purpose, samples were crushed in a mortar, so errors due to possible closed porosity could be avoided. Helium being able to penetrate into the smallest pores, the volume of the solid backbone was derived. Before the experiments, the samples were dried at 120°C in vacuum overnight, in order to avoid the distorting effect of adsorbed water on the volume measurement. Samples were then introduced inside a calibrated volume (1 cm^3), and the induced change of helium pressure was accurately measured. Each determination included 10 helium flushes prior to analysis, in order to clean the volume chamber, and 50 analytical runs [30].

Mercury pycnometry was used for determining the bulk density, ρ_b, of organic and carbon gels. The experiments were carried out in the same apparatus as the one already used for Hg porosimetry (AutoPore IV 9500, Micrometrics). For that purpose, the volume of mercury introduced into a sample holder of known, calibrated, volume, containing the sample formerly under vacuum, was measured at low pressure: 34.5 mbar. In these conditions, mercury neither intruded the pores of the material nor could collapse it, so its volume could be deduced accurately. Bulk density, also called "apparent density", was checked by weighing a number of cylindrical or parallelepiped samples of known dimensions: differences always lower than 10%, and most of times around 5%, were found.

From the values of bulk and skeletal densities, determination of both total porosity, ϕ (dimensionless), and specific pore volume, V_p ($cm^3\ g^{-1}$) of the materials was possible, using equations 10 and 11, respectively:

$$\phi = 1 - \frac{\rho_b}{\rho_s} \tag{10}$$

$$V_p = \frac{1}{\rho_b} - \frac{1}{\rho_s} \tag{11}$$

5.5 Infrared spectroscopy

Generally speaking, spectroscopy is a helpful mean of investigating molecular structure and composition based on the study of the interaction of radiation with matter. The substance

of interest is submitted to an electromagnetic radiation of known incident intensity and frequency, and the transmitted or scattered intensity and frequency are recorded. More exactly, spectra are recorded in the form of graphs showing the resultant intensity after interaction with matter, as a function of wavelength. The mid- infrared region (IR) extends from 4000 cm^{-1} to 400 cm^{-1}. It is surrounded by far-IR region from 400 cm^{-1} to 10 cm^{-1} and near-IR region from 12500 cm^{-1} to 4000 cm^{-1}. Functional groups and other specific groups of atoms usually absorb infrared radiation in a relatively narrow frequency range, regardless of the structure of the rest of the molecule. IR spectroscopy is thus a rather simple, commonly used, identification method of functional groups and other elements of molecule structure. The method is rapid, sensitive, easy to handle and may be used whatever the nature of the sample: gaseous, liquid or solid. Important aspects are the qualitative and quantitative information that can be derived from the spectra [100, 101].

Typical IR spectrum were shown in figure 27 (chapter 3), wherein transmittance [%T] was plotted versus wavelength [cm^{-1}]. From the features of an IR spectrum, such as number of infrared absorption bands, their intensities and their shapes, the various moieties and groups of atoms can be identified. The energy of infrared light is too small to cause electronic excitations, but is sufficient to induce changes in the oscillatory energy of the bonds between atoms. The atoms in molecules vibrate constantly (oscillate around their equilibrium position), and the vibrations corresponding to different energy levels of molecules are called oscillatory levels. As a result of radiation absorption, the molecule is excited to a higher energy level. The differences in energy of vibrational levels typically range from 4 to 40 kJ mol-1. Depending on the kind of vibrational motion, stretching vibrations (changes of bond lengths) and deformation vibrations (changes of bond angles) can be distinguished. Deformation vibrations may be additionally subdivided into bending modes, twisting or torsion modes, wagging and rocking modes. Further subdivision refers to the symmetry of the vibration (e.g., symmetric or antisymmetric, in-plane or out-of-plane) [100].

Characteristic vibrations of groups of atoms are of great help for determining the structure of polyatomic molecules. In organic compounds, characteristic vibrations usually occur at wavelengths ranging from 4000 to 1500 cm^{-1}, whereas inorganic compounds containing heavy atoms may exhibit characteristic vibrations at much lower wavelengths. All wavelengths of organic compounds below 1500 cm^{-1} involve molecular vibrations, usually bending motions, which represent a characteristic fingerprint of the entire molecule or of large fragments of the molecule.

The infrared spectra can be obtained from two different kinds of spectrometers, dispersive and Fourier-transform (FT) spectrometers. The FTIR spectrometers are commonly used because the measurement is much faster and more sensitive. In FTIR spectrometers, radiations of all wavelengths are simultaneously treated, instead of being treated successively in dispersive spectrometers [100]. Figure 34 presents a schematic diagram of an FTIR analyser.

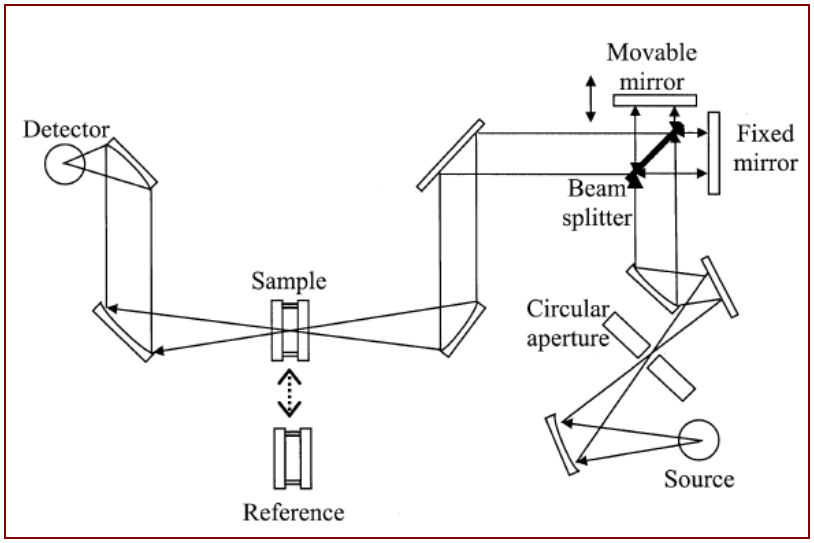

Fig. 34. Diagram of FTIR spectrometer [100].

5.6 Mass spectroscopy

In mass spectroscopy methods, the molecules to be analysed are converted into free gaseous ions and subsequently subjected to magnetic and electric fields in high vacuum where they are separated according to their mass/charge ratios. They are next dispatched toward the detector which measures the abundance of each kind of ion. Depending on structure and physical and chemical properties of the compounds, different kinds of ionization techniques are used. The most known and widely used is Electron Ionisation (EI). This classical ionisation method utilizes an electron beam passing through the sample in the gas phase. As a result of such collision of molecules with electron beam, another electron and a positively charged molecular ion or, more often, ionized fragments corresponding to a certain molecular substructure, are created. The molecules are usually bombarded with electrons with an energy of 70eV, because the ionization energy of a typical organic molecule is less than 15eV. Sputtered electrons transfer an excess energy to newly created molecular ions, which is partly used for breaking covalent bonds having a binding energy within the range 3 - 10 eV. Breaking covalent bonds is usually highly reproducible and characteristic of the investigated

compound, thus the fragmentation process is predictable and hence mass spectroscopy can be the basis of a complete determination of the structure. EI is the oldest and best known ionisation method and can be applied to all volatile and thermally stable compounds. Complex mixtures of compounds that were either enough volatile as such, or which needed to be chemically modified for enhancing their volatility, may be analysed by combined gas chromatography – mass spectrometry (GC-MS) [100].

The molecules may also be ionized by a laser beam. The most commonly used lasers are of two types: based on CO_2, emitting a radiation in the far infrared, and based on solid Nd / YAG that emits radiation in the UV range with a wavelength of 266nm. Therefore, a mass analyser compatible with pulsed ionisation methods has to be used. Typically, time-of-flight (ToF) analysers are employed, but several hybrid systems, such as quadrupole time of flight (Q-ToF) or high resolution Fourier Transform Ion Cyclotron Resonance (FTICR) analysers have been successfully adapted [102]. In Matrix – Assisted Laser Desorption/Ionisation method (MALDI – MS), the samples are first dissolved in a solution containing an excess of a matrix (see below) that contains a chromophore absorbing at the laser wavelength. UV lasers are mainly used for protein analysis, whereas for certain biopolymer classes such as polynucleotide, IR lasers are employed. The laser ionisation scheme is presented in figure 35.

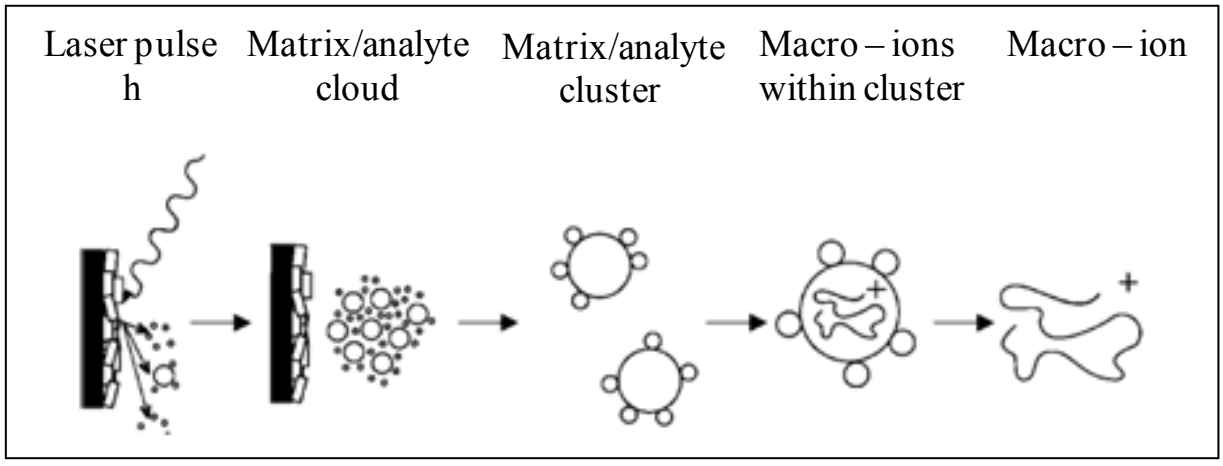

Fig. 35. Diagram of ionisation/desorption in MALDI-MS. A matrix/analyte cloud is desorbed from the microcrystalline matrix/sample preparation by a laser pulse. Proton-transfer from matrix ions is thought to be primarily responsible for the subsequent generation of analyte ions [100].

Two matrices, nicotinic acid and sinapinic acid, absorbing the radiation emitted by the laser used, are widely used and allow to analyze compounds with a molecular weight as high as 200000 – 300000 Da. The sample/matrix mixture is irradiated with laser pulse, causing the desorption of singly charged ions that are accelerated towards the mass analyzer. These ions

have little excess energy and a low tendency to fragmentation, therefore, this method may be used to analyze macromolecules.

5.7 Nuclear Magnetic Resonance

Nuclear magnetic resonance (NMR) is a widely used method for characterizing synthetic and natural materials, finding their structures, and studying chemical reactions. Absorption of electromagnetic radiation in the range of radio waves is carried out by nuclei placed into a strong, homogeneous, magnetic field. Absorption is possible only for atoms whose nuclear spin is non-zero, since such atoms behave as magnets, taking different orientations relative to the applied magnetic field. In the case of the most commonly used methods, atomic nuclei 1H, 13C or 15N have a spin I = 1/2, leading to two orientations of their nuclear moment in the applied field: parallel and anti-parallel to the direction of the field. As a consequence, these orientations possess two energy levels, the difference between them depending on the nucleus and on the magnetic field intensity [100 – 103].

The absorption spectra are obtained by irradiation of samples by radio waves in a narrow frequency range near the characteristic frequency of the spectrometer, which depends on the magnetic field. Radiation absorption occurs when the investigated nuclei in the sample has the suitable frequency in a given applied magnetic field. Figure 36 schematically presents the NMR device.

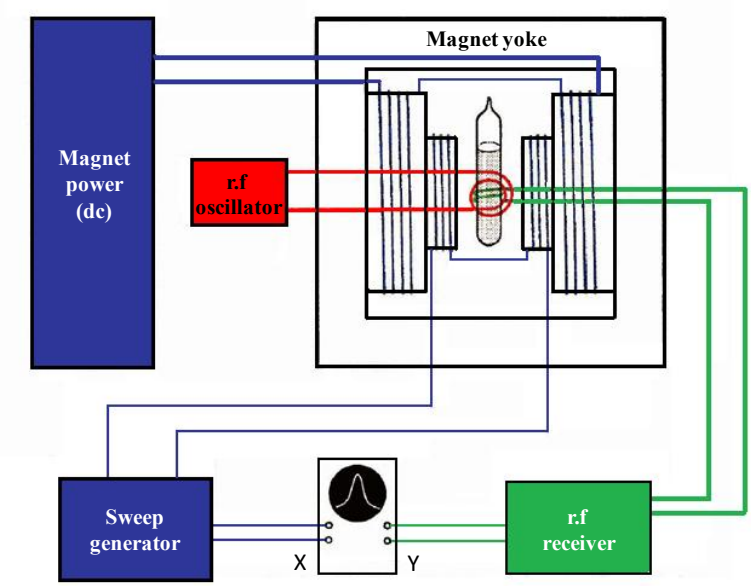

Fig. 36. Diagram of NMR spectrometer [103].

Given that the absorption frequency depends on the intensity of the magnetic field, relative spectra are always produced, so spectra obtained from NMR spectrometers working in different conditions can be compared directly. For that purpose, the absorption frequencies are expressed relatively to that of a reference compound. Such reference molecule absorbs radio wave frequencies that are not absorbed by most other compounds. The position of the signals is determined as a shift versus the reference. The most commonly used reference is tetramethylsilane (TMS). The shift versus the reference is called chemical shift, as it depends on the structure of the molecule. Being a small fraction of the reference absorption, it is generally expressed in ppm according to equation 12.

$$\delta = \frac{\nu - \nu_r}{\nu_r} 106 \text{ ppm} \quad (12)$$

where ν is the observed NMR absorption frequency of the sample, and ν_r is that of the reference molecule [100 – 103]. The chemical shift δ is a function of the electron density around the nuclei, since the electrons are directly involved in the diamagnetic shielding, locally attenuating the applied magnetic field. Because of this, each chemical group has its own chemical shift, so the structure of the molecule can be identified.

Magnetic resonance phenomenon also occurs in the case of 13C nuclei, but their signals are considerably harder to observe than for 1H. This is due to the low abundance of 13C isotope in nature. Molecules of organic compounds contain very few atoms of 13C and recording the signals coming from them requires very sensitive devices and a long accumulation time. 13C NMR spectra contain clearly visible signals from each non-equivalent carbon atoms in the studied molecules. The same principles apply to 1H and 13C NMR spectroscopy, except the following significant differences:

- Signal intensity doesn't strictly depend on the number of atoms.
- Spin - spin coupling does not exist between the carbon atoms, because all signals are single.
- Shift range is much larger and is in the range 0 - 200 ppm (against 0 - 12 ppm for 1H NMR). 13C NMR can thus lead to much more detailed spectra.

5.8 Scanning Electron Microscopy

The idea of a microscope in which an image of the sample surface is obtained through the scanning of an electron beam was first suggested by Knoll in 1935 [104]. Nowadays, the

scanning electron microscope (SEM) is undoubtedly the most widely used of all electron beam instruments. A SEM has several features accountable for its popularity, such as the versatility of its various modes of imaging, the excellent spatial resolution now achievable, the very simple sample preparation and condition, the relatively straightforward interpretation of the acquired images, and the possibility of associating other instruments such as spectroscopy and diffraction techniques. The present generations of microscopes give rise to a wide range of magnifications, from 5 to 500000×, giving access to nearly nanometre dimensions. From the impact of the electron beam on the sample surface, a variety of particles are generated. There are three types of electrons that can be emitted from the interaction of primary (i.e. incident) electrons with the surface of the specimen: secondary electrons with energies <50 eV, Auger electrons produced by the decay of the excited atoms, and backscattered electrons that have energies close to those of the incident electrons.

The generated signals, represented schematically in figure 37, may be utilized to form images or diffraction patterns of the examined samples, or can be analyzed to provide spectroscopic information. De-excitation of atoms formerly excited by the electron beam also produces continuous and characteristic X-rays as well as visible light. These signals can be used to ensure qualitative, semi-quantitative, or quantitative information on the elements or phases present in the investigated regions. Generated signals are the product of strong electron – samples interactions, which depend on the energy of the incident electrons and on the nature of the samples.

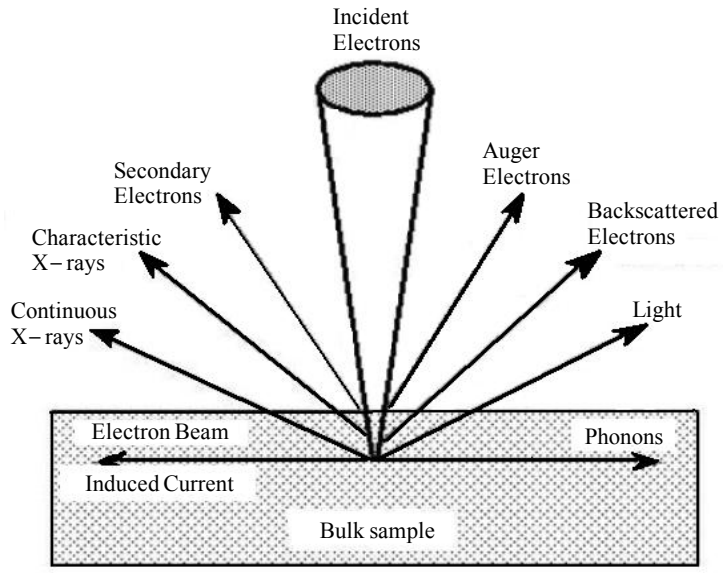

Fig. 37. Illustration of the signals generated inside a scanning electron microscope when an electron beam interacts with a sample [104].

Samples are scanned by the electron beam which is moved and tilted by coils. The deviation of the beam forming the image on the Cathode Ray Tube (CRT) screen is synchronized with that of the beam scanning the sample [104], see Figure 38. The signals from the sample surface, most often due to secondary or reflected electrons, are intercepted by a detector whose main parts are constituted of a scintillator and of a photomultiplier. The scintillation phenomenon allows the transformation of secondary electron energy in light pulses, which are then amplified by a photomultiplier. Output signal from the detector affects the brightness of the image displayed on the CRT screen, while the magnification of microscope is related to the ratio between the sizes of sample's scanned areas and of CRT screen.

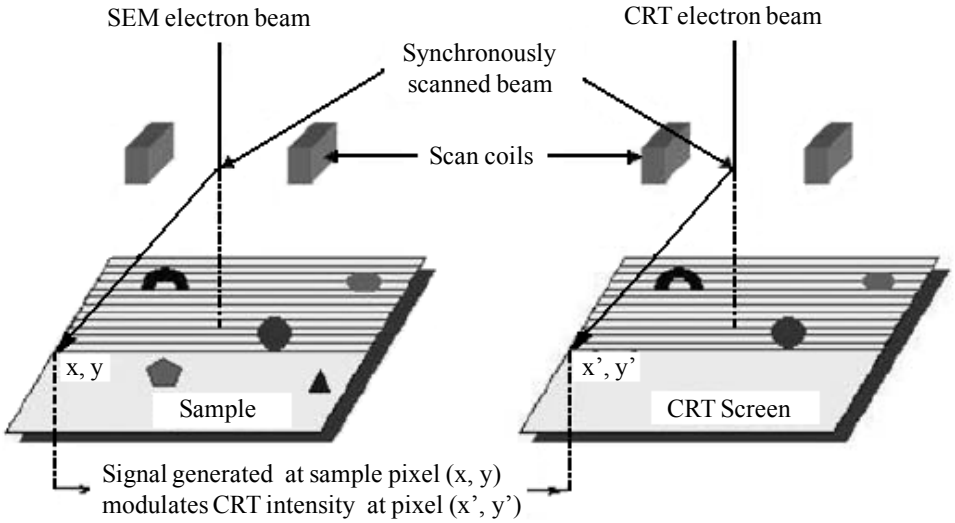

Fig. 38. Schematic diagram illustrating the formation of SEM images.

As a result of elastic scattering of electrons by atoms of the sample, backscattered electrons (BSE) are emitted. The ability of sample atoms to scatter electrons principally depends on their atomic number Z, and increases with it. Information about the chemical composition of the sample can thus be obtained. Difference in Z, and hence in composition, gives visible BSE image contrast, areas of lower atomic numbers being darker, and vice-versa. Other primary electrons absorbed by the sample are non-elastically scattered by subsurface layers of atoms, and gradually lose their energy. This phenomenon leads to the formation of low-energy secondary electrons, which are sensitive to the topography of the sample surface. A lot of secondary electrons leave the ridges of the sample and are detected, while very few remain in the sample and are not seen by the detector, thus allowing the creation of topographic contrast of the sample [104]. Figure 39 presents the example of a carbon aerogel (our work).

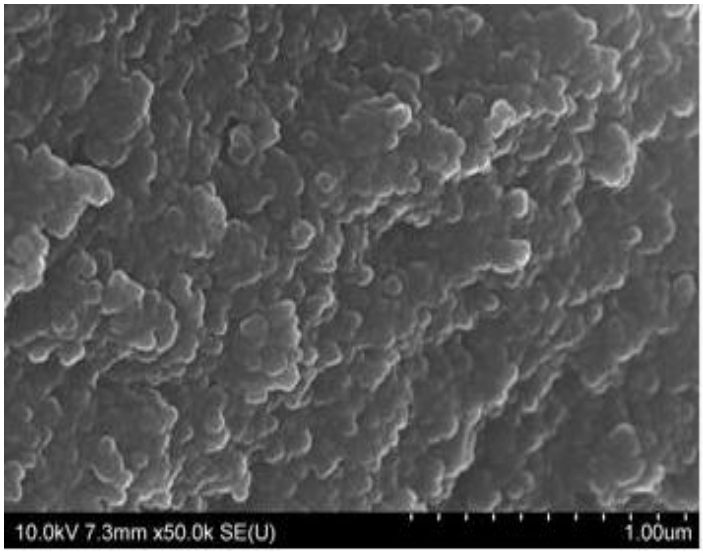

Fig. 39. Secondary electrons SEM image of the surface of an RF carbon aerogel. The nodular structure is clearly seen.

5.9 Electrochemical characterization

Electrochemical properties of carbon gels were determined by measuring the charge capacity of the electrical double-layer which develops at the electrode / electrolyte interface. Electrodes were prepared in the form of pellets, which consisted of 75 – 85 wt% carbon gel, 5wt% acetylene carbon black (highly conductivity additive), and 10wt% polyvinylidene difluoride (binder). The compounds were mixed and pressed into pellets. Two pellets of comparable mass (within the range 4 - 14 mg) and identical composition were then electrically separated by a glassy fibrous paper, placed in a Teflon Swagelok® cell which was filled with 4 M H_2SO_4 aqueous solution. However, the measurements can also be carried out in other electrolytes such as KOH aqueous solution, or in organic solvents such as tetraethylammonium tetrafluoroborate ($TEABF_4$) in acetonitrile [30, 82, 105]. The illustration of the cells we built is presented in figure 40.

Cyclic voltammetry measurements were made, in which the electrodes were charged and discharged periodically at a controlled potential at a rate changing from 2 to 200 mV s-1. Two quantities were thus simultaneously recorded: the potential of the capacitor (X-axis) (within the range 0.05 – 1.05V), and the instantaneous charge / discharge current (Y axis), giving voltammograms as already shown in figure 30 (chapter 4). Galvanostatic charge/discharge experiments were also carried out, leading to the very similar values of specific capacitances (see below).

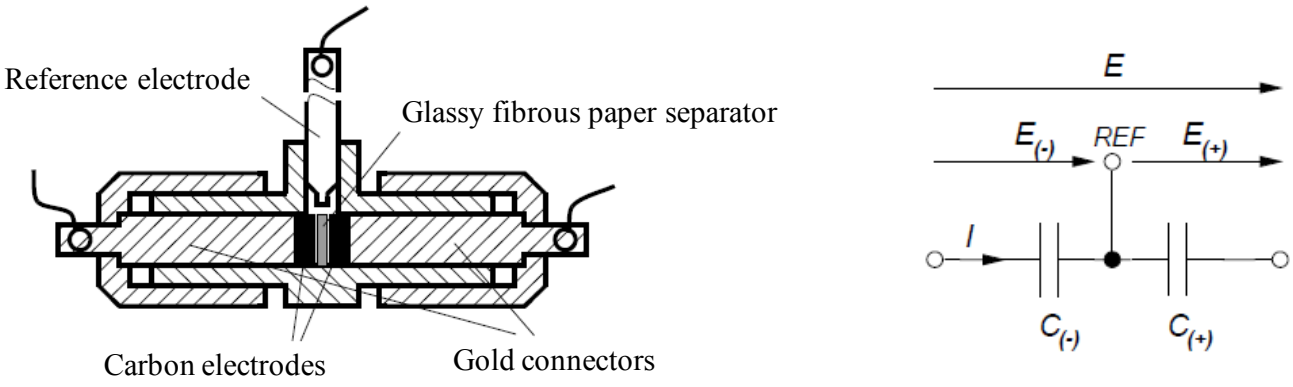

a) b)

Fig. 40. a) Illustration of measurement cell based on two working electrodes made of carbon gels, and one reference electrode; b) Electric diagram of the resultant capacitor [105].

The specific capacitance of the carbon gels, C (F g^{-1}), was estimated from the aforementioned methods. From cyclic voltammetry, C was calculated as:

$$C = \frac{2I}{ms} \tag{13}$$

where I is the measured current (A), m is the mass of active material (hence carbon gel) in the electrode (g), and s is the scan rate (mV s^{-1}).

Galvanostatic charge/discharge measurements were carried out at constant current density adjusted at 0.2 or 1A g^{-1}. In such experiments, the capacitor was cyclically charged and discharged at constant current, and the voltage variations were recorded. From galvanostatic charge/discharge, C was calculated as:

$$C = \frac{I_d \Delta t}{\Delta V} \tag{14}$$

where I_d is the discharge current per gram of active material (A g^{-1}), Δt is the discharge time (s) and ΔV is the voltage drop (V). In both equations (13) and (14), the factor 2 comes from the fact that the capacitance measured from the cell is two equivalent single – electrode capacitors arranged in series. Whether the capacitances were measured by one or the other method, a good agreement was always observed.

Références bibliographiques

1. Henish HK. *Crystal growth in gels*. Penn State University Press, University Park, Pa, 1970
2. Brinker CJ, Scherer GW. *Sol – gel science. The physics and chemistry of Sol – gel processing.* Academic Press Inc., San Diego, 1990.
3. Hench LJ, West JK, *The sol – gel process*. Chemical Reviews 90, 1990, 33 – 72
4. Sakka S., editor. *Handbook of sol – gel science and technology. Processing, characterization and applications.* Springer, 2005.
5. Flory PJ. *Principles of polymer chemistry.* Cornell University Press, Ithaca, NY, 1953
6. Pekala RW. *Organic aerogels from the polycondensation of resorcinol with formaldehyde.* Journal of Materials Science 24(9), 1989, 3221–3227.
7. Tamon H, Ishizaka H, Yamamoto T, Suzuki T. *Preparation of mesoporous carbon by freeze drying.* Carbon 37(12), 1999, 2049–2055.
8. Fricke J, editor. *Aerogels: proceedings of the first international symposium, Würzburg, Fed. Rep. of Germany, September 23-25, 1985.* Springer – Verlag, New York, 1986.
9. Babic B, Kaluderovic B, Vracar L, Krstajic N. *Characterization of carbon cryogel synthesized by sol–gel polycondensation and freeze-drying.* Carbon 42(12-13), 2004, 2617–2624.
10. Leonard A, Job N, Blacher S, Pirard JP, Crine M, Jomaa W. *Suitability of convective air drying for the production of porous resorcinol–formaldehyde and carbon xerogels.* Carbon 43(8), 2005, 1808–1811.
11. Durairaj RB. *Resorcinol: chemistry, technology and applications.* Springer – Verlag, Berlin Heidelberg, 2005
12. Fairén-Jiménez D, Carrasco-Marín F, Moreno-Castilla C. *Porosity and surface area of monolithic carbon aerogels prepared using alkaline carbonates and organic acids as polymerization catalysts.* Carbon 44(11), 2006, 2301–2307.
13. Job N, Pirard R, Marien J, Pirard JP. *Porous carbon xerogels with texture tailored by pH control during sol–gel process.* Carbon 42(3), 2004, 619–628.
14. Szczurek A, Amaral-Labat G, Fierro V, Pizzi A, Celzard A. *The use of tannin to prepare carbon gels. Part II. Carbon cryogels.* Carbon 49(8), 2011, 2785 – 2794.
15. Pizzi A. *The chemistry and development of tannin-based adhesives for exterior plywood.* Journal of Polymer Science 22(8), 1978, 2397–2399.
16. Pizzi A. *Advanced wood adhesives technology.* Marcel Dekker Inc., New York, 1994.

17. Pichelin F, Nakatani M, Pizzi A, Wieland S, Despres A, Rigolet S. *Structural beams from thick wood panels bonded industrially with formaldehyde-free tannin adhesives.* Forest Products Journal 56(5), 2006, 31–36.
18. Tondi G, Fierro V, Pizzi A, Celzard A. *Tannin-based carbon foams.* Carbon 47(6), 2009, 1480–1492.
19. Kraiwattanawong K, Mukai SR, Tamon H, Lothongkum AW. *Preparation of carbon cryogels from wattle tannin and furfural.* Microporous and Mesoporous Materials 98(1–3), 2007, 258–266.
20. Kraiwattanawong K, Mukai SR, Tamon H, Lothongkum AW. *Improvement of mesoporosity of carbon cryogels by acid treatment of hydrogels.* Microporous and Mesoporous Materials 115(3), 2008, 432–439.
21. Sengil IA, Ozacar M. *Biosorption of Cu(II) from aqueous solutions by mimosa tannin gel.* Journal of Hazardous Materials 157(2–3), 2008, 277–285.
22. Ogata T, Nakano Y. *Mechanisms of gold recovery from aqueous solutions using a novel tannin gel adsorbent synthesized from natural condensed tannin.* Water Research 39(18), 2005, 4281–4286.
23. Szczurek A, Amaral-Labat G, Fierro V, Pizzi A, Masson E, Celzard A. *The use of tannin to prepare carbon gels. Part I. Carbon aerogels.* Carbon 49(8), 2011, 2773 – 2784.
24. Job N, Panariello F, Marien J, Crine M, Pirard JP, Leonard A. *Synthesis optimization of organic xerogels produced from convective air-drying of resorcinol–formaldehyde gels.* Journal of Non-Crystalline Solids 352(1), 2006, 24–34.
25. Pizzi A, Stephanou A. *On the chemistry, behavior, and cure acceleration of phenol–formaldehyde resins under very alkaline conditions.* Journal of Applied Polymer Science 49(12), 1993, 2157–2170.
26. Korszak WW, editor. *Technologia Tworzyw Sztucznych.* WNT, Warszawa, 1981.
27. Pekala RW, Alviso CT, Lu X, Gross J, Fricke J. *New organic aerogels based upon a phenolic-furfural reaction.* Journal of Non-Crystalline Solids 188(1-2), 1995, 34-40.
28. Lee KN, Lee HJ, Kim JH. *Synthesis of phenolic/furfural gel microspheres in supercritical CO_2.* Journal of Supercritical Fluids 17(1), 2000, 73–80.
29. Wu D, Fu R, Sun Z, Yu Z. *Low-density organic and carbon aerogels from the sol–gel polymerization of phenol with formaldehyde*. Journal of Non-Crystalline Solids 351(10-11), 2005, 915–921.

30. Szczurek A, Jurewicz K, Amaral-Labat G, Fierro V, Pizzi A, Celzard A. *Structure and electrochemical capacitance of carbon cryogels derived from phenol–formaldehyde resins.* Carbon 48(13), 2010, 3874–3883.
31. Pizzi A. *Wood adhesives chemistry and technology*. Marcel Dekker Inc., New York, 1983.
32. Scopelitis E, Pizzi A. *The chemistry and development of Branched PRF Wood Adhesives of Low Resorcinol Content*. Journal of Applied Polymer Science 47(2), 2003, 351 – 360.
33. Wilson, MJR, Hench LL. *Real Time Monitoring of Silica Gel Drying Behavior. Proceedings of 4th International Conference on Ultrastructure Processine of Ceramics. Glasses and Composites*. Tucson, AZ, 1989
34. Wilson, MJR, Hench LL. *Drying of Gel Silica Monoliths*. Journal of Non-Crystalline Solids 121(1-2), 1990, 915–921.
35. Job N, Sabatier F, Pirard JP, Crine M, Leonard A. *Towards the production of carbon xerogel monoliths by optimizing convective drying conditions*. Carbon 44(12), 2006, 2534–2542.
36. Kistler S. S. *Coherent expanded aerogels and jellies*. Nature 127, 1931, 741.
37. Wu D, Fu R, Zhang S, Dresselhaus MS, Dresselhaus G. *The preparation of carbon aerogels based upon the gelation of resorcinol–furfural in isopropanol with organic base catalyst.* Journal of Non-Crystalline Solids 336(1), 2004, 26–31
38. Qin G, Guo S. *Drying of RF gels with supercritical acetone.* Carbon 37(7), 1999, 1168–1169.
39. Szczurek A, Amaral-Labat G, Fierro V, Pizzi A, Masson E, Celzard A. *Porosity of resorcinol-formaldehyde organic and carbon aerogels exchanged and dried with supercritical organic solvents*. Materials Chemistry and Physics 129(3), 2011, 1221-1232
40. Job N, Thery A, Pirard R, Marien J, Kocon L, Rouzaud JN, et al. *Carbon aerogels, cryogels and xerogels: influence of the drying method on the textural properties of porous carbon materials.* Carbon 43(12), 2005, 2481–2494.
41. Tamon H, Ishizaka H, Yamamoto T, Suzuki T. *Influence of freeze-drying conditions on the mesoporosity of organic gels as carbon precursors.* Carbon 38(7), 2000, 1099–1105.
42. Mastalerz P. *Chemia organiczna*. Wydawnictwo Chemiczne, Wrocław, 2000
43. Burchell TD, editor. *Carbon Materials for Advanced Technologies*. Elsevier Science Ltd. Kidlington, 1999.
44. http://www.chem1.com/acad/webtext/chembond/cb07.html, July 2011.

45. Zazula JM. *On graphite transformations at high temperature and pressure induced by absorption of the LHC beam*. CERN. LHC Project Note 78 / 97, 1997
46. Dresselhaus MS. *Future directions in carbon science*. Annual Review of Materials Science. 27, 1997, 1–34.
47. Hoffman U, Wilm DZ. *The crystal structure of graphite*. Elektrochem. 42, 1936, 504.
48. Franklin RE. *The interpretation of diffuse X-ray diagrams of carbon*. Acta Crystallographica 3, 1950, 107 – 121.
49. Kuhn J, Brandt R, Mehling H, Petricevic R, Fricke R. *In situ infrared observation of the pyrolysis process of carbon aerogels.* Journal of Non-Crystalline Solids 225, 1998, 58–63.
50. Guilminot E, Fischer F, Chatenet M, Rigacci A, Berthon-Fabry S, Achard P, Chainet P. *Use of cellulose-based carbon aerogels as catalyst support for PEM fuel cell electrodes: Electrochemical characterization.* Journal of Power Sources 166(1), 2007, 104–111.
51. Tsioptsias C, Michailof Ch, Stauropoulos G, Panayiotou C. *Chitin and carbon aerogels from chitin alcogels.* Carbohydrate Polymers 76(4), 2009, 535–540.
52. Li WC, Lu AH, Guo SC. *Characterization of the microstructures of organic and carbon aerogels based upon mixed cresol–formaldehyde.* Carbon 39(13), 2001, 1989–1994.
53. Lorjai P, Chaisuwan T, Wongkasemjit S. *Porous structure of polybenzoxazine-based organic aerogel prepared by sol–gel process and their carbon aerogels.* Journal of Sol-Gel Science and Technology 52(1), 2009, 56–64
54. Hanzawa Y, Hatori H, Yoshizawa N, Yamada Y. *Structural changes in carbon aerogels with high temperature treatment.* Carbon 40(4), 2002, 575–581.
55. Kipling JJ, Sherwood JN, Shooter PV, Thompson NR. *The pore structure and surface area of high-temperature polymer carbons.* Carbon 1(3), 1964, 321–328.
56. Théry A. *Relation entre l'organisation multiéchelles des aérogels de carbone et leurs propriétés de stockage électrochimique de l'hydrogène*. Université d'Orléans, 2004.
57. Zhang R, Lu Y, Meng Q, Zhan L, Wu G, Li K, Ling L. *On Porosity of Carbon Aerogels from Sol-Gel Polymerization of Phenolic Novolak and Furfural*. Journal of Porous Materials 10(1), 2003, 57–68.
58. Bock V, Emmerling A, Fricke J. *Influence of monomer and catalyst concentration on RF and carbon aerogel structure.* Journal of Non-Crystalline Solids 225, 1998, 69–73.
59. Horikawa T, Hayashi J, Muroyama M. *Controllability of pore characteristics of resorcinol–formaldehyde carbon aerogel.* Carbon 42(8-9), 2004, 1625–1633

60. Contreras MS, Paez CA, Zubizarreta L, Leonard A, Blacher S, Olivera-Fuentes CG, Arenillas A, Pirard JP, Job N. *A comparison of physical activation of carbon xerogels with carbon dioxide with chemical activation using hydroxides.* Carbon 48(11), 2010, 3175 – 3168.
61. Bansal RCh, Goyal M. *Activated Carbon Adsorption*. Taylor & Francis Group, LLC, Boca Raton, FL, 2005.
62. Fierro V, Torné-Fernández V, A. Celzard. *Methodical study of the chemical activation of Kraft lignin with KOH and NaOH.* Microporous and Mesoporous Materials 101(3), 2007, 419–431.
63. Zubizarreta L, Arenillas A, Pirard JP, Pis JJ, Job N. *Tailoring the textural properties of activated carbon xerogels by chemical activation with KOH.* Microporous and Mesoporous Materials 115(3), 2008, 480–490.
64. Lee YJ, Jung JC, Park S, Seo JG, Baeck SH, Yoon JR, Yi J, Song IK. *Effect of preparation method on electrochemical property of Mn-doped carbon aerogel for supercapacitor.* Current Applied Physics 11(1), 2011, 1-5.
65. Yoshizawa N, Hatori H, Soneda Y, Hanzawa Y, Kaneko K, Dresselhaus MS. *Structure and electrochemical properties of carbon aerogels polymerized in the presence of* Cu^{2+}. Journal of Non-Crystalline Solids 330(1-3), 2003, 99–105.
66. Job N, Pirard R, Vertruyen B, Colomer JF, Marien J, Pirard JP. *Synthesis of transition metal-doped carbon xerogels by cogelation.* Journal of Non-Crystalline Solids 353(24-25), 2007, 2333–2345.
67. Serp P, Figueiredo JL. *Carbon materials for catalysis*. John Wiley and Sons, Inc. New Jersey, 2009
68. Huo J, Song S, Chen X. *Preparation of carbon-encapsulated iron nanoparticles by co-carbonization of aromatic heavy oil and ferrocene*. Carbon 42(15), 2004, 3177–3182.
69. Qiu J, Li Ya, Wang Y, An Y, Zhao Z, Zhou Y, Li W. *Preparation of carbon-coated magnetic iron nanoparticles from composite rods made from coal and iron powders*. Fuel Processing Technology 86(3), 2004, 267– 274.
70. Tian HY, Buckley CE, Sheppard DA, Paskevicius M, Hanna N. *A synthesis method for cobalt doped carbon aerogels with high surface area and their hydrogen storage properties*. International Journal of Hydrogen Energy 35(24), 2010, 13242 – 13246.
71. Zubizarreta L, Menendez JA, Job N, Marco-Lozar JP, Pirard JP, Pis JJ, Linares-Solano A, Cazorla-Amoros D, Arenillas A. *Ni-doped carbon xerogels for* H_2 *storage.* Carbon 48(10), 2010, 2722 – 2733.

72. Yamamoto T, Kataoka S, Ohmori T. *Characterization of carbon cryogel microspheres as adsorbents for VOC.* Journal of Hazardous Materials 177(1-3), 2010, 331–335.
73. Sanchez-Polo M, Rivera-Utrilla J, Salhi E, von Gunten U. *Ag-doped carbon aerogels for removing halide ions in water treatment.* Water Research 41(5), 2007, 1031 – 1037.
74. Maldonado-Hodar FJ, Moreno-Castilla C, Carrasco-Marın F, Perez-Cadenas AF. *Reversible toluene adsorption on monolithic carbon aerogels.* Journal of Hazardous Materials 148(3), 2007, 548–552
75. Sanchez-Polo M, Rivera-Utrilla J, Salhi E, von Gunten U. *Bromide and iodide removal from waters under dynamic conditions by Ag-doped aerogels.* Journal of Colloid and Interface Science 306(1), 2007, 183–186.
76. Haji S, Erkey C. *Removal of Dibenzothiophene from Model Diesel by Adsorption on Carbon Aerogels for Fuel Cell Applications.* Industrial & Engineering Chemistry Research 42(26), 2003, 6933 – 6937.
77. Jayne D, Zhang Y, Haji S, Erkey C. *Dynamics of removal of organosulfur compounds from diesel by adsorption on carbon aerogels for fuel cell applications.* International Journal of Hydrogen Energy 30(11), 2005, 1287– 1293.
78. Tian HY, Buckley CE, Wang SB, Zhou MF. *Enhanced hydrogen storage capacity in carbon aerogels treated with KOH.* Carbon 47(8), 2009, 2112 – 2142.
79. Tian HY, Buckley CE, Paskevicius M, Wang SB. *Carbon aerogels from acetic acid catalysed resorcinol–furfural using supercritical drying for hydrogen storage*. Journal of Supercritical Fluids 55(3), 2011, 1115–1117.
80. Kang KY, Lee BI, Lee JS. *Hydrogen adsorption on nitrogen-doped carbon xerogels.* Carbon 47(4), 2009, 1171 – 1180.
81. Li J, Wang X, Huang Q, Gamboa S, Sebastian PJ. *Studies on preparation and performances of carbon aerogel electrodes for the application of supercapacitor*. Journal of Power Sources 158(1), 2006, 784–788.
82. Frackowiak E, Beguin F. *Carbon materials for the electrochemical storage of energy in capacitors.* Carbon 39(6), 2001, 937–950.
83. Probstle H, Schmitt C, Fricke J. *Button cell supercapacitors with monolithic carbon aerogels*. Journal of Power Sources 105(2), 2002, 189–94.
84. Kinoshita K. *Carbon: electrochemical and physicochemical properties.* John Wiley and Sons, New York, 1988.
85. Qu D, Shi H. *Studies of activated carbons used in double-layers capacitors*. Journal of Power Sources 74(1), 1998, 99–107.

86. Liu Z, Wang A, Wang X, Zhang T, *Reduction of NO by Cu–carbon and Co–carbon xerogels*. Carbon 44(11), 2006, 2345 - 2347.
87. Wu JCS, Chang TY. *VOC deep oxidation over Pt catalysts using hydrophobic supports.* Catalysis Today 44(1-4), 1998, 111 – 118.
88. Garetto TF, Apesteguıa CR. *Structure sensitivity and in situ activation of benzene combustion on Pt/Al_2O_3 catalysts.* Applied Catalysis B: Environmental 32(1-2), 2001, 83 - 94.
89. Gomes HT, Samant PV, Serp P, Kalck P, Figueiredo JL, Faria JL. *Carbon nanotubes and xerogels as supports of well-dispersed Pt catalysts for environmental applications.* Applied Catalysis B: Environmental 54(3), 2004, 175 – 182.
90. http://personal.strath.ac.uk/ashleigh.fletcher/adsorption.htm#, July 2011.
91. IUPAC. *Manual of Symbols and Terminology Appendix 2, Pt. 1. Colloid and Surface.* Pure and Applied Chemistry 31, 1972, 578.
92. Brunauer S., Deming L.S., Deming W.S., Teller E., *On the theory of van der Waals adsorption of gases.* Journal of the American Chemical Society 62(7), 1940, 1723-1732.
93. Brunauer S, Emmet PH, Teller E. *Adsorption of gases in multimolecular layers.* Journal of the American Chemical Society 60(2), 1938, 309–319.
94. Dubinin MM. *Fundamentals of the theory of adsorption in micropores of carbon adsorbents – characteristics of their adsorption properties and microporous structures*. Carbon 27(3), 1989, 457–467.
95. Gregg SJ, Sing KSW. *Adsorption, surface area and porosity. 2nd ed.* Academic Press, London, 1982.
96. Stoeckli F, Slasli A, Hugi-Cleary D, Guillot A. *The characterization of microporosity in carbons with molecular sieve effects.* Microporous and Mesoporous Materials 51(3), 2002, 197–202.
97. Tarazona P. *Solid–fluid transition and interfaces with density functional approaches*. Surf. Sci. 331-333, 1995, 989–94.
98. Job N, Pirard R, Pirard JP, Alie C. *Non intrusive mercury porosimetry: pyrolysis of resorcinol–formaldehyde xerogels.* Particle and Particle Systems Characterization. 23(1), 2006, 72–81.
99. Leonard A, Blacher S, Crine M, Jomaa W. *Evolution of mechanical properties and final textural properties of resorcinol–formaldehyde xerogels during ambient air drying.* Journal of Non-Crystalline Solids 354(10–11), 2008, 831–838.

100. Gauglitz G, Vo-Dinh T, editors. *Handbook of Spectroscopy*. WILEY-VCH Verlag GmbH & Co. KGaA, Weinheim, 2003
101. Mazurkiewicz R, editor. *Metody spektroskopowe i ich zastosowanie do identyfikacji związków organicznych: praca zbiorowa*. WNT, Warszawa, 2000.
102. Silverstein RM, Webster FX, Kiemle DJ. *Spectrometric identification of organic compounds.* John Wiley and Sons, New Jersey, 2005.
103. Roberts JD. *Nuclear Magnetic Resonance. Applications to organic chemistry*. McGraw-Hill Book Company, Inc, New York, 1959.
104. Barbacki A, editor. *Mikroskopia Elektronowa.* Wyd. Politechniki Poznańskiej, 2007.
105. Kierzek K. *Materiały węglowe aktywowane wodorotlenkiem potasu*. Politechnika Wrocławska, 2007.
106. Haile SM. *Fuel cells and components*. Acta Materialia 51(19), 2003, 5981 – 6000.
107. Marie J, Berthon-Fabry S, Chatenet M, Chainet E, Pirard R, Cornet N, Achard P. *Platinum supported on resorcinol–formaldehyde based carbon aerogels for PEMFC electrodes: Influence of the carbon support on electrocatalytic properties.* Journal of Applied Electrochemistry. 37(1), 2007, 147 - 153.
108. Samant PV, Fernandes JB, Rangel CM, Figueiredo JL. *Carbon xerogel supported Pt and Pt–Ni catalysts for electro-oxidation of methanol in basic medium.* Catalysis Today 102–103, 2005, 173 – 176.
109. Samant PV, Rangel CM, Romero MH, Fernandes JB, Figueiredo JL. *Carbon supports for methanol oxidation catalyst*. Journal of Power Sources 151(10), 2005, 79 – 84.
110. Figueiredo JL, Pereira MFR, Serp P, Kalck P, Samant PV, Fernandes JB. *Development of carbon nanotube and carbon xerogels supported catalysts for the electro-oxidation of methanol in fuel cells.* Carbon 44(12), 2006, 2516 - 2522.
111. Du H, Li B, Kang F, Fu R, Zeng Y. *Carbon aerogel supported Pt–Ru catalysts for using as the anode of direct methanol fuel cells.* Carbon 45(2), 2007, 429 – 435.

Publications scientifiques publiées/acceptées

Article n°1

Reaction mechanism of Hydroxymethylated Resorcinol adhesion promoter in Polyurethane adhesives for wood bonding

A. Szczurek, A. Pizzi, L. Delmotte, A. Celzard

Journal of Adhesion Science and Technology 24 (2010) 1577 – 1582

Jusqu'à présent, l'hydroxyméthyl résorcinol (HMR), un composé de faible poids moléculaire additionné à des adhésifs tels qu'époxy ou polyuréthane (PU), était connu pour améliorer le collage du bois. Cette action était comprise sur la base de l'interaction du HMR avec le bois lui-même, mais sa réactivité avec l'adhésif n'avait pas été considérée. L'objet de ce travail était de mettre en évidence les réactions mises en jeu par l'HMR avec une colle PU monocomposante, dans laquelle il reste des groupements isocyanates réactifs capables de donner des réticulations supplémentaires en cours d'application.

Deux produits ont été préparés : un mélange résorcinol – formaldéhyde ajouté à une résine pMDI telle que définie ci-dessus, et un mélange de référence obtenu dans les mêmes conditions mais en l'absence de formaldéhyde. Les deux produits ont été séchés et étudiés par RMN du ^{13}C.

L'analyse de ces spectres, combinée à des données de la littérature, a permis de conclure à la formation de liaisons uréthanes entre les groupes méthylols de l'HMR et les groupements isocyanates toujours réactifs de la colle PU. Cette réaction s'ajoute à celle que permet le résorcinol seul, à savoir la formation de liaisons uréthanes entre les groupes hydroxyls du résorcinol et les groupements isocyanates restants. L'adhésif contenant de l'HMR a donc *in fine* de meilleures performances.

Article n°2

Porosity of resorcinol-formaldehyde organic and carbon aerogels exchanged and dried with supercritical organic solvents

A. Szczurek, G. Amaral-Labat, V. Fierro, A. Pizzi, E. Masson, A. Celzard

Materials Chemistry and Physics 129 (2011) 1221– 1232

Au cours de ce travail, nous avons préparé nos premiers aérogels de carbone RF. Pour en réduire le coût, leurs précurseurs organiques ont été séchés par des solvants supercritiques : acétone ou éthanol. Dans ce but, des hydrogels ont préalablement été préparés à pH et stœchiométrie fixes mais avec différentes dilutions dans l'eau, les plus dilués devant donner logiquement les matériaux les moins denses après séchage. Ces hydrogels ont été échangés par ces deux mêmes solvants liquides, acétone ou éthanol, puis traités en autoclave, dans lequel ils ont été convertis en fluide supercritique. Ce dernier a ensuite été échangé par de l'azote circulant dans l'autoclave à la même pression et à la même température, avant de finalement diminuer la pression puis la température à leurs valeurs à l'ambiante.

Les densités apparentes des aérogels organiques résultants ont été mesurées et comparées à ce qu'elles auraient dû être en l'absence totale de retrait. Le retrait (en % volumique) a ainsi pu être déterminé avant, mais aussi après pyrolyse. Les textures poreuses obtenues sont typiques de celles obtenues par un coûteux séchage au CO_2 supercritique. Nous en avons conclu que l'acétone supercritique est aussi performant que le CO_2 dans le même état pour obtenir des aérogels avec très peu de retrait, et ce, quelle que soit la dilution initiale des gels. En revanche, l'éthanol supercritique ne donne les mêmes résultats que si les gels sont peu dilués, donc aptes à résister aux contraintes mécaniques responsables du retrait.

L'analyse par GC-MS des solvants supercritiques condensés en sortie d'autoclave a aussi montré que l'acétone est dégradée en cours de process. Par contre, les gels sont très peu affectés, un seul composé aromatique ayant été détecté en très faible concentration. L'éthanol est quant à lui moins dégradé, mais ce sont les gels qui le sont davantage, comme en témoigne l'abondance et la diversité des aromatiques détectés.

Article n°3

Bimodal activated carbons derived from resorcinol-formaldehyde cryogels

A. Szczurek, G. Amaral-Labat, V. Fierro, A. Pizzi, A. Celzard

Science and Technology of Advances Materials 12 (2011) 035001 (12pp)

Le second article sur la base de gels RF décrit la synthèse de charbons actifs à partir de cryogels activés à l'acide orthophosphorique. Près de 40 matériaux ont été préparés et étudiés systématiquement en termes de structure poreuse, déterminée en croisant les résultats de différentes techniques. Ce nombre d'échantillons correspond à la multiplication des conditions de synthèse : dilution des hydrogels de départ (au travers du rapport massique résorcinol/eau, compris entre 0.025 et 0.5), concentration de l'acide (entre 0.25 et 4M), et temps de contact gel-acide (entre 0.5 et 12h).

Ces différents paramètres ont mis en évidence un comportement complexe, et des impacts très variés des différents paramètres de synthèse sur la porosité finale. De manière à avoir une référence en termes de texture poreuse, les gels organiques RF correspondant à chaque dilution ont été pyrolysés. Il apparaît ainsi, et pour la toute première fois, que l'activation ne développe la porosité que pour les gels suffisamment dilués au départ, et aussi à condition que la concentration de l'acide soit suffisante. Une concentration trop faible combinée à un gel de départ assez dense conduit à une déstructuration du matériau, avec comme principal effet une réduction considérable de la porosité. Contre toute attente, des échantillons moins poreux que leurs homologues simplement pyrolysés peuvent être obtenus.

Par ordre d'importance, la densité initiale des hydrogels a la plus grande influence sur la porosité finale, suivie de près par la concentration de l'acide. L'effet du temps de contact est moindre. Nous avons également déterminé les conditions optimales d'activation, permettant d'obtenir des surfaces spécifiques record pour ce type de matériau et ce type d'activation, de l'ordre de 2200 m^2/g. Des charbons actifs bimodaux micro/macroporeux ont pu être obtenus, grâce auxquels on s'attend à d'excellentes cinétiques d'adsorption/désorption.

Article n°4

Structure and electrochemical capacitance of carbon cryogels derived from phenol–formaldehyde resins

A. Szczurek, K. Jurewicz, G. Amaral-Labat, V. Fierro, A. Pizzi, A. Celzard

Carbon 48 (2010) 3874 – 3883

Cet article est le premier de la thèse décrivant la préparation de gels de carbone bon marché non RF. Dans ce but, le précurseur et le mode de séchage : résine phénol-formaldéhyde et lyophilisation, respectivement, ont été volontairement choisis pour que les matériaux résultants présent un faible coût. Bien qu'il ne soit pas aisément chiffrable, le coût de production doit être nettement inférieur à celui des aérogels de carbone classiques préparés à partir de résorcinol et séchés par CO_2 supercritique. Le but du travail était de démontrer qu'un tel gel de carbone présente des caractéristiques voisines et des propriétés similaires à celles de matériaux plus onéreux. L'étude a porté sur la synthèse, la détermination des paramètres texturaux et sur les performances électrochimiques. Les deux premières parties ont été réalisées à Epinal, et la dernière (électrochimie) a fait l'objet d'un séjour de 2 semaines à l'Université Technique de Poznan, en Pologne.

Des alcogels phénol-formaldéhyde (PF) ont été préparés à pH fixe mais en variant le rapport molaire P/F de 0.1 à 0.5. De la sorte, différentes textures poreuses ont pu être obtenues après échange par le tert-butanol, lyophilisation puis carbonisation à 900°C. En dépit d'une porosité totale toujours très proche de 90%, ces différents matériaux ont en effet présenté des surfaces spécifiques variant du simple au double (environ 300 à 600 m^2/g), mais restant essentiellement mésoporeux (mésoporosité comprise entre 74 et 85%). Ces valeurs sont proches de celles des aérogels RF. Les différences de paramètres texturaux ont entraîné des différences de comportement électrochimique, les meilleures capacités étant proches de 100 F/g pour les matériaux présentant le meilleur compromis : accessibilité de la surface carbonée – pores de bonne taille pour l'adsorption des ions de l'électrolyte.

Article n°5

The use of tannin to prepare carbon gels. Part I: Carbon aerogels

A. Szczurek, G. Amaral-Labat, V. Fierro, A. Pizzi, E. Masson A. Celzard

Carbon 49 (2011) 2773 – 2784

Cet article a été publié comme le premier d'une série de deux, mais en réalité fait suite aux travaux ayant porté sur les cryogels tannin – résorcinol – formaldéhyde (TRF). Ici, les premiers gels de carbone TF sont rapportés. Une seule dilution et un seul rapport T/F ont été choisis pour réaliser une série d'échantillons, dont on a seulement fait varier le pH initial entre 3 et 8. Cette gamme de pH est plus large que ce qui est habituellement possible pour les gels RF. Ces matériaux ont ensuite été séchés dans l'acétone supercritique selon la méthode déjà évoquée dans l'article n°2 présenté dans ce mémoire. Après pyrolyse, les caractéristiques texturales ont été étudiées selon les méthodes désormais classiques : adsorption de N_2, pycnométrie He, porosimétrie Hg. Des spectres de RMN et FTIR ont aussi été obtenus et discutés. Enfin, l'acétone condensée en sortie d'autoclave a été analysée par GC-MS.

Le chromatogramme de l'acétone est presque exactement le même que celui présenté dans l'article n°2 pour les gels RF. Cela prouve que le gel n'est jamais dégradé au cours de ce traitement. Le pH a un effet considérable sur la porosité, et en particulier sur la mésoporosité. La surface spécifique est néanmoins affectée, les plus faibles valeurs étant obtenues aux pH les plus élevées comme dans le cas des gels de carbone RF, mais n'est jamais inférieure à 600 m^2/g. Ces valeurs sont excellentes, comparativement à celles de la littérature. Nous avons montré que les distributions de tailles de pores présentent exactement la même forme, quel que soit le pH. Seul change l'intensité des pics, donc les volumes de pores correspondants.

Enfin ces gels de carbone, qui présentent donc des textures poreuses très proches de celles de leurs homologues RF séchés par CO_2 supercritique, sont cinq fois moins chers de par leur précurseur (80% du coût) et par le mode de séchage. Bien que ne représentant que 4% du coût total, il est intéressant de noter que le séchage par l'acétone supercritique est 1000 fois moins onéreux que celui utilisant du CO_2 supercritique.

Article n°6

The use of tannin to prepare carbon gels. Part II: Carbon cryogels

A. Szczurek, G. Amaral-Labat, V. Fierro, A. Pizzi, A. Celzard

Carbon 49 (2011) 2785 – 2794

Cet article fait référence à nos premiers travaux sur les tannins de mimosa en tant que précurseur de gel. Nous avons commencé à l'utiliser à raison de 2/3 en poids de tannin pour 1/3 de résorcinol, et en présence de deux quantités différentes de formaldéhyde. Le pH de la solution initiale a alors été varié entre 2 et 8, une gamme nettement plus large qu'avec les gels RF. On en attendait donc des textures poreuses plus variées, et à moindre coût. Les hydrogels ont été échangés par le tert-butanol, lyophilisés et pyrolysés. Les mêmes techniques de caractérisation que dans l'article n°5 précédent ont été mises en œuvre.

La gélation étant assez rapide, nous avons pu déterminer les points de gel pour chaque pH initial. Nous avons observé que le minimum de réactivité était obtenu aux pH voisins de 4 – 5, en accord avec ce qui est connu pour les molécules phénoliques en général vis-à-vis du formaldéhyde. Les spectres RMN et FTIR des cryogels organiques ont montré que les réactions étaient plus avancées à pH plus élevé, et que davantage de formaldéhyde conduisait à davantage de réticulation.

Ainsi, aux pH inférieurs à 5, les plus grandes surfaces spécifiques et les plus grandes porosités ont été obtenues pour les cryogels de carbone. Les pH les plus hauts ont conduit à des matériaux pratiquement non-poreux. Comme prévu, une très large gamme de texture poreuse a ainsi été obtenue. En particulier, un décalage des distributions de tailles de pores a été mis en évidence, les pores devenant de plus en plus étroits au fur et à mesure que le pH augmente. Ce comportement est très différent de celui des précédents aérogels de carbone TF. En combinant tous ces différents matériaux, il est donc possible de préparer des porosités sur mesure, et qui conservent toutes les propriétés traditionnelles de gels de carbone : structure nodulaire, mésoporosité très développée, conductivité électrique, etc.

Article n°7

Oligomer distribution at the gel point of tannin-resorcinol-formaldehyde cold-set wood adhesives

A. Pizzi, H. Pasch, A. Celzard, A. Szczurek

Journal of Adhesion Science and Technology (2011) sous presse

Cette étude par spectrométrie MALDI-ToF des oligomères présents dans un gel TRF obtenu à trois pH différents permet de mieux comprendre les mécanismes réactionnels dans ce type de mélange. La résine TRF était, jusqu'à présent, utilisée comme adhésif pour le bois à pH élevé. Son utilisation comme précurseur de gel à d'autres pH, pour lesquels les réactions sont beaucoup plus lentes, permet l'identification des oligomères étant apparus au point de gels de ces matériaux.

Les spectres MALDI-ToF sont qualitativement les mêmes, quelque soit le pH, seule change l'intensité relative des différents pics et donc la proportion des différents oligomères. Les résultats montrent clairement la prédominance des oligomères résorcinol - formaldéhyde aux pH acide et basique, auxquels la réactivité du résorcinol est la plus grande. A pH intermédiaire, la différence de réactivité entre résorcinol et tannin devient faible, et les adduits tannin – formaldéhyde sont nettement plus nombreux qu'aux pH extrêmes.

Par conséquent, une résine (et donc une colle) TRF n'est pas juste un mélange d'oligomères RF d'une part et TF d'autre part, mais comporte bien une proportion importante (jusqu'à 38%, à pH 4), d'oligomères TRF. Ces derniers se présentent majoritairement comme des oligomères de résorcinol ayant réagi avec des tannins monomères ou dimères.

Article n°8

Oligomer distribution at the gel point of tannin-formaldehyde thermosetting adhesives for wood panels

A. Pizzi, H. Pasch, A. Celzard, A. Szczurek

Journal of Adhesion Science and Technology (2011) sous presse

Cette seconde étude par spectrométrie de masse MALDI-ToF considère cette fois des aérogels organiques TF obtenus par séchage dans l'acétone supercritique (cf. article n°5). La méthode permet la détermination des structures des tannins polymérisés mais aussi les produits de condensation de ces tannins avec le formaldéhyde. Ne perdant pas de vue l'application « adhésifs », pour laquelle les colles à bois tannin de mimosa – formaldéhyde sont préparées à pH 6 – 7, c'est donc l'aérogel obtenu à pH 6.3 qui a été étudié.

L'abondance des oligomères de faible poids moléculaire confirme que le matériau est bien un gel, et pas une résine fortement réticulée. Il s'agit en effet tout au plus de trimères, dans lesquels les liaisons entre flavonoïdes existent soit sous forme de ponts méthylène (donc apparus par réaction avec le formaldéhyde), soit en combinant ces ponts avec des liaisons propres à l'auto-condensation des tannins.

La spectrométrie de masse indique aussi que plus de la moitié des tannins ont réagi au moins partiellement avec le formaldéhyde. Comme c'est un gel qui a été étudié pour arriver à cette conclusion, tout indique donc que la résine adhésive TF une fois durcie sera très largement plus réticulée encore. Enfin, la présence de certains oligomères détectés n'a pu être expliquée qu'en admettant la participation de l'anneau B, habituellement non réactif avec le formaldéhyde, à la formation de groupes méthylols. Ce type de réaction est connu pour les pH très alcalins, typiquement supérieurs à 10, mais n'avait jamais été observée à pH 6. Il semble donc que les conditions de gélation très lentes (plusieurs jours) qui ont conduit à la formation du gel TF ont permis la participation de l'anneau B à la formation du réseau polymérique, induisant donc un taux de réticulation plus élevé dans la résine durcie finale.

Conclusion

L'objectif de cette thèse était, d'une manière générale, la préparation et la caractérisation de nouveaux gels de carbone. Pour être réellement nouveaux, ces matériaux ont été obtenus en modifiant, par rapport aux synthèses déjà publiées, soit le précurseur, soit le mode de séchage, soit les deux. Lorsque les précurseurs ont été changés, ils l'ont été en « détournant » des formulations initialement établies pour en faire des adhésifs pour le bois. En effet, au lieu de vouloir préparer des résines durcies et hautement réticulées, ce sont des matériaux dilués et proches de leur point de gel que l'on a souhaité obtenir. Lorsque c'est le mode de séchage qui a été modifié, c'est en proposant une lyophilisation ou une extraction par des solvants organiques en phase supercritique. Des gels séchés par simple évaporation (xérogels) ont aussi été obtenus, mais n'ont pas été décrits ici.

Cette volonté de synthétiser de nouveaux gels de carbone avait pour origine, bien sûr, de proposer des matériaux carbonés présentant d'autres types de textures poreuses que leurs homologues dérivés de résine résorcinol – formaldéhyde (RF). Ces derniers ont d'ailleurs servi de référence tout au long de ce travail. En science des matériaux carbonés, c'est en effet bien souvent la structure de la porosité qui est à l'origine des propriétés d'adsorption, de catalyse, d'isolation thermique, de diffusion, etc. Les gels RF présentent, pour de nombreuses applications, des caractéristiques convenables, mais souffrent du prix de leur précurseur, qui empêche la production de masse de tels matériaux. Un objectif essentiel était donc, en plus de proposer des matériaux différents, d'offrir des gels beaucoup moins chers à préparer. Si, dans certains cas, les textures de pores étaient très comparables à celles des gels de carbone RF, alors tous les objectifs seraient atteints.

Nous avons donc travaillé selon deux voies parallèles, qui se sont finalement rejointes en dernier année de thèse. D'une part, nous avons optimisé le séchage supercritique en milieu solvant et montré, sur la base de gels RF bien connus, qu'il pouvait donner sous certaines conditions des résultats aussi bons que la très coûteuse extraction par CO_2 supercritique. D'autre part, nous avons pu préparer des gels de propriétés très satisfaisantes à partir de précurseurs comme le phénol et le tannin de mimosa (T), respectivement 5 et 30 fois moins chers que le résorcinol. En combinant tannin et séchage supercritique à l'acétone, ce sont finalement des aérogels 5 fois moins chers que les aérogels RF qui ont été préparés pour la première fois.

De tels résultats constituent la « colonne vertébrale » de cette thèse. Quelques travaux « satellites » ont également été effectués, notamment une étude de la réaction entre l'adduit résorcinol – formaldéhyde et une colle polyuréthane, la préparation de charbons actifs

remarquables (à porosité duale) à partir de gels RF, et la détermination de mécanismes réactionnels dans les résines TRF et TF précurseurs de nos nouveaux gels. Tous ces travaux sont originaux, et ont d'ailleurs tous été publiés dans des journaux de rang A.

Cette thèse a été résolument tournée vers les matériaux carbonés résultant de la pyrolyse de gels organiques. Ces derniers auraient sans doute pu être l'objet de davantage d'attention, afin d'observer, par exemple, comment la texture initiale du gel sec se transformait en celle du carbone, dont on sait qu'elle est assez différente à l'échelle nanométrique. Les gels organiques auraient également pu être testés en tant que biosorbants en phase liquide ou, après dopage, comme catalyseur pour diverses réactions de chimie organique. D'une manière générale, et même si les buts tels que définis en début de thèse ont été atteints, peu de temps a été consacré aux applications des gels, qu'ils soient organiques ou carbonés. Cependant, le manque d'équipements sur place, mais aussi le manque de temps, n'a pas permis de se dédier beaucoup aux propriétés applicatives. Des collaborations ont été initiées pour contourner le problème, qui n'ont pas porté leurs fruits aussi vite que nous l'aurions souhaité. La caractérisation électrochimique d'une partie des matériaux a pu néanmoins être faite, suite à un déplacement de deux semaines dans un laboratoire polonais.

Pour mieux appréhender les aspects qui n'ont été que survolés dans ce travail, une seconde thèse faisant suite à celle-ci a déjà démarré. Un point fondamental qu'elle devra traiter est l'optimisation de la porosité des gels de tannins, qui souffrent pour l'instant d'une trop large fraction de macroporosité. Ces pores sont en effet trop larges pour être réellement utiles dans nombre d'applications. Des gels de même densité, mais dont cette partie de la porosité existerait sous forme de méso ou de micropores, seraient plus intéressants encore. Des caractérisations mécaniques et thermiques, à peine abordées ici, devront aussi être conduites avec des équipements acquis très récemment. Il ne fait pas de doute que les voies qui ont été ouvertes au cours de cette thèse seront un point de départ précieux pour la suite de cette thématique « nouveaux gels organiques et nouveaux gels de carbone dérivés ».

Résumé

Cette thèse décrit de nouveaux gels de carbone moins onéreux, mais aux caractéristiques équivalentes, à celles de leurs traditionnels homologues dérivés de résine résorcinol – formaldéhyde (RF) et séchés par CO_2 supercritique avant pyrolyse. Pour parvenir à ce but, deux voies ont été explorées simultanément : (1) la recherche de précurseurs bon marché capables de former des gels chimiques de densité et de propriétés mécaniques convenables ; (2) la recherche de modes de séchage alternatifs, tels que la lyophilisation et le séchage à l'acétone ou à l'éthanol supercritiques. Après pyrolyse, de nouveaux cryogels et aérogels de carbone, respectivement, ont été obtenus. La moitié du travail présenté ici repose sur l'utilisation de tannins (flavonoïdes) de mimosa, des molécules bon marché d'origine naturelle. On montre que l'utilisation de tannins permet d'obtenir des carbones hautement poreux aux caractéristiques texturales bien plus diversifiées et, dans un certain nombre de cas, équivalentes à celles des homologues dérivés de RF. Ces derniers ont un coût de production cinq fois plus élevé que ceux des aérogels de carbone à base de tannins rapportés ici, qui sont donc les moins chers du marché.

Mots-clés : Aérogels, Cryogels, Tannin, Résorcinol, Séchage supercritique, Lyophilisation, Carbones poreux, Supercondensateurs